UNDERSTANDING THE MECHANISMS THAT GOVERN THE IMPACT BEHAVIOUR OF A FOOTBALL

Katie Louise Mills

A thesis submitted in partial fulfilment of the requirements of Sheffield Hallam University for the degree of Doctor of Philosophy.

April 2024

Collaborating Organisation: Fédération Internationale de Football Association

Candidate Declaration

I hereby declare that,

1. I have not been enrolled for another award of the University, or other academic or professional organisation, whilst undertaking my research degree.

2. None of the material contained in the thesis has been used in any other submission for an academic award.

3. I am aware of and understand the University's policy on plagiarism and certify that this thesis is my own work. The use of all published or other sources of material consulted have been properly and fully acknowledged.

4. The work undertaken towards the thesis has been conducted in accordance with the SHU Principles of Integrity in Research and the SHU Research Ethics Policy.

5. The word count of the thesis is 40,000.

Name	Katie Louise Mills
Date	April 2024
Award	PhD
Research Institute	Health & Wellbeing
Director of Studies	Dr Simon Goodwill

SHEFFIELD HALLAM UNIVERSITY

Sports Engineering Research Group

UNDERSTANDING THE MECHANISMS THAT GOVERN THE IMPACT BEHAVIOUR OF A FOOTBALL

Katie Louise Mills

Submitted for the Degree of Doctor of Philosophy

April 2024

Football is one of the most popular sports in the world. The 2022 FIFA World Cup final was watched by approximately 1.5 billion people, with an estimated 250 million people participating in the sport globally. The ball is a fundamental piece of equipment necessary for participating in the sport and has undergone numerous developments in both the design and materials as manufacturers strive for a competitive advantage.

The Fédération Internationale de Football Association (FIFA), as the international governing body of football, regulate the quality of footballs entering the professional game to uphold the integrity and safety of the sport. However, there is a need to greater understand the dynamic performance of footballs to ensure that the policy remains relevant to assess the standard of balls entering the sport as materials and manufacturing technologies evolve. This thesis details an in-depth investigation into the dynamic impact response of footballs, the development of appropriate experimental test protocols and a mathematical model to investigate the contribution of the mechanical properties of a football on its impact behaviour to inform the standards.

The static and dynamic properties of twelve different footballs were obtained experimentally. Each football was projected at a force platform at a relatively low and high velocity. Measurements were captured using a combination of high-speed video and a force platform to characterise the impact response. The mechanical properties of each football were evaluated from a quasi-static compression test and the loading profile outputted from the force platform.

The relationships between the mechanical properties and the impact response of a football were developed using multivariable regression. The models that used the properties derived from dynamic tests showed better ability to explain the variations in the impact response between the footballs than the properties obtained from static tests. The stiffness of a football showed significant influence on its impact response.

The current policy for regulating the standard of footballs evaluates their ability to dissipate energy upon impact but lacks a direct or indirect quantification of a ball's stiffness. However, the stiffness properties govern aspects such as contact time, deformation and impact force. Therefore, to ensure a comprehensive assessment of the mechanisms that govern the impact behaviour of a football, it is recommended to incorporate an additional measurement of contact time in the FIFA Quality Programme. This measure can easily be incorporated into the existing test protocols to serve as a proxy of dynamic stiffness. This can provide a comprehensive evaluation of the properties of a football that govern its impact behaviour across diverse conditions.

Keywords: football, impact testing, mechanical properties, multivariable regression

Acknowledgments

I would like to thank my supervisors Dr Simon Goodwill, Dr Simon Choppin, Dr Marcus Dunn and Dr John Kelley for their support and guidance throughout the duration of the study. Special thanks are due to Terry Senior for his role in the design and construction of the experimental equipment used in this research.

I would also like to thank Johsan Billingham and Eduardo Tavares, and all other members of the FIFA Technology and Innovation subdivision who have supported and funded this work.

My extended thanks go to members of the Sports Engineering Research Group for their assistance and collaboration throughout the duration of my time here.

Contents

Nomenclature

a	Acceleration of the football ($m \cdot s^{-2}$)
A	Cross-sectional area of the ball (m^2)
c	Dashpot coefficient used to model the hysteresis losses in a ball
C_d	Drag coefficient
C_l	Lift coefficient
COM	Centre-of-mass
COR	Coefficient of restitution
d_a	Actual diameter of football (m)
d_c	diameter of football seen from camera (m)
e_{loss}	Energy loss due to hysteresis (J)
F	Peak impact force (N)
F_b	Force acting on the ball (N)
F_D	Force due to drag (N)
F_{MAX}	Maximum applied force (N)
F_N	Force due to Newtons law of motion (N)
F_w	Weight of a football (N)
F_x	Component of force in the x axis (N)
F_y	Component of force in the y axis (N)
F_z	Component of force in the z axis (N)
FQP	FIFA quality programme
FQPro	FIFA Quality Pro certification mark
g	Acceleration of gravity ($m \cdot s^{-2}$)
I	Impulse (Ns)
k	Aerodynamic drag force factor
k_b	Stiffness coefficient
k_{dyn}	Dynamic stiffness ($N \cdot m^{-1}$)
k_{eq}	Equivalent stiffness ($N \cdot m^{-1}$)
k_s	Static stiffness ($N \cdot m^{-1}$)
l	Contact Length (m)

m_b	Mass of football (kg)
R^2	Coefficient of determination
RMSE	Root-mean-square error
t	Time (s)
T	Contact Time (s)
T_F	Contact time measured using force platform (s)
v	Relative velocity of the football (m·s^{-1})
v_i	Inbound velocity (m·s^{-1})
v_o	Outbound velocity (m·s^{-1})
V_T	Terminal velocity of a football (m·s^{-1})
x	Displacement of ball COM (m)
$\dot{x}$	Velocity of ball COM (m·s^{-1})
$\ddot{x}$	Acceleration of ball COM (m·s^{-2})
Z	Z score
δ_b	Ball deformation (m)
ρ	Density of air (kg·m^{-3})
σ	Standard deviation
ϕ	Phase difference (rad)

1 Introduction

The following chapters describe a three-year study examining the impact response of a football during a collision with a force platform.

(a) Motivation for the study

Football is one of the world's most participated sports that has transcended cultural, geographical, and demographic boundaries. The evolution of the sport has been a gradual process shaped by cultural, social, and technological advancements over centuries. It has transitioned from its diverse ancient forms to the standard rules established by The Football Association in 1863. In the 21st century football has become a global phenomenon, with growing emphasis on fair play, inclusivity, and social responsibility within all aspects of the sport. Players and coaches at the elite level are increasingly skilled and place heightened expectations on the quality of equipment used throughout the sport. Football has seamlessly integrated technology advancements into various facets of the sport, enhancing the accuracy and fairness whilst also elevating the overall experience for players, officials, and fans on a global scale. Beyond officiating, technological advancements have permeated playing equipment, with innovations in boot designs, materials, and wearable technology.

The ball is a fundamental piece of equipment necessary for participating in the sport of football. Its development has primarily been influenced by advancements in material science and industrial engineering. Manufacturers are constantly competing with one another to optimise the performance of the football and use it to showcase unique panel designs and market their brand image. Players of all abilities will encounter a wide range of footballs throughout their careers, possessing different textures, weights, and flight patterns. In 1996 Fédération Internationale de Football Association (FIFA) introduced 'The FIFA Quality Programme (FQP) [1]' to outline the quality of footballs used across elite competitions to protect the integrity of the game and provide players with reliable and consistent playing experiences across different matches and tournaments. This is achieved through a series of laboratory tests designed to evaluate the performance of a football. While these results offer a suitable means for assessing the quality of the materials and manufacturing, they do not thoroughly examine the dynamic performance of footballs.

FIFA has been fast evolving into a governing body that is better equipped to serve the sport, which included a review into the existing standard programmes for verifying the quality of equipment. The organisation is motivated to maintain the integrity of the sport to ensure developments in technology do not detrimentally affect the sport in the future. This has motivated the governing body to embark on research projects aimed at advancing their existing knowledge of the mechanics of the game. The impact response of a football is fundamental to the quality, safety, and overall experience of the game. It influences player performance, game play dynamics and the perception of the sport by both participants and spectators. Understanding and optimising the impact response is a key consideration in the design, testing and regulation of footballs.

Mathematical models have been used extensively in the study of ball impacts, to understand and predict the complex dynamics involved. These models incorporate fundamental principles from physics and engineering to simulate the behaviour of a ball during a collision. The models allow researchers to identify and quantify the influence of individual factors such as the mechanical properties on the overall impact behaviour of the ball. This insight is crucial for identifying the most significant design elements that affect performance and allow informed decisions about the factors that should be considered during the regulation of footballs.

Thousands of footballs have received certification from the FQP for professional use. However, it is essential to evaluate if the existing test programme is effectively regulating the impact behaviour of modern-day football designs. This thesis details an in-depth investigation into the impact response of certified footballs, the development of appropriate experimental test protocols and a mathematical model to investigate how the mechanical properties of the football contribute to its impact behaviour. The research looks to identify and quantify the factors influencing a footballs impact response, to allow a proactive regulation of football performance in safeguarding against potential future developments.

(b) Aims and Objectives

The aim of this programme of research was to develop a greater understanding of the influence that the mechanical properties of a football have on its impact response at a low and at a match-representative velocity.

The objectives were to:

1. To analyse and evaluate existing research relevant to this study.

2. Measure the quasi-static stiffness properties of a football.

3. Validate an experimental set-up to measure the force and deformation during a football-surface impact.

4. Measure the impact response of a football during a collision with a surface at appropriate velocities.

5. Develop a mathematical model between the mechanical properties of a football and appropriate variables that characterise the impact response of a football.

6. Consider the practical applications of the research findings in the context of the FIFA Quality Programme for Footballs.

(c) Structure of the study

The objectives outline a systematic approach to acquire the data that is essential to develop a mathematical model of a football impact. The thesis will first present the findings from a review of relevant literature to synthesise the knowledge in the area and evaluate suitable methodologies to successfully achieve the objectives. The subsequent chapters will document the development and validation of an experimental test procedure, specifically designed for accurate measurement of the footballs impact response. The data derived from relevant experimental investigations will then be used in the development of the model.

2 Literature Review

2.1 Introduction

The pursuit of knowledge in football is multifaceted, spanning across diverse areas of the sport such as its historical evolution, tactical analysis, physiological demands, and technological advancements. Published material within the sport originates from a variety of disciplines including sport science, engineering, physics, biomechanics, psychology, and sociology. Within sports engineering, the quantity of research has greatly expanded in topics including the global impact of the sport, technological advancements in; officiating, equipment, sports surfaces, and systems used to monitor game play.

This study is aimed at developing an understanding of an impact between a football and a surface. A major challenge of protecting the integrity of the game of football is ensuring an in-depth knowledge of the equipment, specifically how the mechanical properties of a football influence both the behaviour during and after impact, which, in, turn, might shape the way the sport is played. This chapter aims to critically analyse the published material with respect to the intended study, it attempts to explain and highlight the existing knowledge in the field. The first step was to gain an understanding of the current certification protocols for footballs and other balls used across different sports. Following this, the focus shifts towards gaining comprehensive insights into the nature of the football itself. The final section will examine the current methods and tools used to analyse the impact behaviour of a football.

The sponsorship of this work by FIFA signifies a critical partnership aimed at enhancing the regulations and standards that govern the sporting equipment used in football. The outcomes and findings derived from this study will be used by them to aid decision making as they seek to refine and possibly introduce new guidelines to maintain the integrity of the sport.

2.2 Governing Body Regulations

The following section discusses the quality control procedures for footballs and for other balls used in sport.

2.2.1 FIFA Quality Programme

The FIFA Quality Programme (FQP) for footballs [1] was introduced in 1996 to standardise the quality of footballs, promoting consistency in performance across global competitions. This consistency is essential for fair and safe competition, as it ensures all players are playing with footballs with similar characteristics, maintaining the integrity of the game. Figure 1 illustrates the 7 characteristics of the football examined during certification. However, these tests are not exhaustive and several aspects of ball design that the programme does not explicitly examine that include the interaction with different playing surfaces, the colour and design, the aerodynamics, player preferences, manufacturing ethics or sustainability.

Figure 1 The tests to examine a football included in the FIFA Quality Programme.

The impact behaviour of a football is assessed by measuring the rebound height for a collision with a rigid flat surface. For a 2 m fall, the football must rebound consistently between 1.25 and 1.55 m.

Following an assessment, if an outdoor football has successfully conformed to the specific technical requirements, the football is allocated one of three marks shown in Figure 2.

Figure 2 The 3 FIFA Quality Marks for Footballs: FIFA Quality Pro, FIFA Quality, and FIFA Basic.

- **FIFA Quality PRO**, the highest level of certification that emphasises first-class performance and safety. Footballs with this quality mark are designed for optimal performance and use at the highest level.

- **FIFA Quality**, an emphasis on durability and safety. Footballs with this quality mark are designed for extensive use, e.g. an acceptable level for training.

- **FIFA Basic**, an emphasis on setting the minimum standards while ensuring affordability for use at all levels of the game. Footballs with this quality mark fulfil basic performance.

When this study began in October 2020 the programme consisted of laboratory testing conducted by a FIFA accredited test institute and a material analysis which outlined the construction of the football that was submitted by the licensee. In October 2022, the material analysis test was removed from the programme due to the ambiguity and inconsistency of the submissions from licensees. In February 2022, the rebound test was updated to allow licensees to set the internal pressure between 0.6-1.1 bar for the rebound test. Previously it had been set at 0.8 bar for all tests. Apart from minor amendments to the range of accepted limits to laboratory tests, the test protocol remains largely unchanged.

2.2.2 The Laws of the Game

The International Football Association Board (IFAB) was established in 1886 with the purpose of developing and preserving the Laws of the Game. The Laws of the Game [2] were created in 1863 to harmonise the sport internationally with a focus on player safety and wellbeing. The laws are fundamental guidelines that ensure fairness, uniformity and consistency in the way football is played. The laws are applicable to all matches under every confederation, country, and level of play. They govern various aspects of the game, including player conduct, field dimensions, the football, fouls, penalties and more.

The intrinsic property requirements of the football are outlined in Law 2.

'The ball must be spherical, made from a suitable material, with given accepted ranges of circumference, weight, and internal pressure. All footballs used in official confederation or FIFA organised competition must have been subjected to the specific technical requirements of the FQP and thus bear one of the three FIFA Quality certifications. [2]*'*

Professional football competitions and matches adhere to both the Laws of the Game and FIFA's quality standards to ensure fair play, safety, and consistency in the sport. The standard of the equipment and products that are accepted in the Laws of the Game are determined and certified by the FQP. The Laws of the Game uses these equipment standards set by the FQP to govern the way the sport is played.

2.2.3 The Certification of Balls in Sport

Major sport governing bodies including: The Fédération Internationale de Volleyball (FIVB) [3], Fédération Internationale de Basketball (FIBA) [4], R&A (Golf) [5], World Baseball Softball Confederation (WBSC) [6], The Fédération Internationale de Hockey (FIH) [7], and International Tennis Federation (ITF) [8] enforce rigorous quality control procedures for the equipment used in their respective sport. There are similarities in the methodologies employed by these organisations and the FQP to certify adherence of their respective balls to established standards. Differences usually revolve around the quantity of balls that are submitted and tested by the relevant institute. However, certain sports, like volleyball and golf incorporate specific tests tailored to the unique playing conditions of their respective sports.

The rebound test is commonly encountered in each respective test programme to assess dynamic behaviour. While protocols vary in drop height, the impact is recorded using a single camera pointed towards the impact plane. The ITF deviate from standard methods and achieve high measurement accuracy by casting only a shadow of the ball onto a frosted screen that incorporates a calibrated scale, using carefully placed light sources and mirrors, as illustrated in Figure 3.

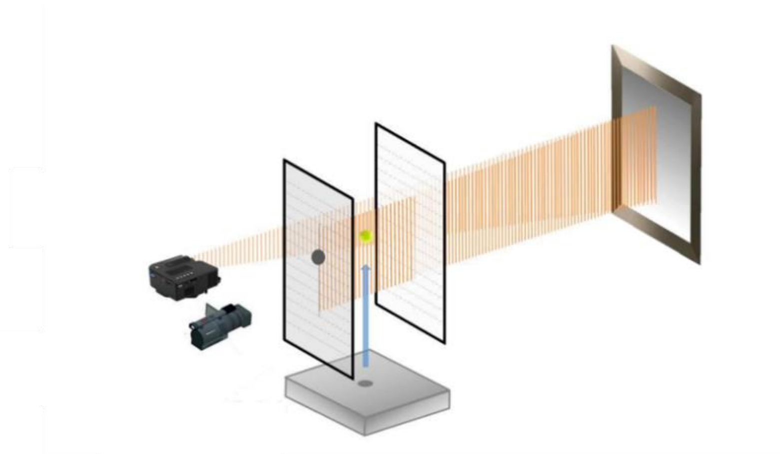

Figure 3 The test apparatus employed by the ITF using a single camera and light source to cast a shadow of the tennis ball to measure the rebound height. Reproduced from [8]

In volleyball (FIVB), a force platform is impacted instead of a rigid surface, to assess the maximum impact force. This measurement is crucial for athlete safety in a sport with frequent contacts between the hand and wrist. The impact force is measured from a relatively low impact speed (around 4 $m \cdot s^{-1}$) following a free-fall drop from 1 m. The R&A perform a distinct test method to evaluate the dynamic performance of golf balls. In this procedure, a mechanical golf robot impacts a golf ball at a club head speed of 120 mph. The collision is videoed, and the outbound velocity, spin and angle of the trajectory must conform to the established limits.

The hardness of hockey and tennis balls is controlled by the respective governing body, each using a different test protocol. In tennis, a static measurement is performed by applying the compressive load and measuring the deformation. While in hockey, a dynamic measurement gauges deceleration using an impactor against the ball. Unlike the test method employed by the ITF, the hockey approach doesn't specify impactor speed, but its dynamic nature allows for replicating match play conditions, addressing certain limitations encountered by the ITF.

2.2.4 Section Summary

For any football used in a FIFA organised competition (professional match played under a FIFA confederation or accredited organisation), it is mandatory to bear a FIFA certification mark. Although the tests performed in the FQP are in line with certification protocols of other governing bodies, these other entities incorporate additional systems like force platforms or mechanical tests to examine further aspects of the ball and its impact behaviour. Despite significant advancements in materials and manufacturing techniques for modern footballs, the FQP protocols have remained largely unchanged since 1996. It remains unknown whether solely measuring the rebound height is sufficient to gauge a footballs impact behaviour. Examining additional properties could offer a more comprehensive understanding of the underlying components contributing to a football's performance.

2.3 The Construction of a Football

The following section discusses the typical construction of a football.

2.3.1 The construction of a football

Footballs are available in three sizes: 3, 4 and 5, each tailored to different age groups and levels of play. The smallest, size 3 footballs, are typically used by children under the age of 8. Size 4 footballs are slightly larger and generally used by children aged 8 to 12. Size 5 footballs are the largest and standard size used by players aged 13 and above and are the official size for professional matches worldwide. Table 1 presents the difference in circumference and mass between the different sized footballs [9].

Table 1 Size and mass ranges for footballs used by different age groups

Size	Age Group	Circumference (mm)	Mass (g)
3	Under 9	600-620	280-310
4	Under 13	635-660	350-390
5	Over 13	680-700	410-450

A football's can be considered a thin-walled pressurised shell, as the volume of material is lower than the volume of pressurised air contained inside the bladder. Manufacturers of footballs will use diverse material compositions and procedures to create their products. Each manufacturer may prioritise different aspects of a ball's performance such as control, power or comfort, depending on the intended use case of a football. This can lead to variations in the thickness, texture and overall composition of the football. Despite variations in material types, the shell of a football can generally be categorised into four layers: the bladder, lining, foam, and outer panelling, shown in Figure 4.

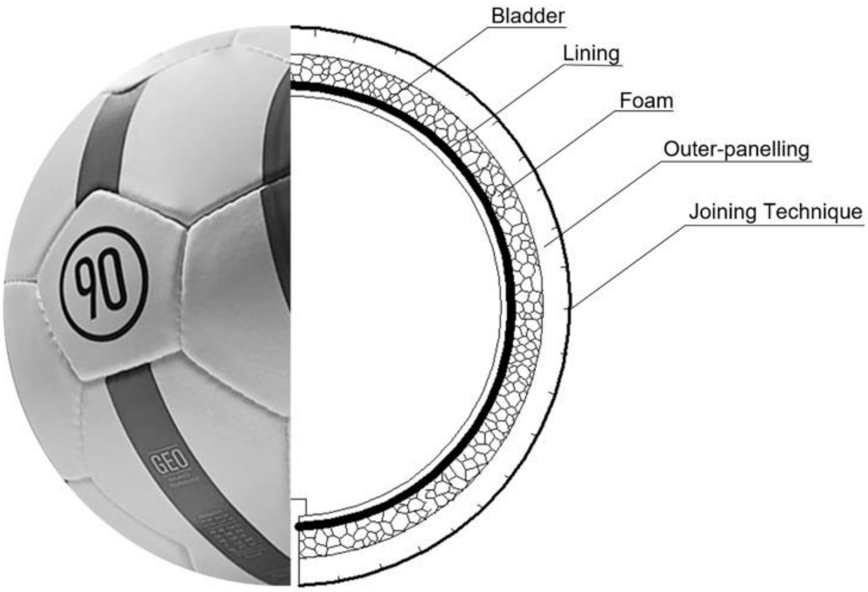

Figure 4 The illustration shows the typical construction of a football and the order of the material layers; bladder, lining, foam, and outer panelling.

The bladder

The bladder is the innermost layer of a football and retains the internal air pressure of the ball. Typically manufactured from hyperplastic polymers like butyl or latex, butyl excels in air retention despite being heavier, while latex offers a softer surface interaction that is suitable for natural grass play. However, micropores in the latex can lead to poorer air retention, requiring more frequent inflation. The valve facilitating air inflow, is integrated into this layer. Certain manufacturers incorporate additional material opposite the valve to counterbalance the mass of the valve to ensure the football’s mass is balanced.

The lining

The bladder is often lined by multiple layers of fabric that are laminated together to provide the structural stiffness of the football [10]. Tensile testing, comparing the stiffness of individual layers to when combined in a manually stitched Adidas football, revealed this layer governed the material response, demonstrating an elastic modulus two times greater than the outer panelling [11]. The bladder and lining are often collectively referred to as the carcass layer.

The foam

The foam layer is a result of the evolution of football design and material developments, not present in traditional models. The layer adds a cushioning effect that improves the perceived comfort and control of the ball. The layer is located between the lining and outer panelling; manufactured from elastomeric polymers, offering high flexibility such as Polyurethane (PU) or Ethylene-vinyl Acetate (EVA). It is typically around 2 to 3 millimetres in thickness. The large energy dissipation of this layer can influence the perceived tactile response of the ball by a player.

The outer panelling

The advancements in material and manufacturing procedures are most evident in the outer panelling. Modern footballs feature outer panelling constructed from polymeric materials, providing superior water repellence compared to traditional leather models. The shift from leather, which gained mass through water absorption, increase impact forces and concerns about head injuries, promoted the change in materials [12]. The outer panelling exhibits much larger material damping due to a higher polymer content than the lining of a football [13]. Three types of polymers are commonly used, determined by the intended level of play for the football.

1. Polyurethane (PU) typically used in elite and match play balls accredited with FIFA Quality and Quality Pro models.

2. Thermoplastic Polyurethane (TPU) is cheaper to manufacture and more commonly used in recreational footballs or those accredited with the FIFA Basic mark.
3. Polyvinyl Chloride (PVC) is used on very basic, low-cost models.

The construction and surface texture of the outer panelling has an overall influence on the impact and flight characteristics of a football [14-18]. The number of panels has been subject to large developments by manufactures due to increasing material and manufacturing options, changes which are often perceived by players [19]. The individual panels that assemble to create the spherical shell of the football are joined using contemporary methods using heat such as thermal bonding and fuse-welding, rather than being stitched together. These methods promote more uniquely shaped curved panel designs as there no longer a requirement of straight edges to stitch along.

2.3.2 Section Summary

A football can be considered as a thin-walled pressurised sphere, with a material shell composed of layers of diverse materials. Typically, this will include a rubber bladder, with the remaining thickness comprising of layers of cloth and foam. The manufacturers of footballs have large flexibility in the material selection, as there are no imposed restrictions. The evolution of footballs has been guided by advancements in material science, making this a crucial area of innovation. The collective selection of the materials shapes the mechanical properties that ultimately influence the overall playability of the football. The next section will review the measurement techniques used to characterise the football properties.

2.4 Static Properties of a Football

The combination of the elastic and viscous properties of the materials used to construct a football make it a viscoelastic object. The properties of the high polymeric content of the football shell allow it to deform under stress, recover its shape and exhibit a time-dependant response to external forces.

2.4.1 Material Phenomenon

a) Material Viscoelasticity

It is necessary to recognise the viscoelastic nature of a football when measuring the static mechanical properties of a football. When subjected to an external force, the material response will be rate-dependant; it does not solely obey Hooke's Law nor Newton's Law of viscosity; instead exhibits both elastic solid and viscous liquid characteristics.

Figure 5 shows the cyclic stress response for an (a) elastic, (b) viscous and (c) viscoelastic material. The phase difference (ϕ) between the total stress and measured strain indicates the extent of a materials viscoelasticity. Price [13] performed dynamic material analysis (DMA) on rectangular sections (40 x 5 mm) of individual constituent material layers for 2 Adidas footballs. The storage and loss moduli and phase difference varied with the frequency showing the materials used in these footballs behaved in a viscoelastic manner. In a dynamic impact, this would mean the peak impact force may occur slightly earlier than the point of maximum ball compression.

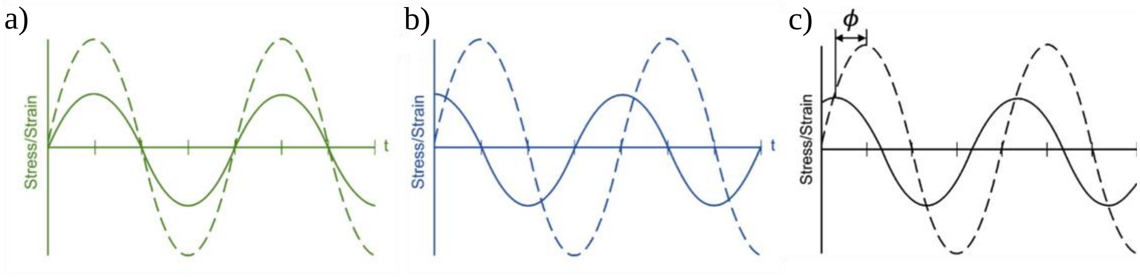

Figure 5 The total stress (-) and measured strain (--) for an (a) elastic, (b) viscous and (c) viscoelastic material. The phase difference between the stress and strain for an elastic (0 °) and viscous (90 °). The phase difference measured for a viscoelastic material demonstrates the level of viscosity exhibited by the material. Figure adapted from [13]

b) Hysteresis

Figure 6 shows the stress-strain plot for a single loading and un-loading cycle of a viscoelastic object. Notably, the unloading path is well below the loading. The area enclosed by the curve is the energy dissipated. Hysteresis is caused by the internal friction of the polymeric materials, resisting the compression and restoration phases. The mathematical explanation for the shape of the hysteresis is outlined in Appendix 10.1.

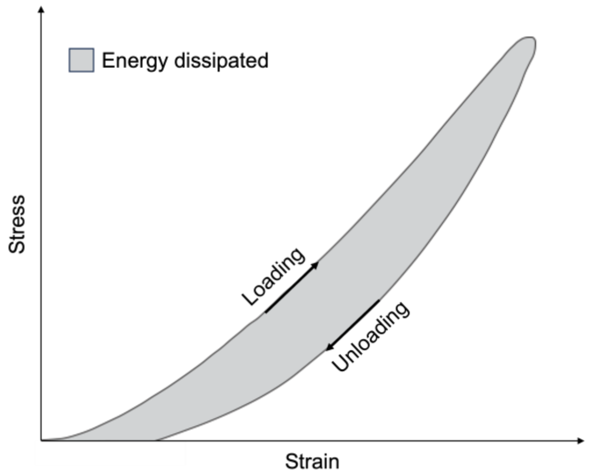

Figure 6 The hysteresis curve showing the relationship between stress and strain during loading and unloading cycles of a compression test. The energy dissipation is signified by the area enclosed by the loop.

c) *Mullins Effect*

Many authors investigating the material or static structural properties of footballs have considered the Mullin's effect during cyclic loading. Materials with significant viscoelastic behaviour and nonlinear stress-strain responses are more prone to the Mullins effect due to their unique microstructural properties than materials such as metals or ceramics that have more stable microstructures under cyclic loading. Viscoelastic materials contain a network of polymer chains and potential filler particles. During cyclic loading, the bonds between these elements can undergo reversible rearrangement which can lead to inaccurate representation of a material's mechanical properties such as stiffness [20]. The stress softening phenomena is characterised by the reduction of stress (σ) observed over repeated cycles of loading and unloading. In an idealised application, the loading path of subsequent cycles would follow the unloading path of the previous cycle, provided the maximum strain (ε) of the first loading cycle is not reached. However, in practice successive extension cycles will exhibit a declining maximum stress value, as shown in Figure 7. The decline of stress between successive loading cycles in viscoelastic objects has been observed to become negligible following 5-10 cycles, where a constant stress amplitude and stabilised hysteresis will be reached.

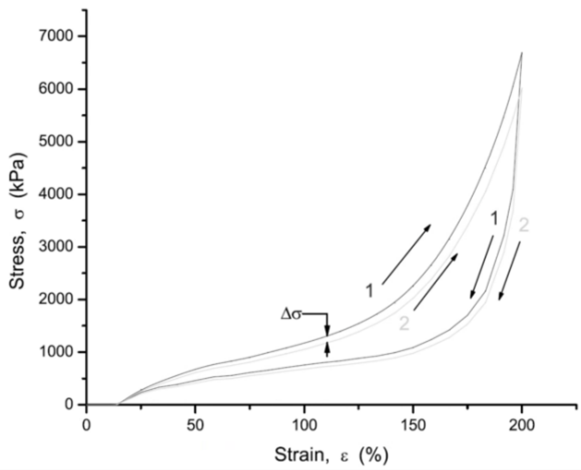

Figure 7 A hysteresis curve demonstrating the Mullins effect, presented by Bauman [18]. The loading of the second cycle (2) does not fully align with the first (1) cycle and exhibits a declining maximum stress value.

2.4.2 Measuring the mechanical properties of a football using static tests

Compression and tensile testing have been performed using commercial mechanical test devices to measure the static mechanical and material properties of sports balls. These approaches differ in the direction of the force applied, the properties measured and applications.

- **Compression testing** involves compressing the whole composite between two plates to characterise the structural mechanical properties.

- **Tensile testing** exerts a pulling force on a section of material along its axis stamped from the whole composite to characterise the material properties, often in a dog-bone shape. This method yields a wealth of information that is required to define the material properties of a ball prior to computational simulations including modulus of elasticity, ultimate tensile strength and yield strength.

Tensile testing gives a global insight into the properties of the materials that are required to define material models in computational simulations. The review of literature will focus on compression testing as this approach characterises the stiffness of the whole structure that is more relevant for impact analysis.

The structural stiffness of a football is defined as the ability of the football to resist deformation when subjected to an external force. It characterises the rigidity or stiffness of the overall structure of the football, including the internal pressure and material composition.

Quasi-static tests cannot replicate the behaviour observed during a dynamic impact [21-25]. There are three differences between quasi-static tests and dynamic impacts; the loading rate, the deformation shape and the type of displacement measured.

1. Loading Rate

   The loading rate and magnitude of force a ball experiences in a static test are far smaller than in a dynamic impact as these are limited to the capabilities of commercial mechanical test devices.

2. Deformation Shape

   In a static test a ball will undergo bilateral symmetrical compression, in a dynamic impact the ball will undergo unilateral asymmetrical deformation [25]. The unilateral asymmetrical deformation shape can be re-created by slicing the ball into two equal parts around its circumference. Research exploring the static properties of balls including cricket [23] or baseball which have rolled core construction; when sawn in half, the ball will retain its shape when a force is applied. However, when compressed the top half of the ball is free to deform outwards as it is not constrained by the other half of the ball which results in a reduced stiffness of the system. Balls with an inflated core such as a tennis ball or a football must be placed on a solid hemispherical cap when compressed as it will not retain its shape when a force is applied. However, this cap will provide a restoring force that is not present during an impact between a ball and a surface [26]. Unlike compressing a ball between two flat plates, this cap introduces an uneven pressure distribution and can create localised deformations that do not accurately represent the overall stiffness of a football.

3. Deformation Measured

   In a quasi-static test, the hysteresis is plotted as a function of ball compression rather than COM displacement. This means the quasi-static and dynamic hysteresis curve that is obtained from an impact with a force platform cannot easily be compared [22]. There have been examples of researchers assuming multiplicative relationships between static and dynamic compression to yield similar values of effective spring constants [22,23]. However, the relationships are highly dependent on the properties of the balls being impacted.

> Quasi-static tests can be used to characterise the mechanical properties of a ball and have been used to explain the behaviours of a ball during a dynamic impact with a surface [27-29]. Quasi-static testing is easier to perform than dynamic impacts as specialised equipment is required to accelerate the balls to a speed considered to best represent match play which introduces uncontrollable variation in the impact (e.g., impact orientation). Whereas quasi-static tests can be performed using standardised test protocols on commercial mechanical test devices. Research examining the impact mechanics of balls in sports including baseball, cricket, tennis, and volleyball [30] have measured the quasi-static stiffness to explain differences in the dynamic impact behaviour between balls of different constructions.

There are only a few examples in published literature where quasi-static compression testing has been performed on a football; none of these have correlated the properties of a football with its dynamic behaviour nor have isolated the contribution of internal pressure to the overall structural stiffness. Karimi et al [31] compared the static mechanical properties of a football to a futsal. A single model of football was compressed to failure between two flat plates at a strain rate of 10 $mm \cdot min^{-1}$. The authors outline the FQP limits for mass, circumference and internal pressure but do not specify if these values were used in their test protocol. Thompsett et al [19] used the structural stiffness as an objective measurement as part of a player perception study to investigate how the design choices in the construction of a football influenced consumer opinions. Three footballs from different licensees, manufactured using different number of panels, different materials and different joining techniques, inflated to 0.9 bar, were compressed between two flat plates using an Instron mechanical test device at a rate of 200 $mm \cdot min^{-1}$ to a force of 2000 N, chosen to represent the force of an instep kick. The force-time and displacement recorded was averaged over five trials, there was no mention of a holding period to allow the displacement to settle in the methodology. The stiffness was calculated using Hooke’s law as a ratio between the magnitude of peak force and corresponding displacement. The stiffness of all three balls was significantly different ($p < 0.05$). The dimensions of the compression plates were not provided in either study.

Dignall [27] and Goodwill [28] have used quasi-static testing to explain the results of a dynamic impact between a tennis ball and a rigid planar surface for different types of tennis balls. The authors held the applied force for a period during a quasi-static compression test between a tennis ball and two flat plates in an attempt to remove strain-rate dependencies, illustrated in Figure 8.

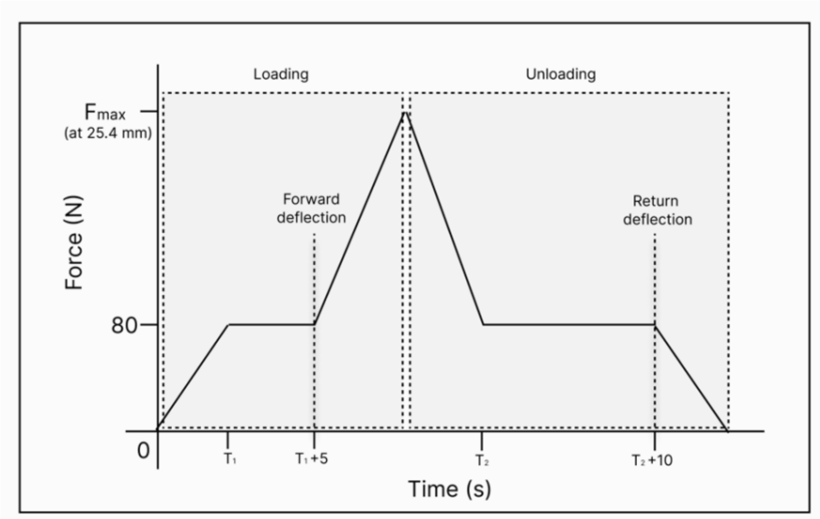

Figure 8 Schematic showing the loading phases for compression testing of a tennis ball. Holding phases were incorporated into the compression cycle in attempt to overcome strain-rate dependencies.

Dignall assessed the viscoelastic properties of a tennis ball by measuring the stiffness of the ball at various strain rates (10-1000 $mm \cdot min^{-1}$). Dignall found above 10 $mm \cdot min^{-1}$ all deformation rates gave identical force-deflection curves. The stiffness contributed purely by the structure of the tennis ball was isolated from the internal pressure contribution by applying a small, drilled hole (around 10 mm) in the ball. This removed any air contained within the volume of the ball. However, Goodwill noted this may not be a true representation of the structural stiffness of the wall due to air leakage occurring during compression. The structural stiffness at various loading levels was calculated by fitting a polynomial to the force-deflection data during the loading cycle. Goodwill found the tennis balls that had a lower quasi-static structural stiffness exhibited greater deformation and longer contact times during high velocity dynamic impacts (~30 $m \cdot s^{-1}$). Hendee et al [32] investigated whether static compression testing could be used to describe the dynamic impact properties of baseballs. They found that static parameters associated to stiffness could be used to predict some dynamic properties (e.g., peak impact force). However, the authors found no way to correlate the hysteresis loss calculated from static tests to the damping properties of the ball (e.g., COR).

2.4.3 Section Summary

Footballs are constructed from layers of polymeric material inflated to give the spherical shape. Standardised mechanical test machines can be used to perform compression tests on a football to quantify the structural stiffness of the football. The material composition of modern footballs exhibits viscoelastic properties, introducing strain rate dependency to the stiffness value obtained these tests. The literature on compression tests for footballs lacks a consistent test protocol and fitting methods for calculating stiffness, with variations in compression speeds and displacement levels. While quasi-static stiffness has been used in conjunction with dynamic impact variables in impact studies for other sports balls, this approach remains unexplored in football.

To successfully achieve objective 2, the quasi-static stiffness of a football can be measured using a compression test performed on a standardised mechanical test machine. The method should consider the material phenomenon effects associated with viscoelastic materials that were discussed in this section. The compression test should be performed across multiple axes to account for the non-homogeneity of the football. Since there is no consistent method of calculation, the research should incorporate evaluating the correlation between the dynamic impact behaviour for different fitting methods.

2.5 Dynamic Impact Behaviour of Footballs

There are standard measurements that are used to characterise the impact behaviour of a football during a collision with an object that are collectively referred to as impact variables. These are the coefficient of restitution (COR), contact time, deformation, and impact forces. The magnitude of these variables will be influenced by the inbound conditions (velocity and impacting surface) and the material composition of the football. They are often used in the discussion about the performance of a football.

2.5.1 Football Launch Methods

To study the impact behaviour of a football, the football is required to be projected at a controllable and repeatable velocity. In literature this has previously been performed using gravity, using mechanical systems, or using players to kick the ball from stationary.

The first method uses gravity by dropping the ball from a range of heights. This method is used in the FIFA Quality Programme (FQP) to measure the rebound height during football certification and has been used to investigate factors affecting the ball-surface interaction [1,33]. The football impacts perpendicular to the surface with no imparted spin. This method gives a highly repeatable and accurate inbound velocity, but the maximum inbound velocity is limited by the drop height, usually to below 8 $m{\cdot}s^{-1}$ which corresponds to a 4 m drop height. This may be suitable for some football-surface interaction investigations but is far below speeds that might be observed in match play. Levendusky [34] achieved a higher inbound velocity using a drop height of 18.09 m corresponding to velocities in the range of 17-18 $m{\cdot}s^{-1}$. Due to the fall time, aerodynamics and magnus effects caused erratic flight that required a large sample size to ensure the impact was located within the correct area.

Many authors [11,35-38] have used mechanical systems to project the football to achieve higher impact velocities that might be more representable of the speed the football would impact the surface during match play. Some authors have used commercially available football launching devices [36,37], whilst others have developed bespoke systems to enclose the rebound of the ball within the testing environment [11,35]. These systems often consist of two or more rotating wheels in the same plane to accelerate the football to speeds between 10-36 $m{\cdot}s^{-1}$. The separation distance of the wheels is often less than the diameter of the football, causing small amounts of compression, which are assumed negligible by the time the football impacts the target that are usually located over 1 m away from the launch device. However, as speed is imparted to the ball during the compression phase, differences in the global properties surface texture between different footballs can lead to small variations in its exit speed. The design of commercially available launching devices requires the football to be launched horizontally. This creates challenges enclosing the testing environment to protect the operator from the co-incident path of the rebound and therefore often requires multiple operators. To overcome this, bespoke systems have been designed to enable a single operator to launch the football within a closed environment. Price developed a bespoke device capable of launching the football up to 36 $m \cdot s^{-1}$ that permitted rotation of the impact surface and rollers to allow both normal and oblique impacts. Wiart [35] used two modified cricket bolas mounted parallel to one another to launch the football normally up to 25 $m \cdot s^{-1}$. These velocities are much higher than can be achieved during drop tests, but Carré [29] noted the use of mechanical systems introduces uncontrollable variability in the orientation and impact location of the ball. To achieve a greater repeatability in impact location, air cylinders can be used. These are employed by the ITF during their tennis ball certification procedures but to date were not found to be used in any football-surface publications [8].

Alternatively, players can impart a velocity onto a football by kicking it from stationary towards a target. Auger [39] noted much higher variation in the inbound velocity when asking players to repeat trials under the same conditions (± 3 $m \cdot s^{-1}$) compared to when mechanical systems are used (Wiart ± 0.2 $m \cdot s^{-1}$). Players are often used in studies when the deformation behaviour of a football around a boot during a kick is the focus [40,41], rather than when accurate and consistent measures are required. However, to achieve a repeatable impact location and velocity, Koizumi [38] used a mechanical arm to simulate a player kicking a ball.

2.5.2 Measuring Dynamic Impact Metrics

The interaction between a football and a surface can be characterised by variables that are measured prior, during and after the impact. These variables can provide understanding of the dynamic response of a football to give an indication of how each component of the football (e.g., internal pressure, shell stiffness) contributes to the dynamic response during an impact with a surface. The parameters that are used to calculate the impact variables include:

1. Linear and angular velocity of the ball prior, during and after the contact with a surface.

2. Football and surface deformation.

3. Contact time.

4. Forces acting on the ball during contact.

The parameters above can be obtained using high-speed video cameras and force platforms.

2.5.3 Impact variables measured using high-speed video

The use of high-speed video cameras is suitable to analyse sports ball impacts since they output individual frames. High-speed video images have previously been used to quantify impact and rebound speeds, contact time and displacement of a football impact between 6 and 30 $m \cdot s^{-1}$ [42,43]. The operating speed and resolution of the camera are dependent on the parameters being extracted and the inbound speed [11,27,28]. It is common that only one high speed camera is used to record video of an impact between a football and a surface. A second camera placed at a stereo angle, allows depth to be measured, which can only be perceived using a single camera. Introducing a second camera minimises camera alignment and parallax errors. An appropriate calibration technique, lighting and camera orientation must be chosen to achieve accurate measurements [44].

A camera calibration is performed to calculate extrinsic (dependant on; camera location and orientation) and intrinsic parameters (dependant on; focal length, field of view, resolution etc) to reconstruct world coordinates from image coordinates to a calculated error. During calibration a set of controlled points are taken to calculate the parameters, that describe the translation from a 3D co-ordinate from object space to a 2D image plane, as shown in Figure 9.

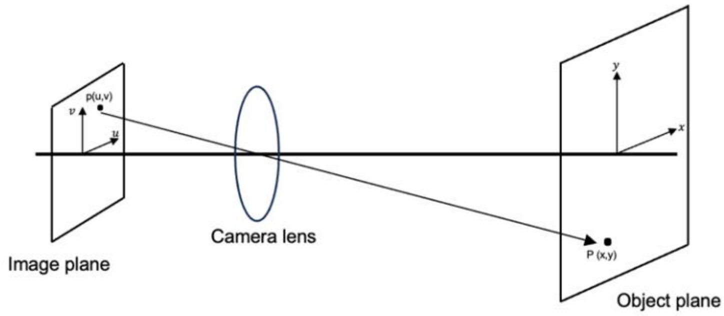

Figure 9 A diagram showing the translation between two reference planes, the image plane, and the object plane.

The error is influenced by the quality of the calibration and the method used. Common methods for calibration include direct linear transform (DLT) and checkerboard planar reconstruction. The two methods are summarised below:

- DLT establishes a relationship between known 3D coordinates of points and their corresponding positions in 2D images, captured by a camera. A system of linear equations are solved to compute the transformation matrix [45].

- Checkerboard planar reconstruction uses known checkerboard patterns with defined dimensions to perform calibration or reconstruction. The translation matrix consists of both rotational and tangential distortions [46,47].

Checkerboard planar reconstruction is the preferred method due to its enhanced accuracy in reconstructing both extrinsic and intrinsic camera parameters compared to other calibration techniques [46]. This technique can be used to calibrate 2D (single camera) and 3D (two or more cameras) environments. Checkerboards can be manufactured to the appropriate size to accurately calibrate different volumes, offering a flexible and cheap method. The checkerboard calibration process can be performed using commercial or bespoke software packages. Check2D[48] and Check3D [49] are software packages developed at Sheffield Hallam University that calculate the intrinsic and extrinsic parameters of a single (2D) or two synchronised (3D) cameras. The software uses the planar calibration technique from the OpenCV function library.

The following variables can be calculated by digitising high-speed video frames:

1. COR
2. Contact Time (T)
3. Contact length (l) and ball deformation (δ_b)

The measurements for contact length and deformation in reference to a football are shown in Figure 10.

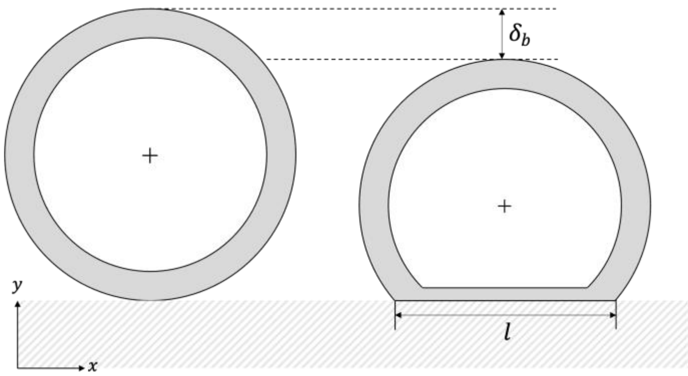

Figure 10 A diagram explaining the measurements of deformation and contact length for a football impacting a rigid surface (hatched rectangle).

During an impact between a football and a surface, the football is compressed by the initial collision until it is momentarily brought to rest. Occurring within milliseconds, the football reasserts its original shape due to the elasticity of the structure and rebounds. However, the height of rebound will not equal the initial drop height due to energy losses occurring across the system as the original shape of the ball is regained [50]

The COR can be calculated as a ratio between the outbound to inbound velocity or between the rebound height and initial drop height. It characterises the energy loss during the impact and is dependent on the properties of both the football and impacting surface [32]. If the impacting surface is rigid (e.g., a slab of concrete), the COR is a sole measure of the football's elastic properties [51]. Homes et al [33] noted difficulty isolating the influence of internal air pressure on rebound height during a normal inbound impact with a natural turf surface due to the mechanical variability of the surface layer. Similar difficulty also occurs when attempting to identify the separation point between a playing boot and the football [52].

In the FIFA rebound test, the COR is determined using the height ratio, with acceptable values ranging from 0.63 to 0.78 for an impact at approximately 6 $m \cdot s^{-1}$. It is widely acknowledged that the COR decreases with increasing inbound velocity during an impact between a football and a rigid surface, with the decrease significantly influenced by the viscoelastic properties of the football. A football can experience a decrease of 0.2 in COR across a 30 $m \cdot s^{-1}$ range [11]. It appears possible to achieve the same COR with balls of different stiffness, suggesting the COR is more influenced by the elastic properties than the stiffness [32,51]. Homes and Bell increased the global stiffness of a football by increasing the internal pressure [53]. In the stress-strain curve, stiffness is represented by the slope of the curve. As pressure increases, the material of the ball's surface is placed under greater tension, that can cause the polymers to move to a steeper part of the curve, indicating that they can withstand higher stress for a given amount of strain. In this higher region of the curve, the material is in a higher energy state which allows the ball to store more energy during the deformation, that means when the ball impacts a surface, it can rebound more efficiently, to a higher height, and thus lower energy is loss during the collision. However, the difference among material composition of the football's was observed to influence the change in rebound height almost three times more than solely increasing the internal air pressure.

Wiart [35] induced a change in the material properties of a football using temperature. When conditioned to the higher temperature (40 °C), the stiffness of the football reduced and experienced more deformation and a longer contact time, but exhibited a higher COR, suggesting a more elastic collision.

The contact time has previously been measured using high-speed video, a force platform or using an electrical circuit [54]. It has been defined using three methods; the time taken for the visual contact between the football and surface, the time over which the impact force acts or as the time taken for the centre-of-mass (COM) displacement to return to zero. For an impact between a football and a rigid surface the value will typically vary between 7 to 10 ms and it is well acknowledged that the contact time decreases with increasing inbound velocity. The contact time is typically an inverse function of structural stiffness; a longer contact time is associated with a lower stiffness.

The change of shape of a ball in impact studies has been characterised using measurements of deformation, contact length and contact area. In the case of table tennis balls [55,56], the shape of the contact area was determined by impacting the ball on a glass surface and observing the resulting impression using a high-speed camera placed below the surface. The ball was observed to buckle across consecutive image frames and adopted a circular-ring shaped contact area once a critical level of deformation was reached. Unlike footballs, table tennis balls derive most of their structural stiffness from the shell material rather than the internal pressure. Price observed a decrease in stress and strain at the centre of a football at maximum deformation in a computational model [11], but there is no evidence determined experimentally to confirm that a football will buckle during the contact with a flat rigid surface. Johnson [54] measured the contact area of a football using a thin layer of chalk covering the impact surface, but only provided a single measurement of the area, without indicating the shape or providing conclusive evidence of buckling. To avoid assumptions of the contact shape influencing the measurements, the change of shape of a football has been quantified using the vertical and lateral deformation using a single camera directed towards the impact area. Typically, these measurements have been used to validate computational models for footballs. However, for a tennis ball a polynomial relationship was developed between deformation and contact length for the compression phase [28]. The relationship was used in a viscoelastic model to allow the damping properties of the ball to vary during the impact.

2.5.4 Impact variables measured using force platforms.

A single [57] or a multi component force platform [39,58,59] has previously been used in conjunction with apparatus to measure inbound and outbound ball velocity. In many biomechanical applications, force data acquisition and image capture have been synchronised [60-63], but systematic errors including time lag and drift must be quantified prior to data collection [64]. Piezo-electric force platforms have typically been preferred to analyse sports ball impacts over strain-gauge force platforms due to their high stiffness relative to the ball, resulting in rapid response times [65].

The first commercially available force platform was introduced by Kistler in 1969, using the piezoelectric principle that quickly established itself as the global benchmark for force measurement. In 1976, Advanced Measuring Technology Incorporated (AMTI) introduced a strain-gauge platform that provided larger surface areas at more affordable prices. Both these commercial force platforms continue to dominant the market and use in research [66].

Commercially available force platforms are available in a variety of sizes and construction types. Systems that have been used in football research include the Kistler 9281E [58,59] , 9287CA [67] and PASCO [39]. The force platform must have sufficient area to ensure the football does not exceed the edge at maximum deformation. An example of a force platform that has been used in football research to measure the ground reaction force is the Kistler 9281 [59], this platform has dimensions of 600 mm x 400 mm x 100 mm, weighs 16 kg and can measure forces in the vertical direction up to 20 kN [68]. This platform is an example of a multicomponent force platform that makes use of four measuring elements to measure the reaction force. For an interaction between a force platform and an object, the force platform can measure six variables in an axis system shown in Figure 11. These include:

1. F_x, F_y, F_z reaction forces in each coordinate axes.

2. Ax, Az coordinates to identify the centre of pressure.

3. My The free moment about the vertical axis.

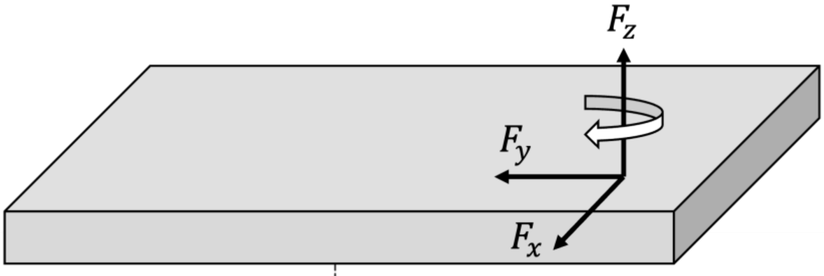

Figure 11 The axis system for a multi-component force platform

A single measurement element is contained in each of the four corners, illustrated in Figure 12. For a Kistler system, these will use the piezo-electric principle to measure the force. The elements contain quartz rings that are mounted between two steel plates in the housing of the sensor. The quartz crystals generate an electrical charge when a force is applied. A total of 12 individual reaction forces are produced by the four measuring elements that are summed to give the overall forces (F_x, F_y, F_z) using Equations 2-1 to 2-3:

$$F_x = F_{x1} + F_{x2} + F_{x3} + F_{x4} \quad \text{2-1}$$

$$F_y = F_{y1} + F_{y2} + F_{y3} + F_{y4} \quad \text{2-2}$$

$$F_z = F_{z1} + F_{z2} + F_{z3} + F_{z4} \quad \text{2-3}$$

These systems can determine the magnitude of forces to much better accuracy than the point of application of the force. Manufacturers of piezoelectric force platforms report errors of below 2% for the magnitude of the force but errors of up to ± 30 mm have been reported in determining the point of force application [69,70]. While correction formulas can be applied, the error is suggested to arise from bending moments in the supporting posts of the force platform [70].

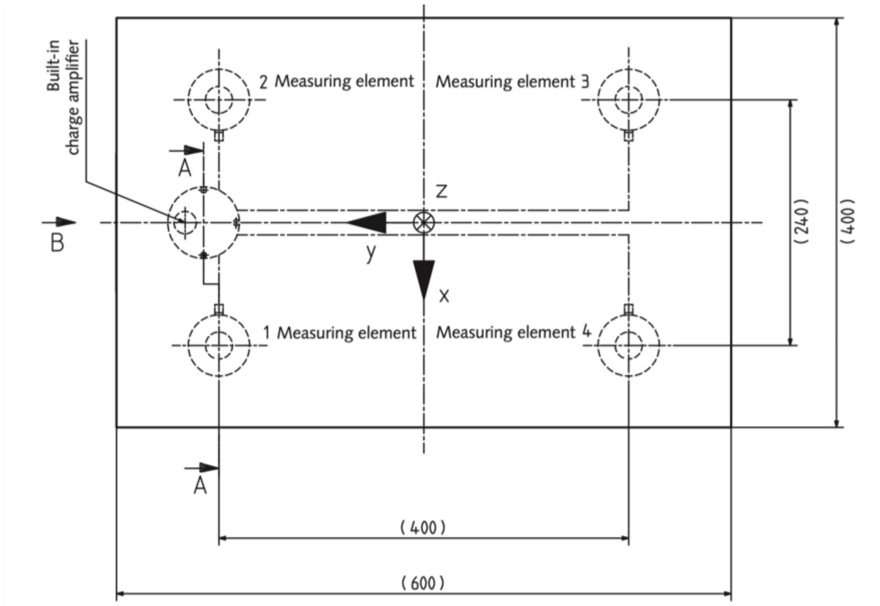

Figure 12 Engineering drawing of the internal arrangement of measurement elements for a Kistler 9281E platform [68]. The elements are contained in each of the four corners.

Force platforms can be used to measure the loading behaviour of a ball throughout impact [34] to allow calculation of discrete loading metrics (e.g., peak impact force, impulse, contact time) as well as calculation of the COM displacement from integration of the force-time plot. The measuring elements are constructed to be sensitive to force in each axis, however they can be highly sensitive to the environment e.g. vibration transmission, so authors have used both stationary and dynamic approaches to validate the accuracy of systems [66,70-72]. Commercial systems designed for biomechanics applications tend to have a low natural frequency ($f < 500$ Hz) as the contact period is larger for human contacts (stance phase for walking is typically between 0.6 and 0.8 s) compared to ball impacts. These systems can suffer from resonant behaviour due to the short contact time of a football impact (typically below 10 ms) relative to the system's natural frequency [73]. This behaviour can be observed in the force-time history where unwanted fluctuations are present in the output that led to inaccuracies.

The sampling frequency is an important input parameter in force platform set ups to avoid information loss during the measurement. The Nyquist frequency specifies the minimum sampling rate that is required to accurately reproduce a discrete-time signal free from aliasing. It is evaluated as one half of the sample period. For example, for an impact of 8 ms (equivalent to a normal inbound impact of a football at 19 $m \cdot s^{-1}$) the Nyquist frequency would be 62.5 Hz. Many biomechanical studies would recommend a sample frequency at least twice this value with many choosing to operate 5-10 times of the frequency of interest, evaluated using the period of the contact [74]. For an 8 ms impact this would be between 625 – 1250 Hz.

In football research, the force-time profile has generally been used to compare discrete values of force or to validate modelling procedures rather than to compare the loading behaviour between different footballs. Koizumi [38] used a force platform to compare a single value of peak impact force for a normal inbound impact between different football models, but do not present any evidence to quantify the reliability or repeatability of the system for this application. In other work, the force-time profile has been used to validate computational and mathematical models.

To have confidence in the output measures and comparisons the repeatability of a force platform system must be assessed, common in biomechanical publications but not presented in any research measuring football impacts. Hori [75] evaluated the repeatability of a force platform (unspecified model) using statistics including the intra-class correlation coefficient and coefficient of variation. Whereas Gudavalli [76] used descriptive statistics including the mean and standard deviation. Discrete-time signals were down sampled in both studies using interpolation. Both authors found measurements associated with time (e.g. time to peak force) were more influenced by sampling frequency than measures of magnitude (e.g. peak force). Guadavill observed greater standard deviations at lower sample frequencies for all measures and highlighted although accuracy was not substantially reduced at lower sample frequencies, the increased standard deviation might have a greater influence on the overall accuracy with small sample sizes.

Outside of football, several authors have used the force and COM displacement to calculate a measure of dynamic stiffness from a normal impact between a ball and a piezo-electric load cell. Whilst static compression tests are used to characterise the overall structural properties of a ball, the magnitude of stiffness from these tests is smaller than in an impact. Smith [77] assumed a softball exhibited linear elastic behaviour during an impact. A single measure of dynamic stiffness was calculated by equating the kinetic energy before the impact with the potential energy at the maximum deformation. However, as discussed earlier, visco-elastic objects do not solely obey Hooke's Law and violate this assumption. Collins [24] speculated a single measure could not be used to evaluate the response of a ball. They observed non-linear behaviour for a solid hurling balls (polymer and cork filled) ball during the compression phase of the force-displacement curve. Two measures were obtained by fitting two first-order polynomial trend lines to the loading curve, as shown in Figure 13. Using this method, the authors revealed differences in impact behaviour between hurling balls of different constructions which were not apparent from rigid-body COR values. Ball constructions containing a greater percentage of polymeric material exhibited greater strain-rate dependencies, indicated by a larger increase in initial stiffness over an approximate 25 $m \cdot s^{-1}$ speed range than traditional cork-yarn constructions.

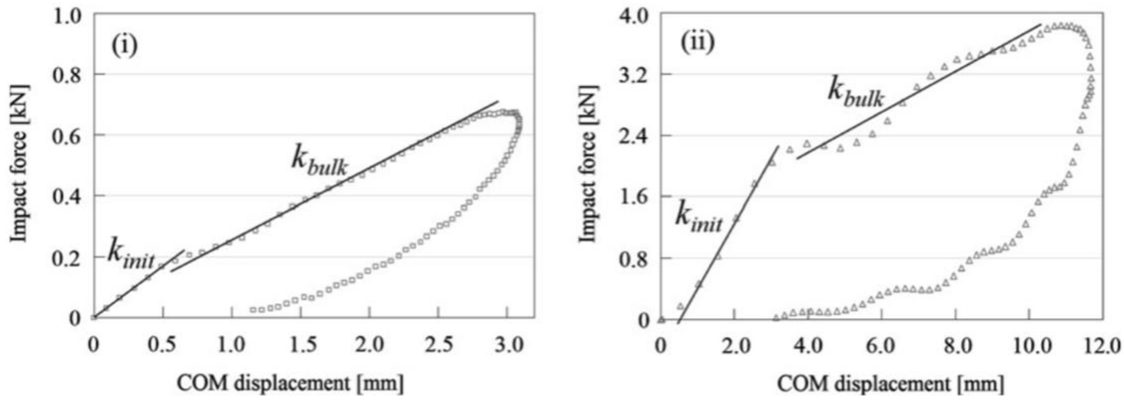

Figure 13 The stiffness of a solid hurling ball was quantified during 2 measurements obtained by fitting two-force order polynomial trend lines to the loading behaviour captured using a force platform at 5 and 25 $m \cdot s^{-1}$. Graphs presented in [24]

Errors can arise in data derived from a digital signal due to inappropriate data processing (e.g. filtering). The impact of a football on a force platform results in a sudden transition from low- to high-frequency components that can have oscillations present in the digital signal. The sudden transition can be minimised by operating at high sampling frequencies or by filtering the signal. Higher sample frequencies capture more data points in a given time, providing a smoother and more accurate representation of rapid changes that occur during a footballs impact. Filtering can be applied to raw data to minimise the amplification of high frequency noise to improve calculations that are performed on the original signal. A comparison of a filtered and non-filtered signal for an in-step kick of a football is shown in Figure 14. However, it is not always necessary and can compromise features of the original signal (e.g., elongating signal or underestimating peak values). For the case of a forehand swing in tennis, Knudson [78] noted that the filtering technique used to smooth velocity data accounted for a large percentage (49 %) of the variance observed between players. Digital low-pass filtering (e.g. Butterworth 4th order) is a common filtering technique used to filter impact data in biomechanics. The cut-off frequency in a low pass filter dictates the frequency above which signal components will be filtered, whilst any components below this will pass through. Cut-off frequencies in biomechanical application have been found using residual analysis [66,79].

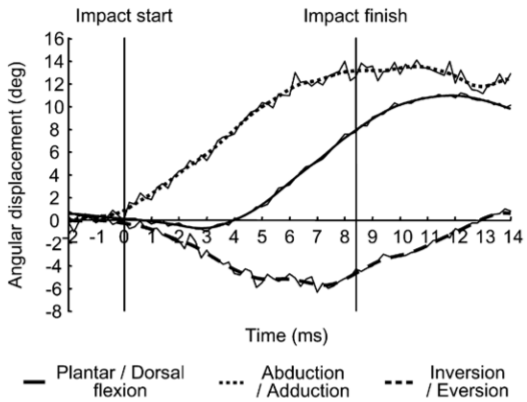

Figure 14 The filtering of data in Shinkai [41], smooths the noise the loading curve obtained from an in-step kick of a football. The raw signal is shown by the solid lines, the filtered signal is shown by dotted or dashed lines.

Iga [36] applied a filter on ball-impact data that was introduced for analysis of limb movement to smooth raw force time data. In the biomechanical study, Shinkai [41] applied a 4th order Butterworth filter with cut-off frequency of 350 Hz to filter velocity data with added padding points. This data was derived from raw displacements acquired using computer vision to give coordinates of markers located on the foot, leg and football. As first presented by G Smith [80], padding points were added using reflection to minimise distortion errors and give better agreement between filtered and raw data. Nunome [81] notes adding padding points does not eliminate the effect of phase distortion and other algorithms may need to be considered to remove noise. Many authors note distortion of kinematic data before and after the impact. Iga did not present any consideration of residuals between features of the raw and filtered data, so it remains unclear whether a filter is necessary and transferable between the biomechanical study by

Shinkai and force platform impact studies. Other studies involving the impact of a football on a force platform either make no reference to filtering or explicitly state no filtering was performed [58].

2.5.5 Section Summary

High-speed video has been the preferred method to measure impact variables that characterise the dynamic impact response of a football. By analysing the footage frame by frame, accurate measurements of the coefficient of restitution, contact time and deformation can be obtained using automated or manual digitisation. Research has shown the viscoelastic properties of the football will influence its impact behaviour; with increasing velocity, the COR and contact time will decrease, and the deformation will increase. Force platforms can be used to measure the loading behaviour of a football during impact; however, their use has mainly been limited to comparing maximums or to validate mathematical or computational models, rather than to compare the loading behaviour of footballs. Consideration must be made to ensure the technical specification of commercially available force platforms is suitable for the challenges that are posed by the short duration impact of a football that tends to fall between 7 to 10 ms. Filtering the output signal of the force platform for impacts with a football may not be necessary, as these impacts typically exhibit a relatively consistent force profile with minimal high-frequency components. This is unlike other dynamic events such as kicking, where rapid changes occur. Therefore, filtering could potentially distort the accurate representation of the impact.

2.6 Mathematical Modelling in Impact Analysis

A football can be considered a flexible thin-walled pressurised sphere that exhibits distinct impact behaviour compared to that of a stiff thin-walled sphere (e.g. a table tennis ball) or a solid sphere (e.g. a ball bearing). This difference will stem from the structural compliance and material properties of the football. A football will deform significant upon impact and will dissipate energy during impact that will influence the rebound characteristics.

Previous approaches to modelling the impact behaviour of a football have varied in complexity, accuracy, and computational requirements. These methods encompass fundamental physics principles, computational models and empirical models that reply on experimental data to predict impact outcomes. The following section critically evaluates relevant modelling techniques employed in studying the impact behaviour of a football or other viscoelastic sports balls.

2.6.1 Mechanisms of Impact

Prior to attempting to understand the components contributing to a football's behaviour in a dynamic impact, the mechanisms of impact must be considered. It is important to gain an understanding of the sequence of events that occur during an impact (shown in Figure 15) to recognise modelling techniques that have suitable assumptions that could be used to represent a football impact.

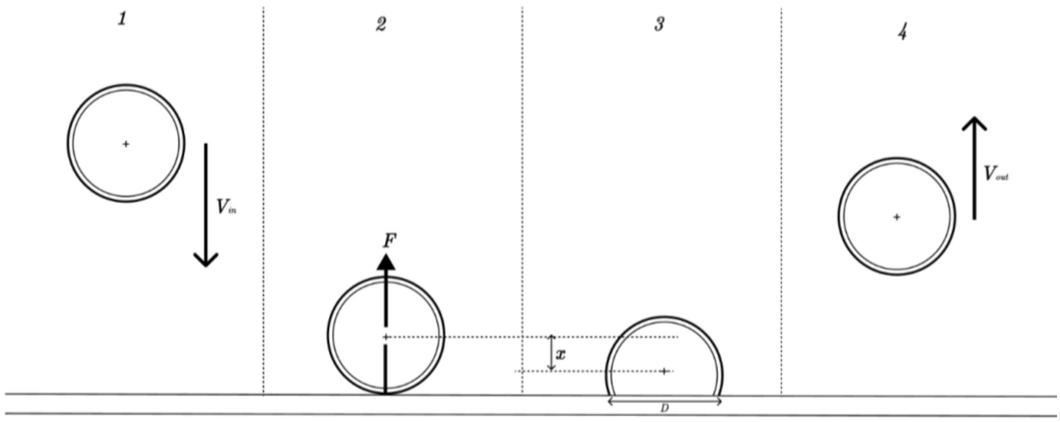

Figure 15 Sequence of events during a football impact with a surface.

For a normal impact, the football will approach a surface perpendicularly at a maximum inbound velocity (1), with motion occurring in a single cartesian direction. During the compression phase, a proportion of the football that was moving towards the surface must be brought to rest. The impact will generate a contact force applied at the bottom of the football (2), opposing the direction of motion causing the football to deform (3). The geometry is that of a sphere intersecting a plane. The shape of deformation will be dependent on the inbound velocity, the material composition of the impacting bodies [82] and the orientation of the football caused by material anisotropy [43]. As the impact speed is increased and the ball deforms to greater levels, the reduction of tension in the flattened part of the ball can permit sideways expansion, that leads to an increase in contact area [83,84]. Figure 16 shows the shape of a football captured using high-speed video for an impact at (b) 6 m·s^{-1} and (c) 20 m·s^{-1}. It could be assumed due to the axisymmetric shape of the football; the shape would be uniform in three-dimensions. The deviation of spherical shape will cause the volume inside of the football to decrease. In accordance with Boyle’s law, when assuming a negligible change in temperature, the internal pressure must increase. The deformation will alter the position of the centre of mass (COM). The COM will displace towards the surface until it reaches a maximum displacement, and the football is momentarily brought to rest.

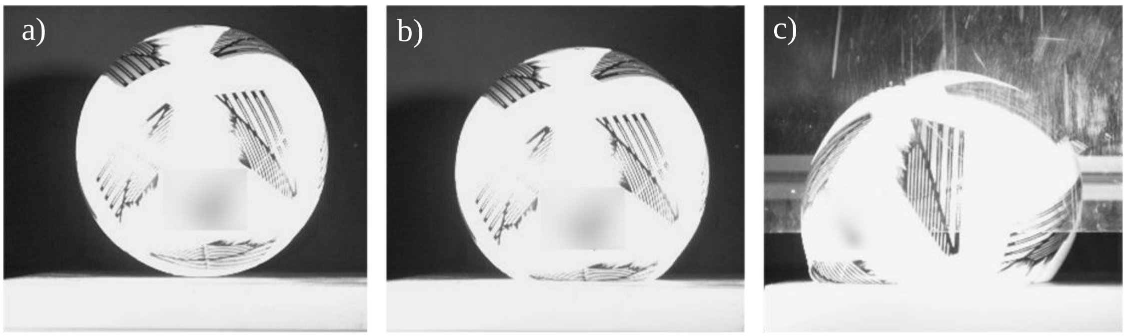

Figure 16 Shape of the football at (a) first contact, (b) the shape of a sphere intersecting a plane encountered at maximum deformation for a 6 m·s^{-1} collision and (c) maximum deformation showing sideways expansion and increased contact area of the football at 20 m·s^{-1}.

As a result of the deformation, energy is stored within the material of the football in the form of strain energy. A restoring force will cause the football to rebound, and it will continue to accelerate until separated from the surface (4). The rebound direction should be coincident with the inbound direction. However, often the orientation and valve position of the football with respect to the surface, can cause the rebounding football to become elongated [11]. This is caused by different portions of the football accelerating away from the surface at different times. The energy returned to the football will not equal the energy stored, some energy losses will occur, causing the outgoing velocity to be lower than the inbound velocity.

Mechanisms of Energy Loss

The energy returned to the football will not equal the energy stored, some energy losses will occur, causing the outgoing velocity to be lower than the inbound velocity. The degree of inelasticity is usually quantified in empirical parameters such as the COR. Bayman [85] described the formation of acoustic waves at the contact point when two solid objects collide. The deformation of the two objects in contact are associated with the propagation of these transverse waves through the objects and their reflection from the surfaces.

Bridge [84] described the formation of surface waves as a source of energy loss for an air-filled ball impacting a flat surface. These waves travel progressively up and down the ball and govern the response of a ball during an impact. The velocity of the transverse waves is governed by the material density and surface tension in the shell material that arises from the internal air pressure. The damping of these waves will contribute to a source of energy loss. Falcon [86] similarly noted the formulation of surface and volume waves that radiated into an inelastic ball as a source of energy loss. However, the author suggested the most significant dissipation of energy emerged from the viscoelastic properties of the ball in comparison to the damping of surface waves and energy loss due to plastic deformation. Another source of energy loss is the friction between the football and impacting surface during the sideways expansion.

2.6.2 Mathematical Models

There have been several different approaches used to model the impact of a ball. These approaches vary in complexity, the assumptions of the model, and predictive capability. In the next section, different mathematical approaches will be discussed.

a) Analytical Modelling

Rigid body analysis is one of the simplest modelling techniques to analyse an impact between a spherical ball and a surface [50]. The motion of the ball is described by

Newtonian mechanics; the ball and surface are assumed to be perfectly rigid and undergo no deformation upon impact, regardless of magnitude. A further assumption is that there is no energy dissipation during the impact, implying that the sum of the kinetic and potential energies are conserved throughout the impact. In real-world situations, especially for a football with deformable materials, this type of analysis may not predict the behaviour accurately. This has been the case for a tennis [22,28,57] and cricket ball [87], that found large disagreements between the experimental and mathematical predictions arising from the assumption that the ball was a solid rigid sphere. Both Daish [50] and James [88,89] noted that the deformation of the impact surface had the effect of rebounding the cricket ball at a steeper angle during an oblique impact than would have been predicted using a Newtonian model.

Analytical equations have been used to describe the behaviour of a spherical shell with internally pressurised core during an impact with a flat surface. These approaches follow the assumptions of flexible body analysis that considers the deformation and flexibility of the sphere during an impact. The assumed profile of the deformed shell is a truncated sphere with no lateral expansion [55].

One of the first examples of a theoretical approach being used to investigate the impact behaviour of a football was performed by Johnson [54]. This approach assumed the football to have negligible flexural stiffness. Equations were developed to describe the relationship between the contact area at maximum deformation and contact time with respect to inbound velocity. Two instances of the internal air pressure were considered to observe the significance of air compressibility; one assuming a constant pressure and one that allowed the pressure to vary adiabatically. The downward acceleration of the football during impact was guided by the motion of the particles in the outer shell of the football, not in contact with the surface. The contact time was attained by assuming the motion of the football was simple harmonic. The area of contact was assumed to be a circular imprint. The theoretical predictions consistently overestimated the contact area due to the neglection of all sources of energy loss.

Hubbard and Stronge [55] also used this approach to describe the behaviour of a table tennis ball bouncing on a flat surface. The stiffness of the ball was described by individual components of the thin-walled spherical shell and an internally pressurised core. This enabled calculation of the deformation and contact forces experienced during impact. The model only accounted for energy losses that arose due to the instantaneous rate of change of momentum of the material shell during impact with the surface. All other mechanisms of energy loss such that arose due to material viscoelasticity effects or due to friction in the contact area were neglected. Ignoring material strain-rate sensitivity in the analytical model led to substantially lower energy losses than in reality. The authors observed a non-linear relationship in the pressure component of the impact force. They noted at larger velocities, the differential of the peak force was largely attributed to the internal gas resisting compression rather than due to lateral expansion of the material shell. In both instances, Johnson and Hubbard [54,55] concluded that the increase in internal pressure during the contact was an important factor in contact behaviour.

More recent mathematical approaches to calculate the impact force using Newtonian physics for an impact between a football and flat surface have used theory based on the displacement of the footballs centre and Hertz contact theory. Shinkai [41] presented the theory that considered the displacement of the geometric centre and centre of gravity. This was later improved by Iga et al [59] to account for the change in surface area and deformation shape of the football during impact. Ishii et al [90] presented the approach using hertz contact theory. Iga acquired experimental data using a force platform to be able to assess the appropriateness of each models' assumptions, as many of the initial models were not validated against a reference force.

The Hertz theory of contact forces is primarily used in the field of contact mechanics to analyse the interaction between two elastic spherical bodies. While this does not perfectly represent the shapes of the interacting bodies, the theory has been used in ball-impact analysis. The theory of contact force is governed by Equation 2-4, where the force between the contact point is proportional to the deformation of the sphere to the power of 3/2. The force is also dependant on the radii of contact, the elastic modulus, and poisons ration of the two contacting bodies.

$$|F_b| = \frac{mV_{b1}}{\int_0^T \delta_b^{\frac{3}{2}} dt} \delta_b^{\frac{3}{2}} \qquad 2\text{-}4$$

This approach has been used to calculate the contact forces for a side-step football kick [91] and for a normal inbound impact between a football and a rigid surface [59]. However, this theory neglects any form of damping or energy loss, which might explain why it proves inaccurate for hollow rubber spheres undergoing significant deformation between two steel plates. The theory consistently overpredicted the forces involved in the impact between a football and a surface, where it exhibited a delay in reaching the peak force compared to the experimental results. These findings suggest the simplifications of the calculations may limit the accuracy, especially for impacts with higher ball deformations.

Shinkai [41] proposed two models to examine the interaction between a single football and a foot during an instep kick. The contact with the foot was modelled as a flat plane, essentially mimicking an impact with a flat surface. In the models, points along the circumference were used to estimate the displacement of the geometric centre of the football. The second approach divided the football into two parts using ball deformation data obtained using high-speed video. The displacements were used to calculate the velocity of the respective central point and Newtons law of motion was applied to calculate the force. When the computations were compared to a reference experimental force, both models exhibited different force curves to the reference and the peak impact force was overestimated at 5 velocities between 9 to 19 $m \cdot s^{-1}$, that became more severe as the velocity increased. Iga [59] further refined the model proposed by Shinkai, to account for the change in surface area throughout the impact and incorporate the experimental observations from analysis of high-speed video of the football to allow the shape to deviate from spherical into a spheroid shape at higher impact velocities. These additional considerations gave more representative estimates of the centre of gravity that led to more comparable relations with the reference force. The findings demonstrated the importance of the assumptions related to the deformation shape of the football. However, as the reference force was only obtained for one football, its uncertain whether the accuracies of these models extend to other footballs made of different constructions, as no study to date has compared the loading curves of multiple footballs. The calculation of force used displacement of the centroid position that was defined from reference points on the football's circumference obtained using high-speed video which omits any consideration for the properties of the football.

b) Material Viscoelasticity Models

In the previous section, model predictions often deviated from experimental results due to the neglection of material viscoelasticity. In these examples, simplification to the model assumptions has led to the overprediction of contact forces, contact area and poor correlation with contact time.

Visco-elastic modelling allows increased versatility compared to the previous models. The values of the stiffness and damping are associated with the material construction of the ball and can be defined as a function of any number of parameters. The modelling approach uses springs to represent the stiffness and dashpot dampers to simulate energy loss. Previous researchers have used a single discrete model to describe the behaviour of ball against a rigid surface. However, increased complexity can be achieved by combining discrete models in series to describe the deformation of a surface. The model is governed by Equation 2-5.

$$m\ddot{x} + c\dot{x} + kx = 0 \quad \text{2-5}$$

Dignall [27] proposed a one degree of freedom model to simulate a normal impact between a tennis ball and surface. Three model components defined the ball behaviour: structural stiffness, material damping and an impulsive reaction force term. The relevant parameters were determined by a combination of quasi-static compression testing and simple dynamic experiments. The model was extended to racket impacts by Goodwill [28] and refined to accommodate for the dependence of the tennis balls structural stiffness and damping on the position of the ball's centre of geometry throughout impact. The structural stiffness parameter was modified to account for the buckling of the shell within the first 0.2 ms of impact, as observed by Cross [57]. An additional damper was included to define the momentum flux that described the impulsive force caused by the material being brought to rest during the compression phase of impact, as previously noted by Hubbard [55]. The model predictions of force showed good agreement with experimental force platform measurements between 13-30 $m \cdot s^{-1}$. For other speeds, the model and experimental values of COR were artificially tuned to agree by determining the relevant level of damping. This approach was used by Goodwill to show the differences in impact behaviour among four different types of tennis balls, each with categorical differences (e.g. Pressurised, pressure-less, oversized and punctured). A single value for the stiffness and damping parameter was derived for each ball type and was used to explain the impact characteristics of each ball. However, in football categorical differences do not exist between the footballs used in professional competitions (FIFA-certified, size 5). It remains uncertain whether this modelling approach could effectively reveal potential similarities or differences in impact behaviour between these footballs. It's possible that certain weaker correlations observed by Goodwill, arising from simplifications in the modelling process, might become more pronounced when applied to a football due to the large volume of material and pressure displaced during an impact.

Christenson et al [92] developed a discrete lumped mass numerical model for the contact football and foot to examine the influence on the impact behaviour of a football. The football was modelled by a single value of stiffness and damping. The stiffness was calculated as a product of the internal air pressure and circumference, as noted in Babbs [93]. The damping was solely dependent on the COR of the football from a rebound test at 3 m, as noted by Nagurka [94]. The model showed general trends for the influence of the internal pressure of an inflated sphere on the impact variables. The findings showed outbound velocity increase, contact time decreased and impact force increase with internal pressure between 0.1 and 1.1 bar. However, the model had no numerical validation. The oversimplifications during the calculation of properties of the football, neglected the influence of construction on the impact behaviour.

c) Computational models

Finite Element Analysis (FEA) is a computational approach to approximate solutions of physical problems involving complex geometries arising across a range of engineering disciplines [95]. FEA involves discretizing a domain, such as a football, into a large number of finite elements. The material properties and external forces acting on the physical body are defined within the software. The behaviour of each element is described using partial differential equations. The computer solves the equations with known boundary conditions using the finite difference method to predict the behaviour of each element, before summing the individual behaviours to predict the behaviour of the complete physical body.

Price, in collaboration with a single equipment provider, conducted a comprehensive investigation into football impact dynamics, which is arguably one of the most extensive studies in the field [11]. The research focussed on optimising the carcass layer for consistent rebound behaviour and encompassed several key aspects; (1) material characterisation using tensile testing, impact testing and computational modelling of two world cup footballs. A series of tensile tests were carried out on the bladder and outer-panelling materials to define material models used in FEA. Impact testing was conducted to measure quantitative data to verify the computational model using impact variables including the COR, contact time and deformation. Additional behaviour was observed during extensive experimental tests including the influence of inbound speed and impact orientation on the impact variables. The computational model was artificially tuned to match experimental results and showed good agreement with the deformation shapes and impact variables obtained experimentally. The model provided insight into the view underneath the football surface and suggested occurrences of buckling, but this behaviour was not experimentally verified. The model facilitated the measurement of strain distributions across the panels of the football. The combination of experimental investigation and computational modelling is one of the first instances where the non-uniform deformation characteristics of a football during an impact were identified, these were attributed to the panel material anisotropy and presence of the stiffer skeletal effects of the seams. During high-speed impacts, the arrangement of the panels relative to the plane of hoop strain was observed to significantly influence the level of deformation. This finding may suggest factors including panel structure and seam length may explain some of the variation in the magnitude of deformation among different footballs. A limitation of this work is that no additional impact variables other than those the model was tuned to match were used to validate the model. An additional impact variable commonly used to validate both mathematical and computational models is impact force.

The primary objective of the work conducted by Taha [37] was to validate a computational model of a football using force measurements. The study aimed to further utilise computational modelling to explore ball-to-head impacts. To achieve this, material properties were acquired from Price's work and revalidated by comparing forces between 10 to 30 $m \cdot s^{-1}$. This was achieved by extrapolating a single value of peak impact force obtained between speeds 3.1 to 6.7 $m \cdot s^{-1}$using linear regression. As with Price, the stiffness proportional damping coefficient was specifically tuned to ensure alignment with experimental data of COR, contact time and deformation. The computational model was found to predict forces with 4% agreement to experimental force data. This finding underlined the reliability of the computational predictions when compared to extrapolated force data.

The overarching aim of the work by Rezaei [58] was to extend the application of a computational model of a football for oblique impacts. The validated model was then used to explore the influence of the coefficient of friction (COF) of the surface on the football impact. As with Taha, to develop the computational model, the material properties obtained were obtained from Price's research. Validation was carried out by obtained experimental data for an oblique impact at approximately the same impact speed (19.1 vs 18.1 $m \cdot s^{-1}$) at two distinct impact angles: 30° and 23° and with top and back-spin applied at approximately the same spin rate (60 vs 58 $rad \cdot s^{-1}$). The validation data included COR, contact time, deformation, and impact force. As observed for oblique impacts in other ball sports, significant changes in rebound angle were found for instances with initial spin [96,97]. The simulations illustrated that variations in the COF of the surface directly influenced the impact behaviour of the football, as has also been studied in golf [98]. Beyond a certain threshold, alterations in the COF significantly affected the rebound velocity and angle, indicating behaviour changes during the contact phase between the football and the surface [99-101].

d) Statistical models

Statistical models encompass various techniques that are used to analyse data and infer relationships between variables. Previous approaches used to analyse the impact dynamics of a football include linear regression and factor analysis derived from principal component analysis. These models are driven by empirical data, so whilst requiring extensive experimental input, have the capacity to identify relationships in datasets with very high dimensionality. They are adaptable to variations within the data, particularly relevant to analyse football impacts where variation in impact behaviour can arise due to uncontrollable variation within the experiment design. Whilst the modelling techniques discussed above in sections a) to c) solely evaluate the performance of the model itself, statistical models can be used to monitor the effect of changes in individual parameters on the outcome of the response or prediction model to provide insight into the mechanisms governing the behaviour of a ball during a collision.

Multivariable regression analysis is an extension of simple single-variable regression, to the situation where multiple independent variables are considered to comprehend their combined impact on an outcome or response variable. This approach enables the assessment of the interactive effects among two or more independent variables [102]. Wiart [35] investigated the relationship between the temperature condition and the change in impact variables such as the COR, contact time and deformation for a size 5 football. The research employed a stepwise multiple linear regression to ascertain whether changes in normal inbound velocity and temperature had an observable effect on these impact variables. A significance level of 0.05 was used. The study revealed a direct positive relationship between temperature and the impact metrics. These findings aligned with previous observations for the effect of temperature on the impact behaviour of a ball [83,103-105]. When both variables were considered in the multivariable model, they significantly influenced the impact behaviour of the football. The models coefficient of determination demonstrated high values for COR (R^2=0.88), contact time (R^2=0.93) and deformation (R^2=0.93). The relationships were used to simulate a shot on goal and illustrated that higher temperatures could reduce the reaction time for a goalkeeper, implying potential implications for match scenarios in elevated temperature conditions.

When multiple independent variables are used, the validation of a relationship cannot be visually compared, additional statistical tools must be employed to assess the performance and applicability to new datasets. The performance of model can be evaluated using metrics such as the coefficient of determination (R^2) and the root-mean square error (RMSE) that calculate the discrepancy between predictions and experiment data. These metrics have been employed by Choppin [106] to assess a second-order polynomial multivariable regression model. The model investigated the relationship between five independent variables that described the interaction between a tennis ball and the racket on the outbound velocity of the tennis ball. The ability of the model to generalise to new datasets is often investigated by employing a cross-validation procedure. This involves portioning the available dataset into multiple folds. By evaluating the model's performance on multiple validation sets, cross-validation helps to detect overfitting.

Exploratory factor analysis aims to identify the fundamental factors that contribute to variation within a dataset. Smith [107] explored the inter-relationships among 3D biomechanical variables involved in the kicking action of a football. Kinematic variables describing the position of body segments and joint angles were measured from video captured in a laboratory environment of 20 mixed-sex participants performing a right-footed lofted instep kick. Exploratory factor analysis was employed to reveal the underlying relationships or latent factors among the observed factors. The knowledge of these associations among movement patterns has potential benefit to enhance a player's technique and improve the feedback from a coach by avoiding assumptions related to these inter-relationships. Interpretation of the factors provided practical insight into the complexities of the movement; the factors extracted accounted for 67% of the variance in kicking distance. The inter-relationships uncovered by the analysis can be used to indicate how aspects of the kick may be influenced by a coach's intervention and whether increasing or decreasing the magnitude of a specific movement will give the desired response.

2.6.3 Trajectory Models in Football

The trajectory of a football is influenced by the initial velocity of the football, the launch angle, and the aerodynamic effect. The flight path and direction of the football will determine the strategies and actions of both offensive and defensive players during a match. The trajectory will influence the timing and anticipation required for receiving or intercepting the football, impacting players' positioning, movement and decision making on the field. Variations in trajectories e.g. driven shots or curve-ball techniques, can create diverse opportunities for attacking teams to capitalize on offensive plays to challenge the goalkeeper, that can ultimately shape the outcome of the match.

Trajectory models have been employed to analyse the effect of changing launch conditions or football properties on match-play actions including free-kicks [108], throw-ins [109], and penalty kicks [35]. Equations that describe the 2D motion of a football in x-y coordinates have been developed by considering the magnus, drag and gravity forces. The equations presented in 2-6 and 2-7, have been widely adopted to model the trajectory of a ball under various launch conditions.

$$\frac{d^2y}{dt^2} = -kv\left\{C_d\frac{dy}{dt} + C_l\frac{dz}{dt}\right\} \quad \text{2-6}$$

$$\frac{d^2z}{dt^2} = -g + kv\left\{C_l\frac{dy}{dt} - C_d\frac{dz}{dt}\right\} \quad \text{2-7}$$

Where,

$$k = \frac{1}{2m}\rho A \quad \text{2-8}$$

Bray and Kerwin [108] experimentally determined the optimum magnitude of drag and lift coefficients for direct free kicks, 18.2 m from goal, between 23 to 28 $m\cdot s^{-1}$ with varying levels of spin. The drag coefficient ranged between 0.25 to 0.30 with an error of ± 0.03. The lift coefficient ranged between 0.23 and 0.29 with an error of ± 0.05. The trajectory model, with these coefficients, was used to investigate the likely outcome for a direct free-kick on goal by varying the launch conditions, for the football to clear a defensive wall, its position in the goal frame and the reaction time for the keeper.

Previous studies have determined the coefficient of lift and drag using a stationary football placed in a wind-tunnel [110,111]. Typically, these footballs are filled with polyfoam and held stationary using a metal rod into the football. Researchers have demonstrated the decrease and stabilisation in the drag coefficient for two world cup footballs (2010; Jabulani and 2014; Brazuca) across a velocity spectrum of 6 to 35 $m \cdot s^{-1}$. Like Bray and Kerwin, Goff [110] utilised the coefficients to explore the effect of the aerodynamic behaviour of the two difference footballs on a shot on goal. However, in contrast to the trajectory the model by Goff, assumed zero lift.

2.6.4 Section Summary

There are a wide array of modelling techniques that have been used to analyse the impact behaviour of a ball. These techniques vary in complexity and effectiveness to describe different characteristics of a ball (e.g. flexible sphere over solid sphere). The choice of modelling technique depends on the nature of the research question of the intended study.

Analytical models are typically developed based on specific material properties and geometrics and may not generalise well to a wide range of football designs. These models tend to oversimplify complex phenomena that can overlook important interactions between football properties in real-world data. For the motivation of this work, the use of a single analytical model may not be able to accurately capture the unique characteristics of different footballs.

Research has employed sophisticated visco-elastic models to enhance the understanding of forces and energy dissipation in ball-to-surface impacts. This type of model has been effective to distinguish behavioural traits between balls that exhibit distinct characteristics such as pressure-less versus pressurised tennis balls but may not be effective to extend to footballs that cannot be categorised in such a way.

Computational modelling requires detailed knowledge of the material properties and complex algorithms to accurately simulate the impact dynamics of a football. While these simulations can provide valuable insights into specific cases or scenario's, they may not be practical or effective to investigate the impact response of a wider population of footballs.

Statistical modelling techniques possess the ability to generalise findings across large sample sizes without requiring extensive computational resources. They are particularly adept to handing inherent variability within the data and allow multiple variables to be considered simultaneously that can assess the combined effects of the mechanical properties of a football on its impact response. This allows for the identification of patterns and correlations that may be obscured or too complex to capture through purely mechanical methods. This flexibility is crucial in real-world scenarios where exact measurements, for example in inbound velocity, are rarely achievable. This makes statistical analysis a very powerful tool for achieving a comprehensive understanding of how different properties of a football collectively influence the balls behaviour upon impact.

The review revealed contemporary modelling techniques including analytical, viscoelastic, and computational modelling are appropriate for assessing the impact behaviour of a football with low sample sizes or balls with distinctive behavioural traits. However, statistical models present significant advantages, particularly when dealing with larger sample sizes and more diverse footballs. These models offer the opportunity to explore interactive effects between various properties and impact parameters, providing a more comprehensive understanding of the multifaceted nature of impact behaviour. They can uncover new insights into how different properties interact, which may be missed by traditional modelling techniques. Furthermore, statistical models can accommodate the variability and randomness encountered in the experimental data of football impacts, making them robust and reliable for capturing the complex realities of football impact dynamics. This approach not only enhances the generalisability of the findings but also leads to deeper, more actionable learnings about the mechanisms that govern the impact behaviour of a football.

2.7 Conclusions

The FIFA Quality Programme does not restrict the composition of a football, allowing manufacturers to produce balls with diverse materials tailored to specific applications. While footballs used in the professional game must conform to regulatory standards for physical properties and rebound, these standards primarily assess the manufacturing quality and are not exhaustive. It is possible to meet the requirements of the FQP using various combinations of materials. Existing research has demonstrated that the impact behaviour of a football is influenced by multiple factors including size, composition, impact velocity and internal air pressure.

However, the impact behaviour of a ball encompasses much more than just the rebound height that is measured in the FQP. Evidence from other sports shows that balls can rebound to similar heights, especially during low-speed collisions, yet exhibit different interactions with the surface such as impact force and contact time. These differences can affect a player's perception of a ball and their playing technique, ultimately influencing match behaviour and outcomes. As new materials and manufacturing techniques emerge, they can significantly alter the behaviour and characteristics of a football. The primary aim of the doctoral study is to understand the influence of the mechanical properties of a football on its impact response. This knowledge ensures that the standards of the FQP evolve alongside these innovations, maintaining the quality and consistency of footballs used in the professional game. By understanding the mechanisms that govern the impact response of a football, FIFA can ensure that innovations in ball design do not compromise the playability or safety of the sport.

An experimental approach was chosen to directly observe and measure the impact response of different footballs. This approach is particularly effective for relatively large sample sizes as it captures the actual behaviour of footballs whilst considering factors such as material composition, manufacturing variations and environmental conditions, that may be difficult to discern from computational simulation assumptions and simplifications, particularly if the material properties are unknown. However, the inconsistency in previous experimental approaches presents a challenge in synthesising findings across different studies. Differences in internal air pressures, velocity choices and experimental conditions inhibits the ability to generalise results across different research studies to contribute to the wider body of knowledge. Whilst overall trends can be extracted from the individual studies, for example the decrease of contact time with respect to increasing inbound velocity, the inconsistency of the experimental protocols does not allow meaningful comparisons of the results to be able to conclude the influence of a ball's properties on its impact behaviour.

The literature review discussed relevant experimental procedures to measure the mechanical properties of footballs using quasi-static methods. However, there were no examples where the properties of multiple footballs had been used to explain variations in the impact behaviour. Given that footballs exhibit viscoelastic properties meaning that the ball will demonstrate strain rate-dependant mechanical properties, it is essential to scrutinise the validity of the rebound test in the FQP. Many previous impact studies have employed velocities above 10 $m \cdot s^{-1}$, so the impact at 6 $m \cdot s^{-1}$ in the rebound test could be considered low compared to typical match-play impact velocities. To examine this, two velocities will be incorporated into the doctoral study, the first at 6 $m \cdot s^{-1}$ and another at a higher impact velocity exceeding 14 $m \cdot s^{-1}$, reflecting the velocity following a kick by a player. The inclusion of a higher velocity aims to highlight the influence of the construction on the impact variables, increasing the likelihood of detecting meaningful differences among the properties of the footballs used in global competitive matches.

A wide array of modelling techniques have been used to analyse the impact behaviour of a ball. The main weakness of the published material is the small sample size considered during the development of previous models, often featuring a single football. Whilst this approach has suited the research conducted in collaboration with a single manufacturer for the development of a single football, the findings may not represent the wider population of footballs. There needs to be more understanding of the inherent variations among the properties of footballs used across international competitive play. Each football, despite complying with standardised regulations, possesses distinct characteristics that are shaped by manufacturing methods, material composition and design specifics (e.g. panel shape). These subtle differences can significantly influence the footballs behaviour during various game scenarios, including impacts, shots, and flight trajectories. It is essential to consider a broader population of footballs to truly understand the mechanisms that govern the impact response of a football.

3 Quasi-Static Stiffness of a Football

3.1 Introduction

The structural stiffness of a football is influenced by the material composition, panel arrangement and internal air pressure. This property influences the football's ability to resist deformation when a force is applied, such as during an impact with a surface. A football with a higher stiffness will typically exhibit less deformation, shorter contact times and better energy transfer during impacts. The structural stiffness of a football can be measured using standard test protocols that involve compressing the ball to a known deflection or by a specified magnitude of force and measuring the output from a commercially available test machine.

While quasi-static stiffness measurements have been used extensively in sports ball research such as baseball, tennis, and volleyball in conjunction with dynamic measurements to explain the variations in the impact behaviour between different ball constructions [27,28,30,32], their use in football remains limited. This chapter presents and discusses a study to measure the quasi-static stiffness of several FIFA-certified footballs that was conducted to successfully achieve objective 2 of the doctoral study. This chapter outlines: the selection of appropriate footballs used in the research, the methods for measuring the quasi-static stiffness and presents the results.

3.2 Methods

3.2.1 Football Specimens

It was essential to consider a range of different footballs to represent the range available in the public domain. The physical characteristics of the footballs was limited to size 5. This size of football is common practice in research studies, as these are the standard and most widely used footballs in professional and competitive matches worldwide. It was sensible to use this type of football to ensure consistency with previous studies and allow for better comparability and reliability of research outcomes. The footballs were inflated to 0.80 bar, this was chosen in line with the specifications of the FIFA Quality Programme (FQP) rebound test at the time of the data collection.

a) Inclusion Criteria

The material composition of a football is the intellectual property (IP) of each respective manufacturer. However, it was necessary to ensure footballs of varying constructions were chosen. To overcome the issue of IP, the results of the FQP certification tests were used to maximise the spread of the characteristics and performance in each of the tests relevant to impact behaviour. A request for information was sent to all certified football licensees by FIFA to permit anonymous data sharing of the FQP test reports with Sheffield Hallam University. All procedures were approved by Sheffield Hallam University Research Ethics Board (ER37533830). The test report contains the results from each of the tests in the FQP for a single football model. Thirty-six licensees agreed to share the results and a total of 1,081 reports were received. It would be impractical to try and obtain over 1000 footballs for the research study, so it was necessary to reduce this number to a workable solution. The following systematic filtering process was followed.

1) Footballs must have a valid licence past January 2021

The reports provided by FIFA contained all records between 1999 to 2021 for each licensee that had agreed to data sharing, that included footballs that had both failed and had an expired licence. The reports were first filtered to only include footballs that held a valid licence *(n = 429)*. Informal conversations with licensees revealed that the patterns and materials of footballs were often retired when footballs were close to their expiry date. The selection of footballs was limited to those that held a valid licence past January 2021 as this would ensure the football was still available in the public domain and could be obtained for the research study. *The number of footballs that met this criterion was 155.*

2) FIFA Quality-Pro (FQPro) certification mark

FQPro footballs are designed to meet the highest performance standards for the professional game. For this reason, they are often designed using the newest innovative materials and manufacturing techniques, making them a reliable benchmark for assessing football performance. Since these footballs are all manufactured to a similar standard that undergo rigorous testing and certification processes, it assures the quality and reliability between the manufacture of samples that may be relevant if multiple samples of the same football are required. *The number of footballs that met criterion was 69.*

3) 32 Panel number

The number of panels used to construct the shell of the football will dictate the shape of the panels and the seam length. These aspects will influence the impact response of a football. The panel number was filtered to minimise the variation between the surface interaction of the footballs, to ensure the variations in impact response reflected the mechanical properties of the footballs rather than differences in design. The number of footballs with 32 panels (n = 34) far exceeded the number of footballs with other panel numbers (e.g. 12 panels with n = 9 and other n = 21). This number suggests that while high-profile tournaments often feature footballs with various panel designs, the overall market continues to predominantly use 32-panel footballs. *The number of footballs that met criterion was 32.*

4) Thermally bonded joining technique

The remaining reports were finally filtered to only include footballs that were thermally bonded. Of the 32 reports that met the previous criteria, thermally bonded dominated other joining techniques. Informal conversations with licensees revealed that the hand-stitched footballs were slowly being phased out due to the evolution of football design. Examination of the licence dates of footballs revealed that many hand-stitched footballs had closer expiry dates than thermally bonded footballs, that indicated the decreasing popularity of hand-stitched methods. *The number of footballs that met criterion was 17.*

b) FIFA Quality Reports

After identifying footballs that met the inclusion criteria, it was essential to ensure these were a representative sample of footballs that pass the FQP, rather than all having performance characteristics concentrated around the same values.

The passing criteria of the tests in the FQP limit the variability that can exist among Pro-certified footballs. Given the absence of established data on the extent of variation among the mechanical properties and impact response of FIFA-certified footballs, an approach was taken to maximise the variation in the performance characteristics of the footballs measured during the tests in the FQP. This approach seeks to enhance the likelihood of detecting significant differences in impact response.

The passing criteria and range for each test in the FQP and an overview of the variability of the results for the 17 football specimens that met the inclusion criteria are shown in Table 1.

Table 2 Variability across test results for football samples that met the inclusion criteria.

FIFA Quality Programme			Football Specimens identified for the study			
Tests	Passing Limits	Range	Limits	Range	Mean ± std	IQR
Circumference (cm)	[68.5, 69.5]	1	[68.5,69.2]	0.7	68.9 ± 0.15	[68.8,69.0]
Sphericity (%)	Max. 1.5	-	[0.7, 1.2]	0.5	0.9 ± 0.1	[0.8,1.1]
Rebound height (cm)						
20 °C	135-155	20	[137, 150.3]	13.3	144 ± 3.5	[141,147]
5 °C	Min. 125	-	[128,143]	15	135 ± 4	[131,138]
Water absorption (%)	Max. 10	-	[0.2, 3]	2.8	0.6 ± 0.7	[0.2,0.7]
Weighing Value (g)	[420,445]	25	[424.5,438.9]	14.4	432 ± 4.45	[429,436]
Loss of pressure (%)	Max. 15	-	[3.2,10.1]	6.9	7.0 ± 1.8	[6,8.5]

Std. standard deviation, IQR inter-quartile range

The rebound height of the footballs showed a 13 cm variation among the 17 footballs at both temperatures. In this study, the impact tests will be performed at room temperature. Figure 17 shows the mean rebound height taken from the FQP reports for the football specimens at 20 ºC, all inflated to 0.8 bar. The mean is shown by the solid red line, and the interquartile range is shown by dashed lines.

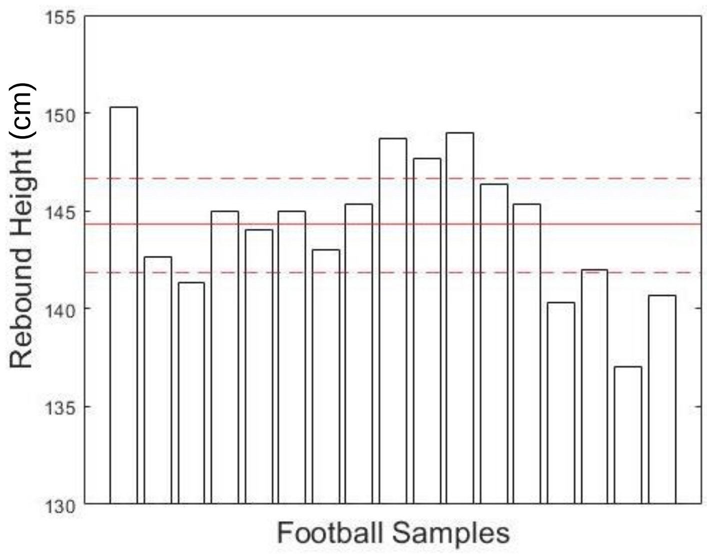

Figure 17 The FQP results for rebound height at 20 ºC for the 17 footballs that met the inclusion criteria. Each bar represents a single football.

The variation among the footballs in rebound height is encouraging to suggest variations in the mechanical properties among the footballs identified, since rebound height is directly influenced by the properties of stiffness, elasticity, and energy absorption.

An acquisition request was made by FIFA to the licensees of the 17 footballs identified. A total of 15 different footballs arrived at Sheffield Hallam University, 1 was discarded as a duplicate and 3 were discarded due to a different panel configuration than the traditional hexagon-pentagon 32 panel design as shown in Figure 18. A final sample of 12 footballs were included in this study. The characteristics of the 12 footballs are shown in Table 3. This outlines key information including the bladder material, number of layers, foam thickness and outer-panelling texture. The footballs typically had between 4 and 5 layers, with the foam thickness accounting for between 38 to 78% of the total material thickness (approximately 5 to 7 mm). Each football was randomly allocated a letter between A to L, to remain anonymous during the analysis to avoid biasing.

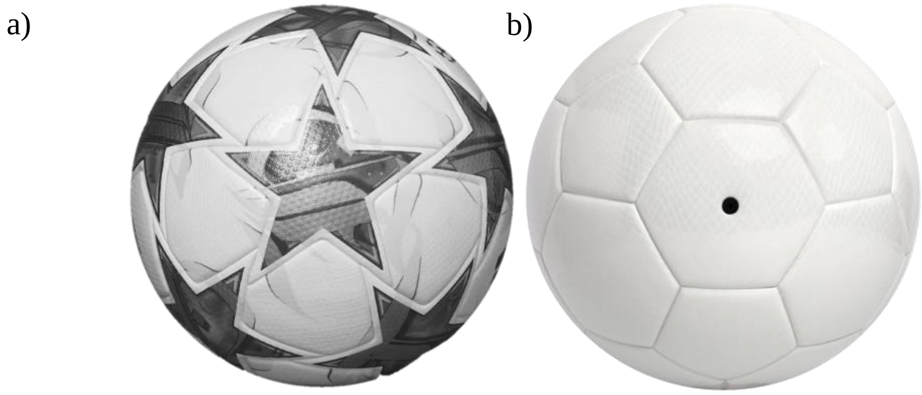

Figure 18 (a) Panel design of the UEFA Champions League football; a football made up of 32 panels in a star shape configuration compared to (b) the traditional hexagon-pentagon 32-panel design.

Table 3 The individual ball characteristics of the footballs tested in the study

Manufacturer Country	Bladder Material	Number of Layers (mm)	Total Thickness (mm)	Foam Thickness (mm)	Outer-panelling Texture
Denmark	Latex (D)*	4	6.24*	4.5 *(72%)*	Dimpled, high gloss
Japan	Latex (I)*	5	5.63	2.5 *(44%)*	Embossed, high gloss
Australia	Butyl (I)	4	6.69	3.5 *(52%)*	Embossed, Low gloss
Pakistan	Butyl (I)	5	5.13	4 *(78%)*	High Embossed, Low gloss,
Japan	Latex (I)	4	5.69	3.5 *(62%)*	Smooth, high gloss
Italy	Butyl (I)	4	6.43	4 *(57%)*	Embossed, Low gloss
China	Butyl (I)	4	6.36	4 *(62%)*	Embossed, Matte
Germany	Butyl (I)	5	5.32	2 *(38%)*	Embossed, Low gloss
Denmark	Latex (D)	4	5.86*	4 *(68%)*	Embossed, high gloss
Denmark	Latex (D)	6	6.75*	3 *(44%)*	Embossed, high gloss
Germany	Butyl (I)	4	5.86	3.5 *(60%)*	Embossed, Matte
Japan	Latex (D)	5	5.44*	3 *(55%)*	Embossed, Matte

I* integrated bladder, D* detached bladder. Where bladder was detached the material thickness does not include the bladder measurement. Embossed: displaying raised patterns or designs on the surface. Dimpled: covered with small indentations, similar to golf ball. Smooth: Even finish, Matte: A non-shiny, flat finish. Glossy: A shiny, smooth finish (low and high).

3.2.2 Equipment and Methods

All procedures were approved by Sheffield Hallam University Research Ethics Board (ER47223536). The mechanical properties of the footballs were measured using an Instron EC3000 test machine (Model No: 2663-901). The machine allowed for control of the rate and magnitude of the deflection within specified limits (deflection limit; ± 30 mm, force limit ± 3 kN). The deflection was applied through the top compression platen, whilst the bottom one remained stationary, shown in Figure 19. To prevent bulging, the footballs were compressed between two rectangular mild steel plates that were larger than the contact area of the compressed football (200 mm x 300 mm) to an overall deflection of 45 mm at a rate of 1000 $mm \cdot min^{-1}$. The deflection of 45 mm was based on the deformation measured during a pilot test of the 20 $m \cdot s^{-1}$ impact tests presented in Chapter 4. To ensure the measure of stiffness solely reflected the footballs resistance to deflection under an applied force, silicone oil was applied to the surface of the plates to mimic a frictionless surface between the plates and the football. This allowed for smooth expansion of the contact area during compression to ensure that the lateral stiffness did not influence the result.

Figure 19 Compression of a football by 45 mm between two plates.

The test sequence was designed using WaveMatrix 2 (Version; 2.0.6, Illinois Tools Work Inc). A schematic of the test sequence is shown in Figure 20. A preload of 25 N was applied to account for the variation in size between the footballs and to ensure they did not lose contact with the plates during the compression cycles. The deflection at 25 N was set as the origin position before any further deflection. The football was cyclically loaded

4 times to 1000 N, this was performed to overcome the viscoelastic effects of the materials associated with the Mullins effect. The football was held at the 25 N preload for 20 s before the final deflection cycle was performed. After the initial loading cycle, the force required for a 45 mm deflection was held for 10 s for the force and deflection to settle before the force was recorded. Raw data were exported to a .csv file and imported into MATLAB (The MathWorks. Inc Version; R2021b) to calculate the stiffness.

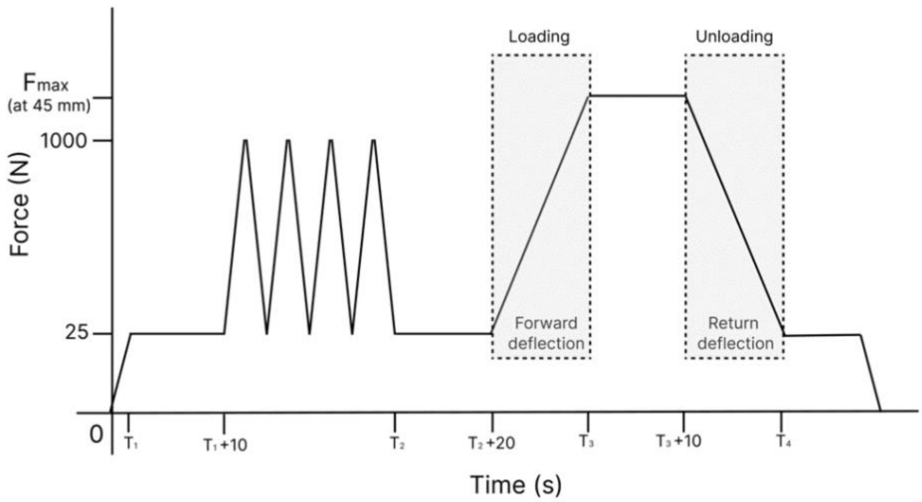

Figure 20 A schematic diagram outlining the test sequence for the compression testing

Force and deflection were measured in three orientations of the football to give an indication of the homogeneity of the stiffness around the circumference for each football model. The three loading orientations are shown below in Figure 21; the first was loaded through (a) the hexagon panel with the valve orientated 90º to the right, the second (c) was on the seam between the two panels testing (21°) and the final (b) was on the adjacent pentagon panel (39°). Each loading direction was repeated twice with the ball removed between trials.

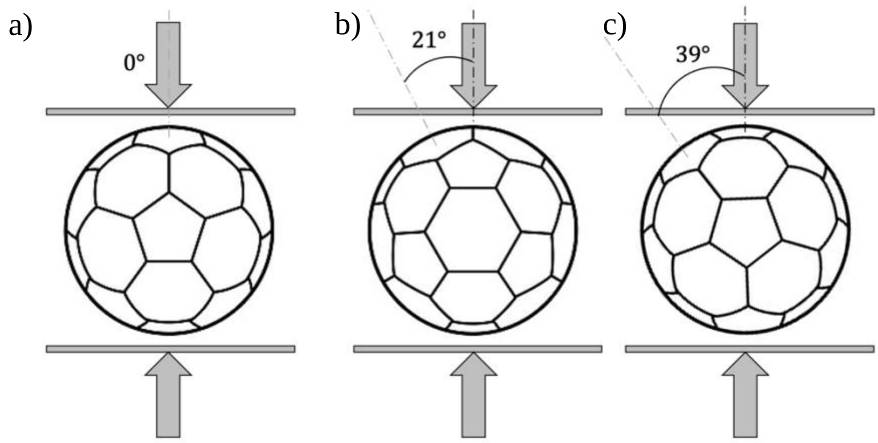

Figure 21 The three orientations of the football during the loading. The initial position loaded through the axes of (a) the hexagonal panel, (b) the seam and (c) pentagon-shaped panel. The angle is given with respect to centre of the hexagonal panel.

The literature review identified various approaches for calculating the structural stiffness of a football from quasi-static compression tests [27-29]. Given the conflicting claims among the literature to whether quasi-static stiffness of a football correlates to dynamic impact performance, it seemed appropriate to evaluate the stiffness using the different calculations proposed in existing research. This approach would determine whether the calculation method affected the measurement and subsequent correlation to dynamic impact variables. This insight could prove crucial to successfully achieving objective 5 of the doctoral study during the development of a mathematical model that contains the mechanical properties of the football.

The two calculation methods were:

1) Stiffness calculated as a ratio of maximum applied force and corresponding deflection. This method will be referred to as ‘calculation 1’.

2) Stiffness calculated using the differential of a 2nd order polynomial fitted to the loading curve during forward deflection. The polynomial will be evaluated at two deflections; 3mm (referred to as ‘calculation 2’) and 30 mm (referred to as ‘calculation 3’).

3.3 Results

The viscoelastic properties of the footballs were evident in the force-deflection curves in each loading direction. This was characterised by a slight decrease in the applied force necessary to sustain a 45 mm deflection during the holding period, that is present in the force-deflection curves shown in Figure 22.

All footballs exhibited a level of non-homogenous behaviour as there was a variation in the maximum force required to reach the maximum deflection across the three loading directions. In some instances (shown in Figure 22a) the 3 loading directions exhibited slightly different force-deflection curves, whereas for other footballs, 2 loading directions exhibited similar force-deflection curves whilst a single axis exhibited either a higher (Figure 22b) or a lower (Figure 22c) stiffness. However, there was no single loading direction across the footballs that consistently required a greater force to reach the 45 mm deflection. The force-deflection plots for all other footballs are shown in Appendix 10.2. The scatter in the data between the repeated loading in a single direction is represented by error bars, that were typically lower than the difference in the maximum applied force.

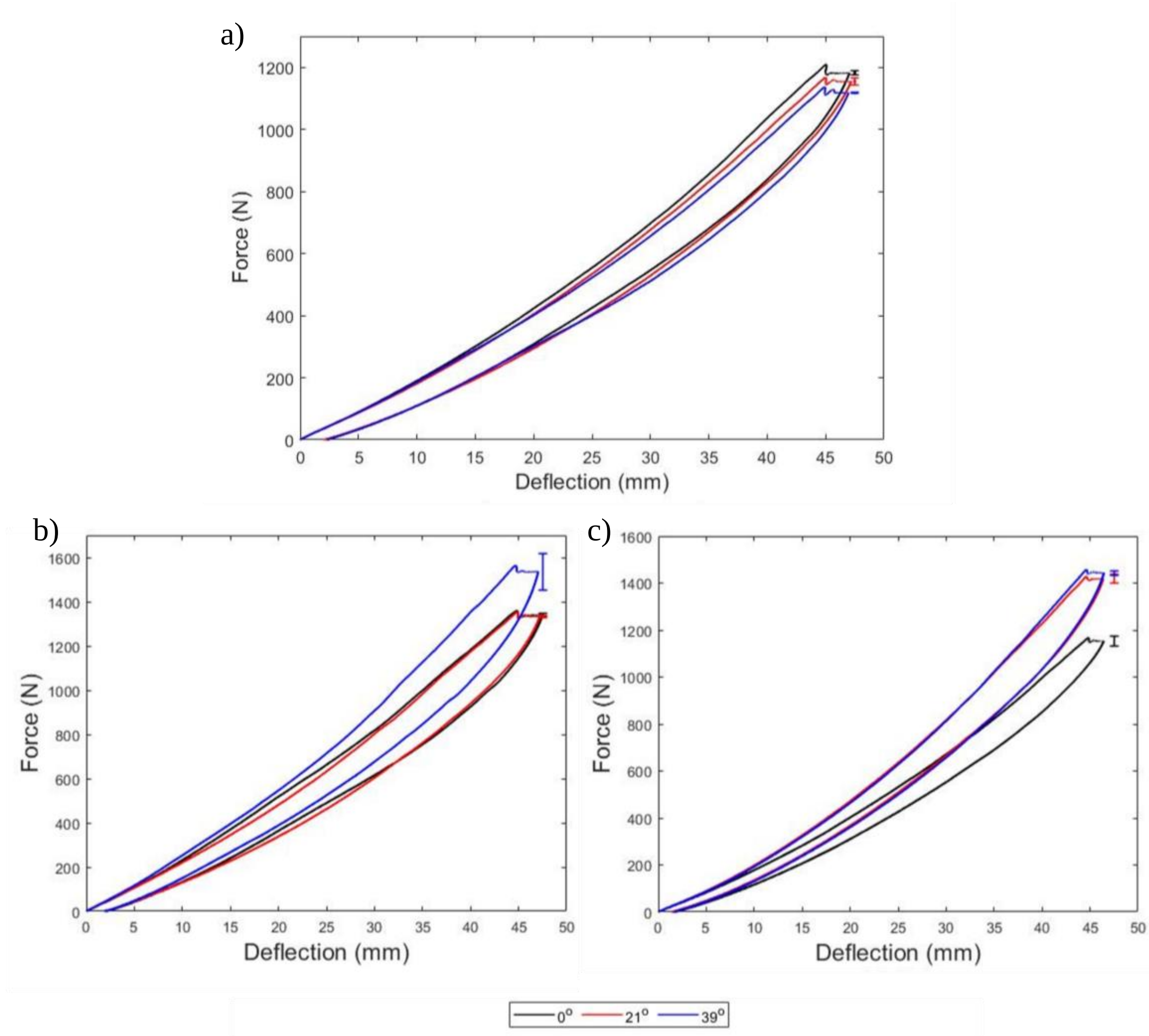

Figure 22 The force-deflection curve for 3 footballs for the three loading directions: (a) Ball K, (b) Ball E and (c) Ball H. The hexagonal panel (0°) (black), seam (21°) (red) and pentagon panel (39°) (blue). The error bars represent the scatter in the data between the repeats.

The scatter of the applied maximum force required to achieve the 45 mm deflection is reflected in the variation of structural stiffness between the footballs, shown in Figure 23**.** All footballs exhibited an initial stiffness between 20 to 25 kNm^{-1}. The stiffness then reduces sharply before increasing with deflection. In four instances, the scatter in the repeats, represented by the error bars overlaps two or more footballs that may suggest several of the footballs may exhibit a similar magnitude of stiffness. The stiffness values for each football are presented in Table 4.

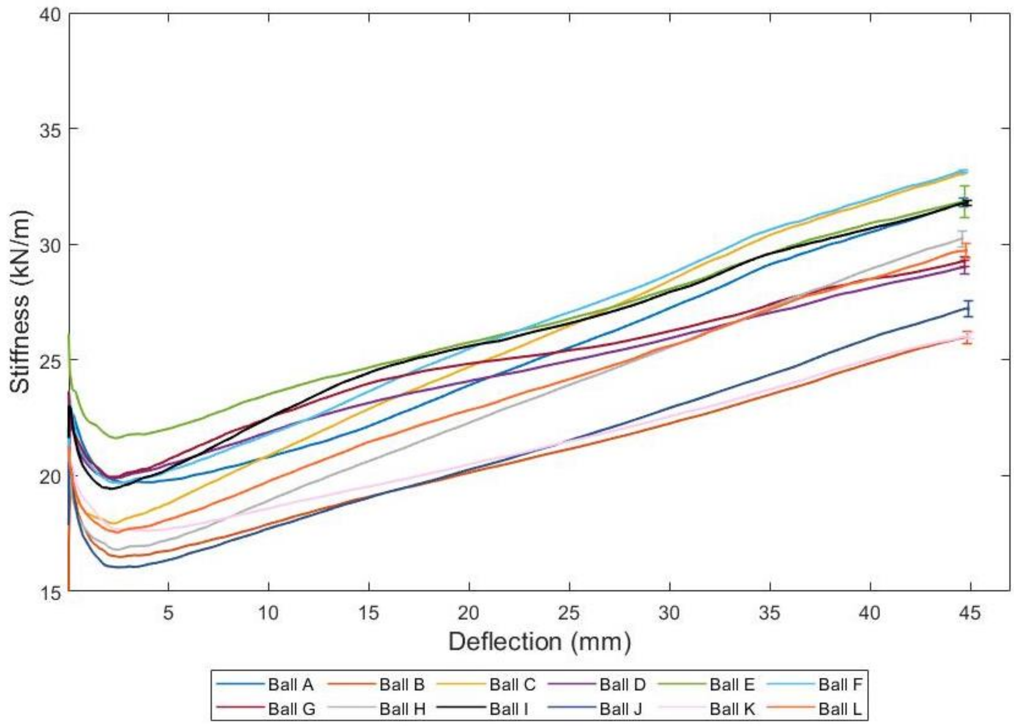

Figure 23 The mean stiffness for each football is calculated by dividing the force by the deflection during the loading period. The error bars represent the scatter in the data between the repeats. Each football model has been issued an anonymised label for confidentiality and to prevent unconscious bias.

Table 4 Mean result of stiffness for each football model for the 3 calculations of stiffness.

Calculation method	Stiffness (kNm^{-1}) A	B	C	D	E	F	G	H	I	J	K	L
1	31.8	26.2	31.3	27.6	29.3	33.2	27.3	28.6	29.5	27.4	24.4	27.8
2	19.4	16.6	20.7	21.2	22.2	21.4	22.0	17.8	22.3	16.1	16.9	19.1
3	34.5	31.7	38.4	32.3	34.9	35.7	31.9	34.9	35.5	29.3	29.2	33.7

3.4 Discussion

This chapter presented the experimental results of the quasi-static stiffness of 12 FIFA Quality Pro footballs. These footballs were identified following a filtering process of FQP test reports acquired directly from FIFA. They were chosen to represent the spread of footballs available in the public domain that could be used in the professional game.

An Instron EC3000 test machine was used to measure the force and corresponding deflection for 12 footballs during a 45 mm deflection. The quasi-static stiffness was evaluated as a ratio of force to deflection and by fitting a 2^{nd} order polynomial to the loading phase of the compression. The choice of the 2^{nd}-order polynomial was informed by previous literature [27,28], which indicated that high-order polynomials could be skewed by uncertain deflection during the initial loading phase [27]. The polynomial was evaluated at two deflection points: 3 mm and 30 mm. The 3 mm was chosen to capture the true stiffness of the football after the initial reduction in stiffness but before it increased with deflection again. The choice of 30 mm was arbitrary, intending to avoid proximity to the maximum deflection, where the stiffness results could be influenced by the polynomial behaviour towards the endpoint. The stiffness was evaluated in 3 loading directions to assess the homogeneity of the football. To account for the variability the reported stiffness value was the mean value from the 3 loading directions. Loading directly through the valve was avoided to its inherent structural vulnerability and differing mechanical properties compared to the ball mains body.

During the test procedure, the force at maximum deflection was held for 10 s, to allow the deflection to settle to ensure calculations using these two variables were accurate [27,28]. At maximum deflection, all footballs exhibited a noticeable drop in the force required to maintain the 45 mm deflection. This is typical for viscoelastic materials due to the phase difference between the applied stress and strain [112]. Larger deflections were measured during the unloading cycle due to the hysteresis loss associated with the football's materials during compression, causing the deflection to not return to zero at zero force. Across all the footballs the stiffness varied $\pm$ 2.5 $kN{\cdot}m^{-1}$ across the 3 loading directions, confirming that footballs exhibited non-homogenous loading behaviour around the circumference.

In the current FQP there is no test that imposes any limit of the amount of deflection for a given applied force. As there is no standardised guidelines or thresholds dictating the stiffness of the football, it is natural to observe differences in the force required to achieve a specified deflection among the 12 footballs. The results demonstrated that the stiffness of all footballs increased with deflection, as evidenced by the stiffness values obtained from the polynomial. Previous studies had solely calculated the stiffness of a football using Hooke's Law [19], but it was observed this method resulted in a lower value of stiffness compared to the polynomial. This discrepancy suggests that the linear assumptions associated with Hooke's Law do not adequately describe the viscoelastic behaviour of the football.

The methods in this chapter measured the stiffness of the football using a quasi-static compression test. The loading rate of 1000 $mm \cdot min^{-1}$, is significantly lower than the deformation rate that is encountered in dynamic impacts, that would be in the order of 10^5 $mm \cdot min^{-1}$. Standardised test machines are unable to recreate deformation rates of this order, alternatively the mechanical properties can be captured during a dynamic impact test against a force platform [30,77], or by approximating the properties using dynamic impact variables [22,28,77]. The stiffness values obtained only capture the structural properties of the entire football and do not decouple the contribution of the material composition over the internal air pressure. Therefore, the stiffness values are only relevant when the football is inflated to 0.8 bar and can be directly compared to the condition of the footballs used in the impact study in Chapter 4.

3.5 Conclusions

The results of the quasi-static compression test revealed differences in the stiffness properties among 12 different footballs available in the public domain. These differences could account for the variations observed among the results of the rebound test for the footballs in the FQP. The stiffness of the football was non-homogenous around the circumference of the ball. The relative stiffness of the footballs was dependant on the magnitude of the deflection, and thus different values were obtained using the two calculation methods that had been used in previous literature. This finding suggests that the method used to calculate the stiffness may influence the strength and significance of the correlation between quasi-static and dynamic measurements. Future research should explore the correlation between the stiffness values and dynamic measurements to identify which value best represents the quasi-static stiffness properties of the football, which is crucial for developing accurate mathematical models.

4 Dynamic Behaviour of a Football – Equipment and Methods

4.1 Introduction

In chapter 3, the quasi-static stiffness of 12 footballs was measured. To understand how the mechanical properties of a football are reflected in its dynamic impact response, it is necessary to establish suitable methodologies to measure the impact behaviour of a football. The impact between a football and a pitch involves a complex interaction between the material composition and internal air pressure of the football and the surface properties. Impacting a football against a rigid surface provides a consistent and controlled environment to study the football's behaviour during collisions. A normal inbound impact ensures the response of the football is free from the influence of surface friction and spin associated with oblique impacts.

The viscoelastic behaviour of a football can significantly influence the magnitude of the impact variables, such as contact time or deformation, that are measured at varying inbound velocities [113]. It is essential to consider the inbound velocities that might be experienced during real-match situations to ensure the velocities chosen for the data collection are both practical and capable of revealing distinctions among different footballs.

This chapter outlines the laboratory equipment, methods, and quantifies the precision of the equipment used to measure the impact variables for a football colliding with a force platform. This works towards fulfilling objective 3 of the doctoral study. The chapter is structured in three sections that discuss, (1) the laboratory equipment, (2) the inbound velocities observed during certification and in real match situations and (3) the methods and precision of the equipment used to measure the impact variables.

4.2 Laboratory Equipment

In this doctoral study, the football must be projected towards a force platform. The rebound test in the FQP was replicated by dropping the football using a vacuum, shown in Figure 24. The height of the vertical drop was measured using a laser distance tool (Leica Disto D210) and could be adjusted using a mobile elevating lifting platform (MELP) that housed the vacuum. This method was designed so that the football was released without spin.

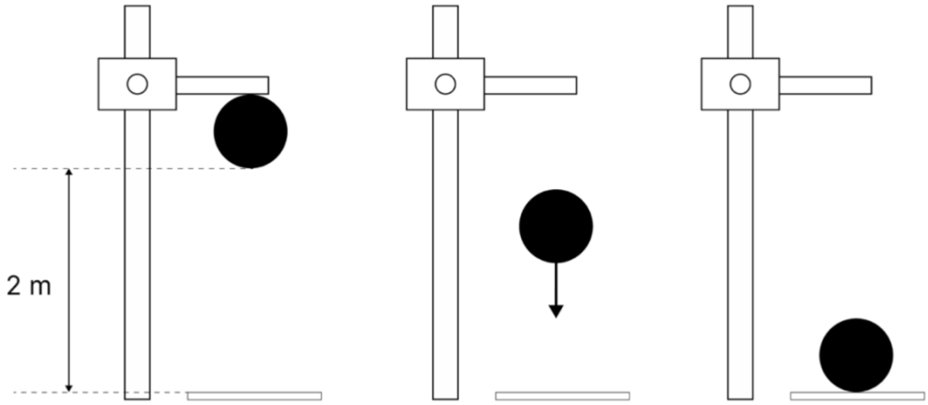

Figure 24 Simplified schematic of rebound test performed from 2 m.

The maximum permitted drop height in the laboratory was 7 m, approximately 11 $m \cdot s^{-1}$, but this would require an operator to be located on the MELP and place the football at this height which is unfeasible for many repeats. Higher velocity impacts were achieved using a custom-made motorised device that projected the football vertically downwards. The design is shown in Figure 25, it uses four rotating wheels to impart velocity on the football as it passes through. The maximum speed that the device could achieve was approximately 40 $m \cdot s^{-1}$.

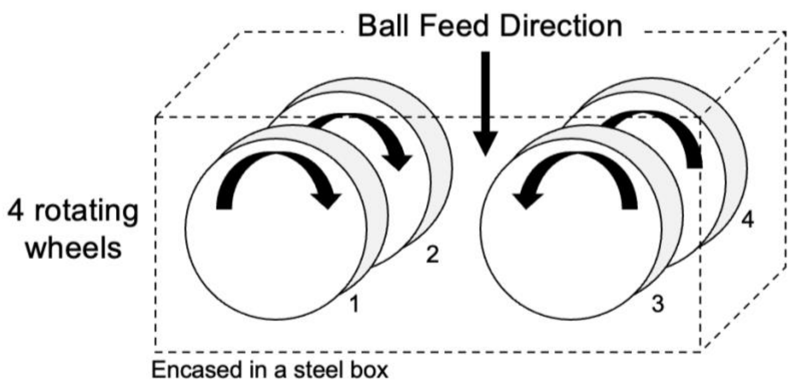

Figure 25 Schematic of the internal arrangement of the bespoke device

The arrangement of the laboratory equipment is shown in Figure 26**.** The systems were designed to allow a single operator to measure the impact variables of footballs.

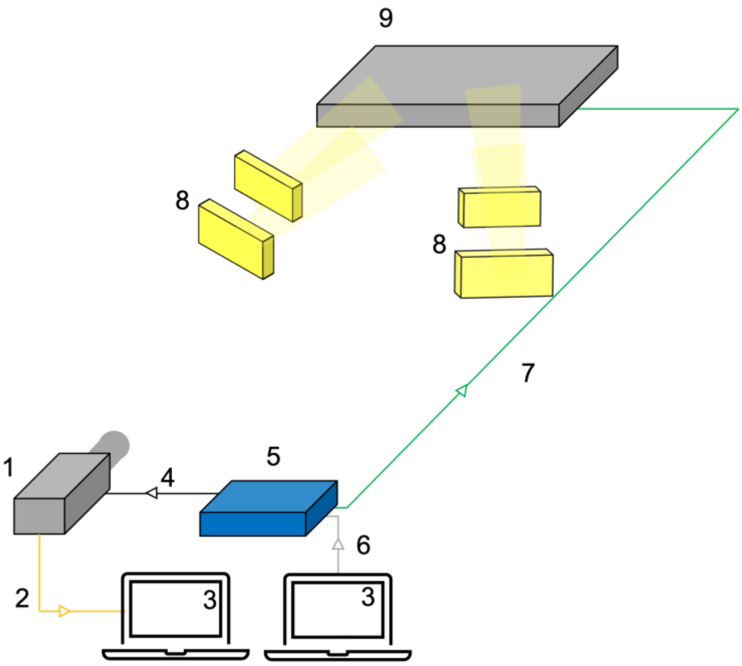

Figure 26 Laboratory equipment and arrangement. 1. High speed camera, 2. Ethernet cable to laptop 1 3. Laptops 4. Bespoke cable to enable trigger-synchronisation between 5. DAQ and the camera, 6. USB cable to connect laptop 2 with 5. 7. Connecting cable for force platform, 8. LED lights (x4), 9. Force Platform

A single phantom MIRO R311 high-speed camera was used to record the impacts. The camera has a maximum resolution of 1280 x 800 p while operating at a sampling frequency of 3200 fps. The camera was positioned perpendicular to the impact plane to minimise perspective errors [88]. Spatial errors and out-of-plane errors were quantified prior to the data collection, these are discussed in Appendix 10.3. The camera should be placed at a minimum distance of 4 m to minimise these errors during the analysis of high-speed video.

Two different lens and camera settings were used in the experiment depending on the hardware available at the time of the data collection and the inbound velocity. For both inbound velocities the camera sampled at 10,000 Hz, to allow frame synchronisation to the force platform.

1. **Drop test:** The camera was positioned 4 m away from the force platform edge. A Nikon lens (35-70 mm) was used to capture images at a resolution of 320 x 800 p. The resolution was chosen to ensure that sufficient images were captured in the vertical direction during the fall for the velocity to be calculated accurately.

2. **Impacts using the mechanical device:** The camera was positioned 6.5 m away from the force platform edge for the higher velocity impacts. A Nikon lens (70-210 mm) was used to capture images at a resolution of 380 x 700 p. The use of a longer lens allowed for a greater distance between the camera and force platform distance without sacrificing image quality. Since the errors associated with out-of-plane were more prevalent using the mechanical launch device (Appendix 10.3), it was logical to increase the distance to reduce the errors. The width of the resolution was increased to accommodate the increased lateral expansion of the football and the change in the position of the camera.

The footballs impacted a Kistler 9281EA force platform that was floor-mounted at a recommended torque of 75 Nm [114]. The selection and appropriateness of this force platform to measure forces for a football impact is discussed in 4.5.2 and 4.5.3. The force platform sampled at 10,000 Hz and was operated using Bioware (5.4.3.0, Kistler Holding AG). A bespoke cable was made to connect the data acquisition device (Kistler DAQ Type 5695) to the high-speed camera to allow trigger synchronisation.

4.3 Inbound Velocities

The primary aim of this work is to quantify the effect of the mechanical properties of a football on its impact response, rather than to quantify the relationship for a single impact variable with respect to increasing inbound velocity. This approach will identify the appropriate properties or impact variables that should be regulated by FIFA to ensure consistent outbound performance between footballs. Existing research has highlighted the pivotal role of impact velocity in shaping the impact behaviour of a football due to its viscoelastic properties. Particularly at impact speeds above 14 $m \cdot s^{-1}$, the influence of the construction of a football is accentuated in impact variables like the coefficient of restitution (COR) [11,32]. Whilst the footballs performance at one set impact speed (6 $m \cdot s^{-1}$) is regulated by the FQP, the relevance of the behaviour assessed at this speed compared to higher velocities often encountered in match play is unknown. To understand the relevance of the certification test programme to higher-speed impacts, testing was limited to two distinct inbound velocities; the predefined certification test speed (referred to as 'CT' velocity) and a single higher impact speed (referred to as 'HV') representing the upper limit of match-encountered impact speeds. This focused approach ensures the findings are applicable to both standardised testing protocols within the FQP and real game conditions.

Certification Test (CT) Velocity

The FQP outlines the procedure to measure the rebound height during certification.

'The apparatus must allow the ball to free fall vertically from a height of 2.00 ± 0.01 m, without imparting any spin to rebound a metal surface for outdoor balls. [1]'

The FQP manual specifies an inbound velocity of 6.25 ± 0.15 $m \cdot s^{-1}$. However, this calculation overlooks the effect of air resistance and may not accurately represent the inbound velocities encountered during laboratory testing. The forces acting on the football falling from a height are shown in Figure 27a. A more representative approximation of the inbound velocity (v) was obtained by resolving the forces due to the football's weight (F_w) and the drag force (F_D) caused by air resistance. A drag coefficient of 0.5, instead of the 0.4 specified in the FIFA manual. This decision was based on a study involving non-rotating balls by Goff [110], which found a drag coefficient of 0.5 more accurately represented the air behaviour for the conditions being studied. The derivation (outlined in appendix 10.4) gives an equation that expresses velocity as a function of time (4-1), shown graphically in Figure 27b. The time taken for a football to fall from 2 m was applied to equation 4-1 to give an inbound velocity of 5.98 $m \cdot s^{-1}$. Whilst this appears lower than the minimum velocity outlined in the FIFA test manual; 6.1 $m \cdot s^{-1}$ at maximum air resistance, this can be attributed to the change in drag coefficient.

$$v(t) = V_T \tanh\left(\frac{gt}{V_T}\right) \quad \text{4-1}$$

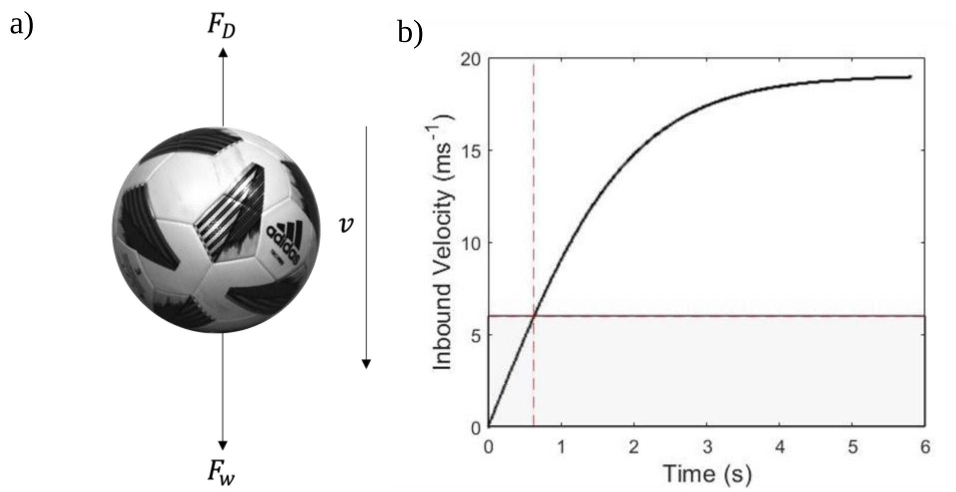

Figure 27 (a) Free body diagram for a free-falling football. (b) Inbound velocity plotted as a function of time. C_d=0.5, ρ =1.23 $kg \cdot m^{-3}$, A=0.04 m^2 g=9.81 $m \cdot s^{-2}$ m=430g.

Higher Inbound Velocity

The velocity imparted by a player to a football is influenced by factors including age [115-117], gender [118] , the type of kick [119-122], the emphasis of the kick [119,120,122,123]; speed or accuracy, shot preparation and speed of approach [124], and playing position [116,125]. The speeds were observed to be between 19 to 35 $m \cdot s^{-1}$, with higher speeds observed when players had no constraints on angle, speed of approach or accuracy. When distance was emphasised the kicking angle was around 45°, commonly observed during goal kicks [126]. The playing position influenced the speed imparted by players to a football in professional players, midfielders were found to impart higher ball velocities compared to defenders or strikers [125]. These studies all feature velocities obtained in laboratory environments rather than in real-match play, so the extent to which these occur in the game of football is unknown.

Goal kicks are an example where a player would impart a maximum velocity to the football to maximise the distance travelled [126]. The upper bound of velocities observed in literature (35 $m \cdot s^{-1}$) was applied to a trajectory model [127], solved using Runge-Kutta, to calculate the upper limit of velocities that a football could impact the surface with during match-play. This trajectory model allowed initial inputs of imparted velocity and angle whilst accounting for lift and drag during the flight. In contrast to equation 4-1, that assumed the football starting from a stationary position.

$$\frac{d^2y}{dt^2} = -kv\left\{C_d\frac{dy}{dt} + C_l\frac{dz}{dt}\right\} \quad \text{4-2}$$

$$\frac{d^2z}{dt^2} = -g + kv\left\{C_l\frac{dy}{dt} - C_d\frac{dz}{dt}\right\} \quad \text{4-3}$$

Figure 28 illustrates the influence of the kicking angle on the trajectory of a football when imparted by 35 $m \cdot s^{-1}$. Air resistance causes the optimal launch angle for distance to be about 25° rather than 45°. When kicked at 45°, the football reaches its peak height more quickly and spends less time travelling horizontally before descending. The shallower launch angle minimises the effect of air resistance, that further contributes to the longer distance travelled.

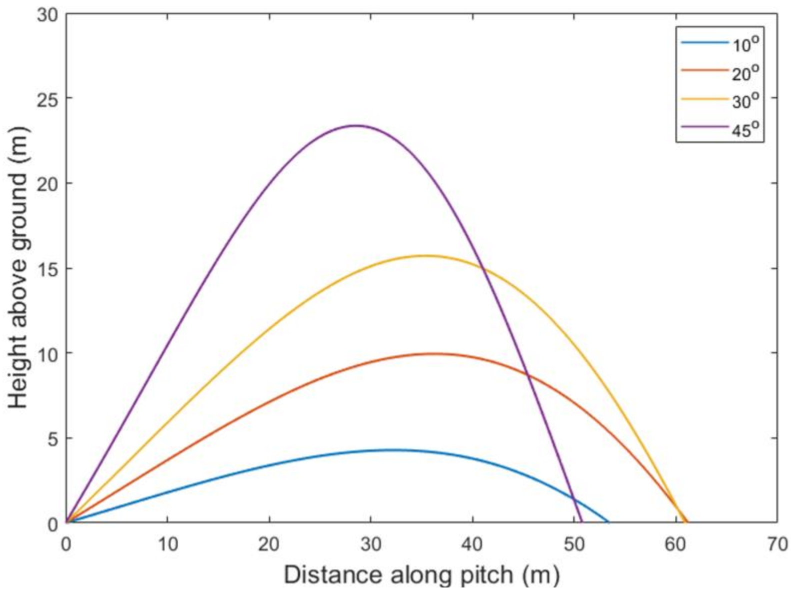

Figure 28 The trajectory of a football imparted with 35 m·s-1 of velocity at a kicking angle between 10, 20, 30 and 45 degrees. Where, m= 0.45 kg, r= 0.11 m, ρ=1.225 kgm^{-3}, g = 9.81 m·s^{-2} C_d=0.23 and C_l=0.24

Previously, two FIFA-certified footballs have exhibited similar values of COR for an 8 m·s^{-1} inbound velocity [11]. At higher inbound velocities the football possesses greater kinetic energy compared to impacts at lower velocities. This results in increased deformation due to higher forces and the energy transfer becomes more pronounced, accentuating the viscoelastic behaviour of the football. More prominent variations in rebound characteristics have been measured between FIFA-certified footballs above 14 m·s^{-1}. The maximum vertical component of inbound velocity across the 4 trajectories in Figure 28 was 18.04 m·s^{-1}, which was around 12 m·s^{-1} below the upper limit of velocities that had previously been tested [43]. The vertical component directly influences the force and behaviour of a football during an impact, making it more relevant than the resultant component. By focusing on the maximum vertical component, the study can replicate and analyse the behaviour of the football during these specific types of impacts. This approach indicates that the tested velocities should not exceed 20 m·s^{-1}, aligning with the upper limit of velocities used in recent studies [36,58].

4.3.1 Summary

The dynamic impact response of a football will be measured at two discrete velocities of approximately 6 and below 20 $m \cdot s^{-1}$. The inclusion of a 6 $m \cdot s^{-1}$ velocity was stipulated by the FQP and a higher inbound velocity was essential to assess the relevance of the certification test to velocities encountered in match-play scenarios. As all of the footballs that will be used in the study (identified in section 3.2.1) had passed the FIFA certification test, based on previous findings it was reasonable to assume that they might exhibit consistent COR values within a given range for an inbound velocity of approximately 6 $m \cdot s^{-1}$. The inclusion of a single higher impact velocity was chosen to accentuate the influence of the material composition and physical properties of a football on its dynamic response to allow comparisons between the impact variables of different footballs to a level of significance.

4.4 Measuring Impact Variables using High-Speed Video

Quantitative analysis of high-speed camera images was performed to measure impact variables that characterise the deformation and energy loss behaviour of a football during a collision with a force platform. Two-dimensional pixel coordinates were extracted during the digitising process. The pixel coordinates were transformed to real-world coordinates by scaling them according to the results of a calibration procedure. Following this, they were used to calculate velocities and distances. This section outlines the data capture and processing procedures that are vital to ensure high-quality measurements are taken.

4.4.1 Camera Settings - Spatial and Temporal Sampling

The spatial and temporal sampling will influence the image quality and the accuracy of the measurements taken.

a) Spatial Sampling

Spatial sampling determines the level of detail, clarity, and sharpness of the image. The focus is determined by manually adjusting the camera lens to converge light to give a sharp and clear image at a specific distance as shown in Figure 29a. The resolution determines the density of these pixels. Achieving the correct focus is essential for realising the full potential of a camera's resolution. It must be noted, the focus cannot be changed after the calibration, so it is essential to consider the visibility of the calibration tool and the different colours and patterns on the outer panelling of the football's models. Incorrectly focusing on the volume as shown in Figure 29b gives a blurred image that can lead to errors in the calibration and image measurements.

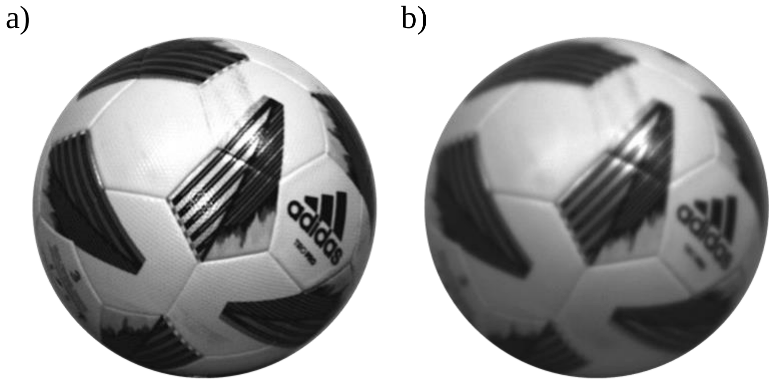

Figure 29 (a) Correctly focusing the camera produces a sharp image where aspects of the football are clearly defined compared to (b) blurred image due to incorrect focusing.

b) Temporal Sampling

Temporal sampling is the process of capturing a series of discrete images at regular time intervals. The frame rate, shutter speed, exposure and lighting will determine the appearance and perceived speed of motion of the football in consecutive images.

The camera was used to record consecutive images during the data collection. The camera uses a global shutter to prevent distortion effects associated with rolling shutters [128,129]. To establish the correct camera settings there is a trade-off between frame rate and resolution. A higher frame rate will require a lower resolution or will limit the maximum recording duration, as the frequency of image capture will require a larger portion of the camera bandwidth [128]. Similarly, each time the frame rate is doubled, the exposure time for each frame is halved which means higher frame rates require additional illumination of the control volume [128,129]. Four LEDS light boxes (LT-v8-15, GS Vitec) all directed towards the impact area were used to increase the illumination and allow the camera to achieve a lower exposure time to reduce motion blur for a 10,000 fps sample rate [128-130].

The motion blur (displacement observed during exposure) can be calculated by multiplying the shutter speed and the speed of the object [130]. Figure 30 shows the decrease in motion blur by decreasing the exposure time with a 10,000 fps sample rate. The amount of motion blur is presented in Table 5. When the exposure rate is decreased from 80 to 20 μs, the motion blur is reduced by 0.4 and 1.2 mm for a 6 and 20 $m{\cdot}s^{-1}$ inbound velocity.

Table 5. Motion blur for a football with two levels of exposure

Inbound velocity (ms^{-1})	Motion Blur (mm)	
	100 μs	20 μs
6	0.5	0.1
20	1.6	0.4

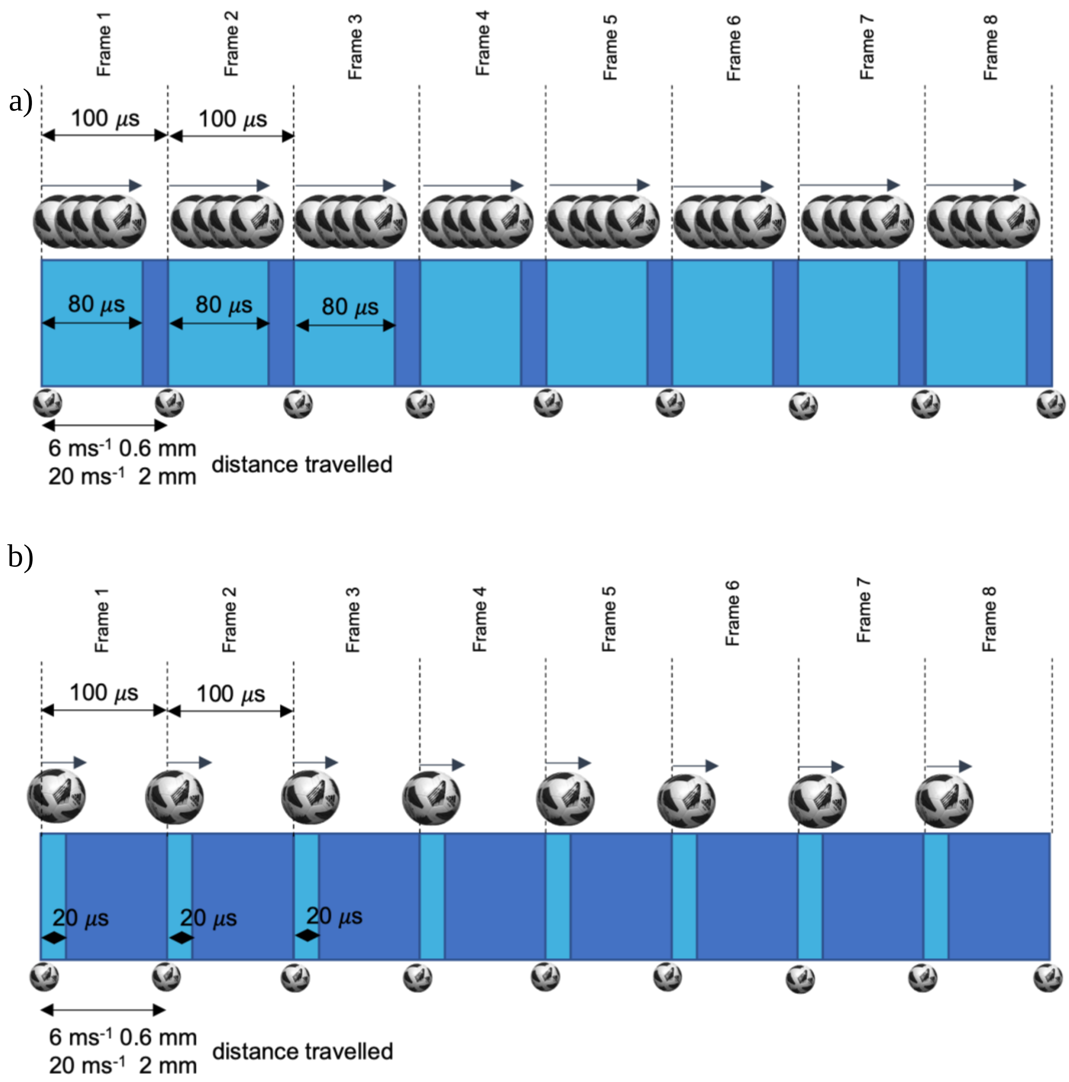

Figure 30 The motion blur for a football travelling at 6 and 20 ms^{-1} with an exposure time of (a) 80 μs and (b) 20 μs. The exposure time is illustrated by the light blue shade and the dark blue shade illustrates the remainder of time where light does not enter the sensor for a sample rate of 10,000fps.

4.4.2 Calibration Procedure

To be able to measure the impact variables using the camera images, a planar checkerboard calibration procedure was carried out to calculate rotation and translation matrices to convert the camera to world coordinates. The checkerboard is moved around the volume and should maximise the lens coverage where measurements are taken.

Aspects of the checkerboard which will influence the quality of the calibration procedure include:

1. Checkerboard Size
   The entire checkerboard must be visible by the camera without any corners being out of view [131].

2. Checkerboard manufacture
   The accuracy of the calibration relies on the physical size of the checkerboard squares to be accurate since the calibration uses the size of each square to scale the calibration volume. Systematic errors will be introduced if the size is measured incorrectly. The checkerboard should be placed on a hard-backing surface to ensure no bowing during the measurements.

3. Checkerboard orientation
   The angle of the checkerboard has been shown to influence the projection accuracy [47]. Checkerboards of higher angle orientations (e.g., above 60°) make intersection detection difficult due to image foreshortening. A variety of angles and orientations are taken to ensure a well-calibrated volume.

4. Visual coverage
   Consecutive images were captured using the continuous recording mode of the Phantom camera. To reduce the errors, 30 – 50 images were used for each calibration.

A series of calibration images were loaded into Check2D (Sports Engineering Research Group, Sheffield Hallam University, UK) to calculate the intrinsic and extrinsic camera parameters. The software has been developed at Sheffield Hallam University and uses the planar camera calibration technique [46,47,132] from the OpenCV function library. The function detects grid patterns within images to return the top corner point of the checkerboard. The software extracts the intersections between the black and white squares of the checkerboard through interpolation, as shown in Figure 31. The intrinsic camera parameters (focal length, principal point and pixel skewness) define the geometric and optical properties of the camera.

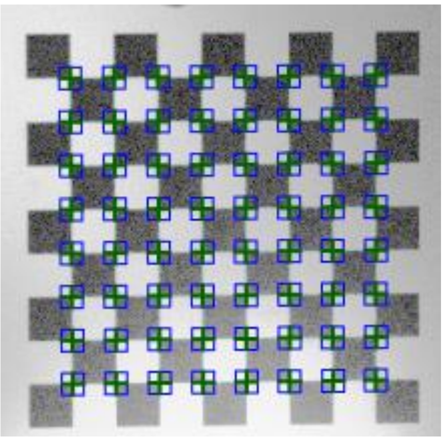

Figure 31 A checkerboard image showing the software extracted positions of the intersections between the black and white squares.

A reprojection error is returned by the software, which is dependent on the quality of the calibration images. The pixel distance between the detected and reprojected points is plotted in u-v coordinates for each image (as shown in Figure 32) and an average error is given. The software allows the user to exclude images that may have irregular reprojection errors. The calibration can be re-run and may result in an improvement.

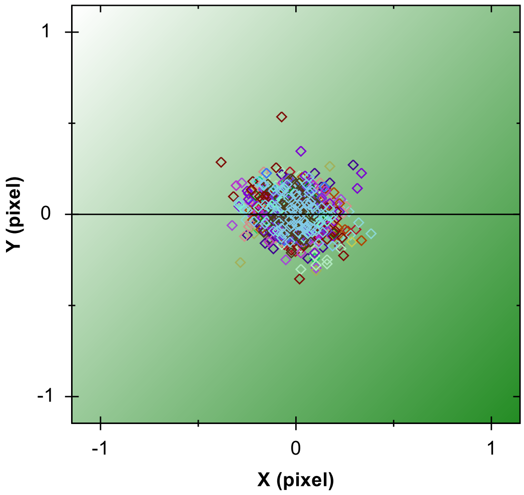

Figure 32 The reprojection error for a calibration carried out by the software. The average reprojection error is 0.127.

The extrinsic parameters are generated following manual extraction of the intersection point for a single checkerboard image placed in the plane of motion. The user manually selects the intersection points of the image and enters the corresponding distances.

The errors associated with the data collection for the study are shown in Table 6. As the two data collections were carried out with different lens settings to accommodate the impacts at the higher velocity, two camera calibrations were required.

Table 6. Calibration details for the data collections.

Condition	Images	Reprojection error (mm)
CT	30	0.127
HV	43	0.158

CT: Certification test velocity (~ 6 $m \cdot s^{-1}$) HV: High velocity (~ 20 $m \cdot s^{-1}$)

4.4.3 Image processing to measure impact variables

The high-speed videos (.cine) were converted into images (.bmp) to enable manual digitisation in Check2D. Impact variables of deformation, contact length and contact time were measured using the images.

Contact Time (T)

The contact time was calculated by visual analysis of high-speed video frames. It was defined as the time taken between when the football first contacts the plate to when contact is lost.

Deformation (δ_b) *and contact length* (l)

A circular marker was manually aligned to the circumference of the football to measure deformation. The uncompressed position on the circumference was defined by the initial image showing when the football was first in contact with the force platform. The magnitude of deformation was measured between the initial frame and the frame where the football was fully compressed, as illustrated in Figure 33.

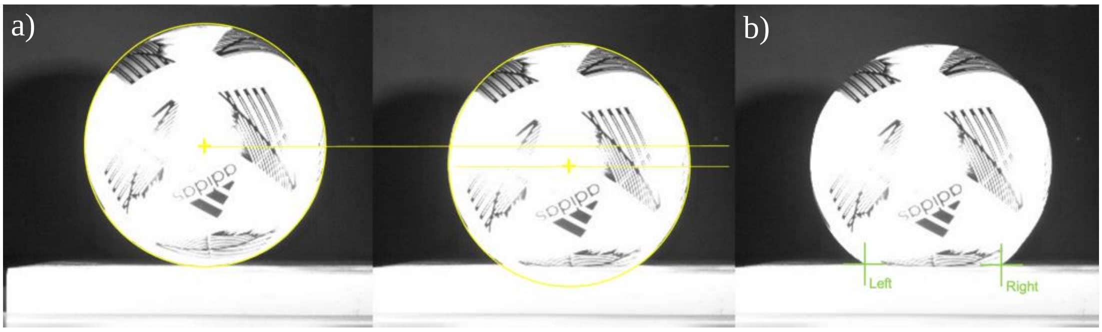

Figure 33 Manually digitised images used to measure (a) deformation and (b) contact length.

The average of two repeat measures were used for the ball deformation and contact length. This was because repeating the measurements and using the mean value improved the inter-reliability (ICC) to above 0.9 compared to 0.65 when only a single measure was taken. A repeatability study (Table 3) was conducted to determine the accuracy of the manual digitisation for measuring the deformation, contact length, and contact time. A repeatability analysis was carried out to calculate the standard error of measurement (SEM) and minimal detectable difference (MDD). The MDD represents the minimum difference between the measurements that can be considered a real difference, beyond the measurement error. It was calculated using the standard error of measurement (SEM) with 95% confidence intervals [133,134]: The SEM and MDD are calculated using equations 4-4 and 4-5.

$$SEM = SD * \sqrt{1 - ICC} \quad (4\text{-}4)$$

$$MDD = 1.96 * SEM * \sqrt{2} \quad (4\text{-}5)$$

SD: Standard deviation

To assess the repeatability of the measures of deformation and contact length, 75 repeat measures were used across 3 footballs (300 measurements). The normality of each impact variable was assessed using the Shapiro-Wilk tests. Paired t-tests ($\alpha = 0.05$) were used to measure the correlation between repeat measures, High repeatability was observed for all measurements ($r > 0.9$). The SEM and MDD are presented in Table 7.

Table 7. Summary of repeatability statistics for contact time, deformation, and contact length.

Impact Variable	CT velocity		HV Condition	
	SEM	MDD	SEM	MDD
Contact Time (ms)	0.05	0.2	0.04	0.1
Deformation (mm)	0.34	0.93	0.42	1.16
Contact Length (mm)	0.89	2.48	0.63	1.75

Coefficient of restitution (COR)

The instantaneous velocities of the football were calculated by plotting the vertical position obtained using a computer vision algorithm and digital processing. The image (.bmp) files were imported into MATLAB, and a circular Hough transform for finding circles was applied [135]. This method was used due to its robustness in the presence of noise, occlusion and varying illumination which was suitable for this application. The method was particularly robust against the different patterns on the footballs. An inbuilt MATLAB function (imfindcircles.m) was used to apply the circle Hough transform. on consecutive high-speed video frames. In section 4.3, the effect of air resistance on impact velocity during a 2 m free-fall was observed. For the lower velocity, a 2nd order polynomial was fitted to the data to consider the air resistance [27,28] and gravity acting on the football. This method assumes the acceleration due to air resistance is constant. The time at a specific position was applied to ensure consistency between footballs, as depicted in Figure 34.

The observations during analysis aligned with existing research, where the use of a 2nd order polynomial was seen to become disproportionately influenced by activity at the endpoints leading to over-fitting for the 20 $m \cdot s^{-1}$ inbound velocity [136]. To overcome this, a linear fit was used to estimate the inbound velocity at the higher velocity impacts. This assumed that the short distance between the exit of the launcher and the force platform did not allow the transition from laminar to turbulent flow. A ratio of the out-to-in-bound velocities for each impact was used to calculate the coefficient of restitution (COR).

As with the other impact variables the SEM and MDD for the COR were calculated using the same method. A total of 100 repeat measurements were performed across 4 randomly selected footballs. The SEM and MDD are presented in Table 8.

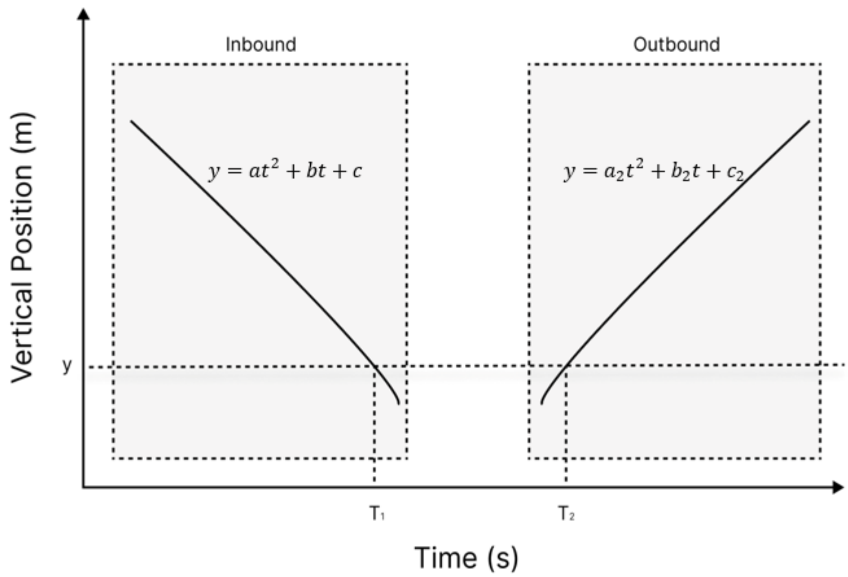

Figure 34 Schematic illustrating the fitting of a polynomial to position data to calculate impact and outbound velocities.

Table 8. Summary of repeatability statistics for inbound velocity and COR.

Impact Variable	CT Velocity		Higher Velocity	
	SEM	MDD	SEM	MDD
COR	0.01	0.03	0.01	0.01

4.5 Impacts on a Force Platform

Force platforms can be used to provide valuable insights into the impact response of the football revealing the deformation characteristics, phases of contact, energy transfer and overall performance. In previous work the outputted signal had been used to validate modelling procedures. In this research study, the signal will be used to compare the loading behaviour between different footballs.

4.5.1 Evaluating available systems

Three commercially available force platforms were investigated for their suitability to measure the impact force throughout contact for a football. These were: the Kistler 9281EA and 9286B and AMTI BMS600900-2K. They were chosen as these were available at Sheffield Hallam University and used different force sensors; the AMTI plate used a strain gauge system, whilst the Kistler force platforms used piezoelectric force transducers. The system properties are outlined in Table 9.

Table 9. Relevant system properties for 3 commercially available force platforms available at Sheffield Hallam University

	9281EA	9286B	BMS600900-2K
Sensing Mechanism	Piezoelectric	Piezoelectric	Strain gauge
Maximum Capacity (Fz)	20 kN	10 kN	8.9 kN
Natural Frequency	1000 Hz	200 Hz	550 Hz
Rigidity (Fz)	30 $N\cdot \mu m^{-1}$	8 $N\cdot \mu m^{-1}$	Not outlined
Sampling Frequency (Fz)	< 125 kHz	< 125 kHz	1.2 kHz
Installation method	Floor	Portable	Floor

The natural frequency of the force platform was a crucial consideration to avoid the amplitude of the natural frequency vibrations corrupting the output signal during short-duration impacts [66]. To find an appropriate natural frequency, a Fast-Fourier transform was carried out on the force-time data from a 20 $m\cdot s^{-1}$ impact. The minimum natural frequency of the platform for this application was found to be 900 Hz. The requirement of the sampling frequency of the force platform to avoid missed or aliased data is outlined in Appendix 10.5. This revealed a minimum sampling frequency of 5 kHz was required. The Kistler 9286B and AMTI BMS600900-2K did not meet these requirements.

The Kistler 9281EA exhibited appropriate technical specifications for the application. The appropriateness of this force platform was reiterated by its use in [59] to measure the impact force of a single football at 19 $m\cdot s^{-1}$. Quantification of the errors and repeatability was carried out and is detailed in the following sections to confirm its appropriateness for the study.

4.5.2 Quantification of errors

The quality of measurements from the force platform are reliant on a suitable natural frequency for the application, low hysteresis, low crosstalk, and high linearity. Psycharakis and Miller [71] noted many authors have previously taken force-plate measurements as being error-free and outlined a procedure to quantify these errors. In Chapter 5, the force platform will be used to measure impact force and impulse, any error in the force platform will propagate in subsequent calculations, so it was essential to quantify these errors and ensure they fell within acceptable limits prior to the data collection.

Hysteresis

Hysteresis refers to the phenomenon where there is a temporal lag between the applied force and the force being measured by the force platform. An example of the cause of hysteresis errors is due to the properties of the deforming materials used in the construction of force platforms [66]. The procedure outlined by Psycharakis and Miller [39] was used to assess the hysteresis errors.

The force platform sampled at 1,000 Hz. Five 20 kg plates were stacked in the middle of the force platform and added in 10 s increments. Once the fifth plate had remained on the platform for 10 s the plates were removed in the same sequence. The maximum difference between the force during the loading and then unloading of the plate was recorded. The hysteresis was expressed as a percentage of the maximum difference in these readings and the full-scale output.

Table 10. Force values recorded during the procedure of calculating hysteresis. (a=loading, b=unloading).

Loading Sequence	Maximum Force (N)	Average Force (N)	Average Difference (N)	Maximum Difference (N)	Relative Error (%)
1a	194.6	191.9	1.35	6.66	3.4
1 b	195.9	193.3			
2 a	388.4	385.9	0.84	6.25	1.6
2 b	389.7	386.8			

3 a	580.2	577.5	0.84	6.26	1.1
3 b	581.0	578.3			
4 a	771.1	768.5	0.08	5.95	0.8
4 b	771.6	768.6			

Table 10 presents maximum and average forces recorded during the procedure to estimate the errors due to hysteresis. The largest relative error, 3.4%, was recorded during the loading sequence of the first plate which corresponded to a full-scale output error of 0.03%. Bartlett [66] suggested a value below 0.5% of the full-scale output was suitable, therefore, the error of hysteresis for the force platform was acceptable.

Non-linearity

Non-linearity refers to the deviation of a linear response between the actual load applied to the plate and the corresponding measured output by the force platform. To assess this difference the output readings from the Kistler 9281EA platform were compared the output readings of an AMTI force platform (Model: BMS600900-2K). The five plates were loaded into the middle of both platforms. The non-linearity was quantified at various load levels by comparing the measured value to the expected linear response.

Table 11. Difference in forces calculated during the procedure of calculating the non-linearity.

Loading Sequence	Average Difference (N)	Relative Error (%)
1	2.3	1.2
2	5.4	1.4
3	8.1	1.4
4	10.9	1.4

The linear response between the two readings was 0.99. The maximum difference between corresponded to a full-scale output error of 0.05% which was considerably lower the recommended acceptable value of 0.5% [66].

Crosstalk

Crosstalk refers to the interference of forces between channels in orthogonal axes which arises due to misalignment of the piezoelectric sensors within the platform. The forces in the Fx and Fy directions were measured when a single plate was placed in the centre of the force platform. The crosstalk was assessed for different loading durations between 5 to 240 s.

Table 12. Forces measured in the x and y directions during the procedure of measuring crosstalk when only a vertical force (z) is applied.

Duration (s)	F_x			F_y		
	Minimum Force (N)	Maximum Force (N)	Average (N)	Minimum Force (N)	Maximum Force (N)	Average (N)
5	-2.32	-1.02	-1.67	-3.10	-1.31	-2.20
90	-3.46	-3.46	-1.02	-5.77	-1.31	-3.54
240	-1.02	-5.71	-5.71	-11.68	-1.31	-6.49

The relative error was influenced by the duration of the loading period. Crosstalk was observed to be smallest during shorter duration loading. The maximum error was observed for the 240 s duration, measuring a relative error of 1.71 % and 3.29 % in the Fx and Fy direction. This equated to a full-scale output error of 0.02 % and 0.03 %. The contact time for a football at 6 $m \cdot s^{-1}$ is approximately 10 ms, therefore the influence crosstalk during this loading duration is assumed negligible.

The errors for hysteresis (0.03 %), non-linearity (0.02 %) and crosstalk (0.03 %) all fell within the acceptable recommendations outlined by Bartlett [66]. Psycharakis and Miller [39] quote the maximum error as a combination of hysteresis and non-linearity when a vertical force only is applied, in this study this would result in 5.5 % (hysteresis 3.4 % and crosstalk 2.1 %).

4.5.3 Measuring impact variables using a force platform

Operating the force platform and HSV using a single trigger

The acquisition of force data is controlled using the Kistler Bioware software. The force platform can be operated using two trigger options; triggering when a threshold voltage level is reached or manually triggering using the laptop. However, the Kistler BioWare software cannot receive a trigger.

Selecting an appropriate trigger method to allow trigger-synchronisation between the force platform and camera provided several advantages; it simplified the experimental set up, allowed for comparison between the visual and force data and reduced post-processing to align the datasets manually.

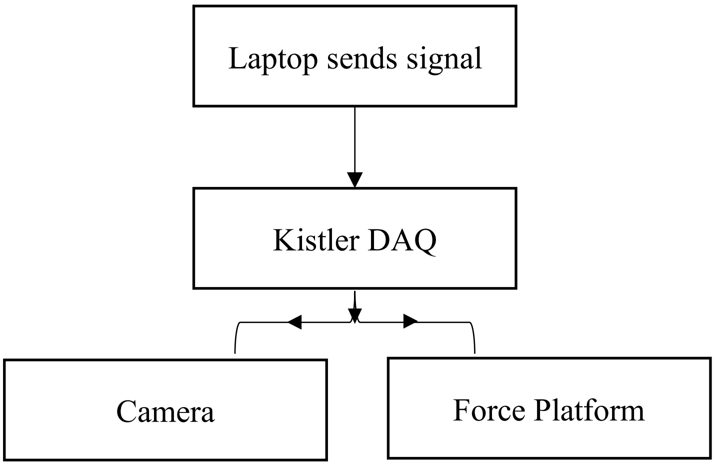

Figure 35 Path of signal to trigger the acquisition of video and force.

The control port of the DAQ included a trigger-emitting pin [137]. To achieve trigger synchronisation between the force platform and camera, a custom cable connected the DAQ to the camera was made, with the laptop serving as the master trigger. The signal was emitted by Bioware to begin the acquisition, which was then split between the camera and force platform, as depicted in Figure 35. Using an oscilloscope, it was determined that the signal was a 5 V square waveform triggered on the leading edge. Camera settings were adjusted accordingly to match this signal. Verification of trigger synchronisation was carried out using a rigid impact hammer, which revealed the alignment of the time stamp between the camera frame displaying initial contact and the initial increase in the force platform dataset.

Data Processing

A function was scripted in MATLAB to automatically extract force-time profiles for each impact from the output of the force platform. The unfiltered force-time data was exported from Bioware and processed using the function on MATLAB. The function searched for consecutive increases in the data to define the start position of the loading phase. The endpoint was defined when the data returned to zero. The number of specified points was 15 and 25 for the impacts at 6 and 20 m·s^{-1}, respectively. A verification assessment confirmed the functions accuracy, aligning with the image frame where the football appeared to make first contact with the force platform within ± 2 frames for 25 impacts.

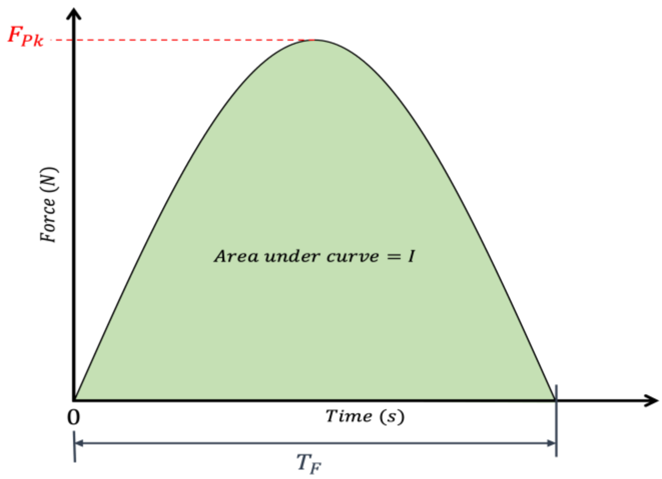

Figure 36 Schematic showing where measurements of impact variables are made using the force-time profile

Peak Force (F) *and Impulse* (I)

The peak force was extracted by finding the maximum value in the series extracted. The impulse was calculated by integrating the series using the trapezium rule. Both variables are shown in Figure 36**.**

Contact Time (T_F)

The force platform provides an additional method to define the contact time that is more automated than manual digitisation. It is defined as the time taken for the force to return to zero, as depicted in Figure 36**.**

Deformation (x)

The displacement of the centre-of-mass (COM) was obtained through integration. The acceleration of the football is obtained by dividing the force by the mass of the football. The acceleration was integrated using the trapezium rule to attain velocity. The constant was found by applying the inbound velocity (measured using the HSV) at time t = 0. The velocity was integrated to give the displacement. The constant was found by applying zero displacement at time t = 0. The three curves are shown below in Figure 37.

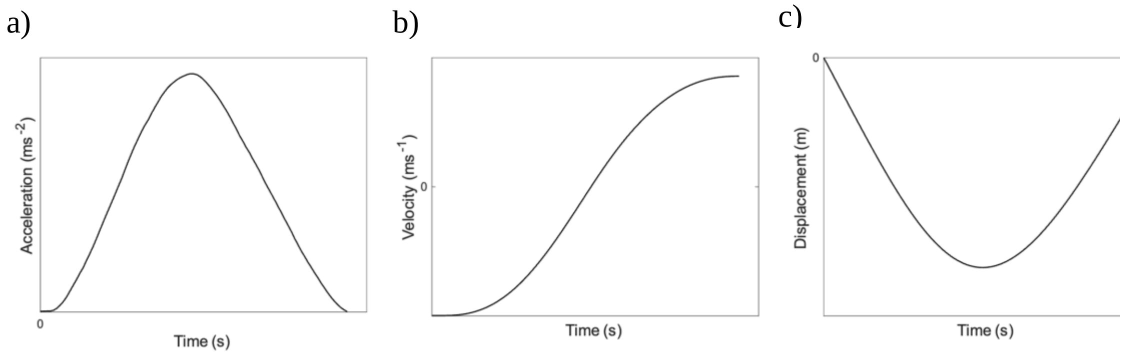

Figure 37 Examples of the curves calculated using the force-time data for a football impacting a force platform: (a) acceleration-time (b) velocity-time and (c) displacement-time.

4.6 Repeatability of Force Platform Measurements

Understanding the sensitively or precision of the equipment used to measure the impact response of a football is crucial to be able to make valid comparisons between different footballs. The literature review did not reveal any evidence to suggest the sensitivity or precision of force platforms had been quantified before using it to make comparisons. To compare the loading behaviour of the 12 footballs accurately and reliably it is necessary to quantify these statistics. To investigate whether the precision of the force platform is suitable to make comparisons, the minimal detectable difference (MDD) will signify the smallest change in a measure impact variable that can be reliably distinguished from noise in the measurement process. This section outlines the procedures to determine the repeatability of the force platforms to ensure an appropriate precision to enable accurate comparisons between different football models in Chapter 5.

4.6.1 Methods

Experimental Procedure

All procedures were approved by Sheffield Hallam University Research Ethics Board (ER40333305). Four FIFA Quality Pro certified footballs (Adidas Tiro Pro; size 5, 32 panel, thermally bonded, mass = 434.0 ± 1.1 g) were inflated to an internal pressure of 0.80 ± 0.01 bar. Each football sample was conditioned (temperature 20 °C; humidity 65%) using a climate chamber (Climacell 404; MMM Medcenter Einrichtungen GmbH) for at least 24 hours prior to impacting. Two samples were used at the certification test velocity (6 $m \cdot s^{-1}$) and the other two samples were used at a higher velocity (20 $m \cdot s^{-1}$). Fifty repeated impacts were performed at each velocity condition. The footballs were accelerated towards the force platform using the launch methods outlined in section 4.2.The orientation of the football was controlled prior to release to avoid direct impacts on the valve. The football impacted a floor-mounted piezoelectric force platform (9281EA, Kistler Holding AG, dimensions; 600 x 400 mm, natural frequency; 1 kHz) without spin and above one of the corner sensors to reduce undesirable oscillations in the system. Two high-speed cameras were positioned at a stereo angle of 45° to ensure that at maximum deformation the football did not encroach the side or front edge of the force platform. All impact tests were performed on separate days in a laboratory at room temperature 20.7 ± 0.75 °C at a relative humidity of 35.8 ± 5.5%.

Statistical Analysis

The first five impacts for each football were discarded to account for the Mullins effect, outlined in Section 2.4.1. Unfiltered force-time data were acquired from the force platform using BioWare (5.4.3.0, Kistler Holding AG). These were processed in MATALB using the method outlined in 4.5.3 to calculate the peak impact force and the impulse.

Normality of each impact metric was assessed using Shapiro-Wilk tests, P ≥ 0.005 (SPSS, 26.0.0.1, IBM Corporation). The impulse at the certification test velocity and peak impact force at the higher velocity exhibited a skewed distribution, these were log-transformed prior to analysis. Paired t-tests ($\alpha = 0.05$) were used to compare the means of the impact variables between the two footballs at each inbound velocity. The results were used to detect statistical differences between the footballs. Percentiles and the intraclass correlation coefficient $(ICC)_{(2,1)}$ were calculated to test the relative repeatability of each metric. Absolute repeatability was assessed using the coefficient of variation (CV) and MDD. ICC values ≥ 0.9 and CV values ≤ 10% were interpreted as high repeatability [138].

Where data had been transformed, the MDD was converted to the scale of the original dataset using the back transformation and arithmetic mean of the transformed dataset ($mean_{ln}$) [139]:

$$MDD_{raw} = \exp(mean_{ln}) - \exp\,(mean_{ln} - MDD_{ln}) \qquad \text{4-6}$$

To verify the accuracy of the magnitude and duration of the impact, the experimental impulse (I_t) (calculated from the velocity change measured by the high-speed camera) was compared to the theoretical calculated impulse (I_e) (calculated from the force trace measured by the force platform) for impacts between the two samples using the root-mean square error (RMSE):

$$RMSE = \sqrt{\sum_{i-1}^{n} (I_{it} - I_{ie})^2} \qquad \text{4-7}$$

4.6.2 Results

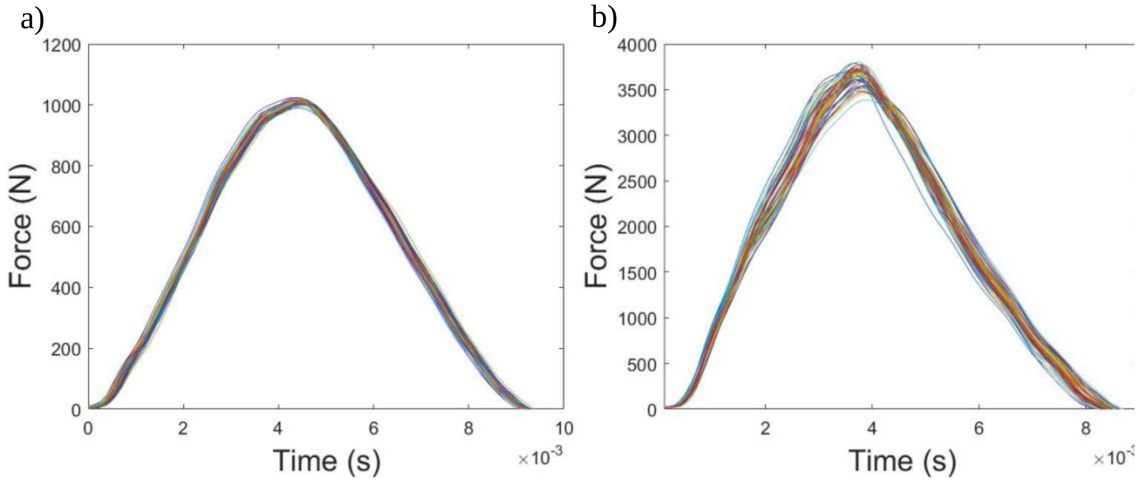

Figure 38 Raw force-time output signal for all impacts at (a) 6.04 m·s^{-1} and (b) 19.4 m·s^{-1}.

Figure 38 presents the raw output signals from the force platform at both impact conditions for all trials. The magnitude of error between the theoretical and experimental estimation of impulse accounted for less than 1% of the median value (19.4 m·s^{-1}; 0.06 Ns, 6.04 m·s^{-1}; 0.04 Ns). No statistical differences were found for any metric between samples (R = 0.76-0.98, $P \leq 0.001$). All metrics indicated good agreement between samples at each velocity: 19.4 m·s^{-1} ($ICC_{2,1}$ = 0.94-0.98) and 6.04 m·s^{-1} ($ICC_{2,1}$ = 0.96-0.98). The MDDs are presented in Table 13, for all variables, the MDD accounted for 15% of the confidence interval between the 5% and 95% percentiles. Figure 39 shows the distribution curves for the impact variables at 6.04 m·s^{-1}; the non-parametric distribution of impulse is visually apparent (P = 0.000). Likewise in Figure 38, the non-parametric distribution of peak impact force is visually apparent at 19.4 m·s^{-1} (P = 0.000).

Table 13. Summary of statistics for impact variables measured from a normal inbound football impact

Inbound Velocity (m·s^{-1})	Metric	Median	5% Percentile	95% Percentile	Range	Sd	ICC	MDD	CV (%)
6.04	Peak Force (N)	1011.2	1003.9	1019.5	15.6	4.56	0.98	1.96	0.45
	Impulse (Ns)	4.81	4.79	4.83	0.05	0.01	0.96	0.01	0.18

19.4	Peak Force (N)	3693.6	3445.4	3786.3	340.90	73.46	0.98	28.5	0.25
	Impulse (Ns)	14.80	14.71	14.91	0.20	0.06	0.95	0.04	0.39

sd standard deviation, ICC intraclass correlation coefficient, MDD minimum detectable difference, CV coefficient of variation in percentage

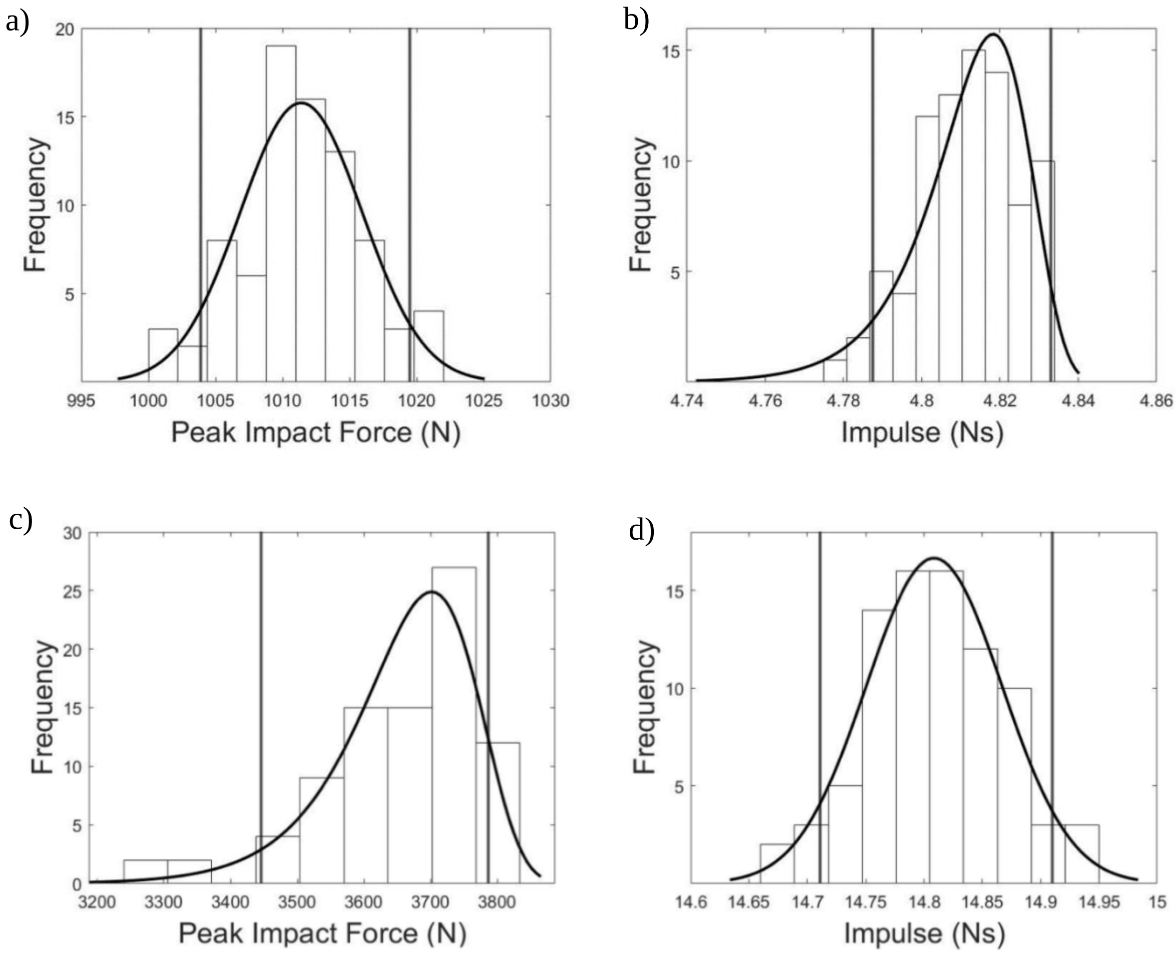

Figure 39 Histograms with distribution fit for (a) peak force and (b) impulse at 6.04 m·s^{-1} and (c) peak force and (d) impulse at 19. 4 m·s$^{-1.}$

4.6.3 Sample Size Calculations

In sections 4.4.3 and 4.6., the precision of the measuring equipment was determined. It was necessary to calculate a suitable sample size that would allow statistically significant comparisons between footballs. The standard deviation (σ) and minimal difference (MD) were used with a confidence level of 95 % to calculate the sample size shown in equation 4-8 [140].

$$n = \frac{(Z^2 \cdot \sigma^2)}{MD^2} \qquad 4\text{-}8$$

The MD represents the smallest difference between the mean of the impact variables between footballs. The MD is a critical component of sample size calculations as it determines the number of repeated impacts required to be able to detect the effect of interest.

The sample size was guided by the peak impact force as this measure exhibited the highest variation compared to the other variables. The variation across the repeated impacts of a single sample (n = 50 impacts) was used as the standard deviation in the calculation. To identify a suitable sample size, iterations were performed using different suitably chosen values of MD for peak impact force. The iterations were based on differences observed between the mean value between the three footballs used in the study outlined in 4.6. The results of the calculations are shown in Table 14. The standard deviation for the certification test velocity was 10 N and 160 N at the higher velocity.

The number of repeated impacts fell considerably as the MD increased, indicating that a larger difference between the mean impact variables of different footballs allowed for reduced sample sizes. It is crucial to balance the time and resources during the data collection while ensuring statistical significance among the results. The average difference between the mean peak impact force between the footballs used in the repeatability test was 17 N and 82 N, to meet this minimal difference a sample size of 1 and 15 would be required. As the differences between the footballs that will be used is unknown, a sample size 25 was chosen. This would allow differences above 4 N and 63 N to be determined to a degree of statistical significance. This gave a total sample size of 300 for each impact variable for the12 footballs.

Table 14. Summary of statistics for sample size calculations

Velocity	MD (n)	Sample Size
Certification Test Velocity	2	96
	5	15
	10	4
	25	1
Higher velocity	30	109
	50	39
	80	15
	100	10

4.6.4 Discussion

Previous research had not required the SEM and MDD to be quantified as the force-time trace obtained using a commercially available force platform had been used to validate mathematical models rather than to compare the impact variables between footballs. It was essential to quantify the measurement precision prior to the data collection to understand the smallest change that can be reliably detected within a set of repeated measurements. This informed whether the force platform was suitable for the application of comparing load behaviour between footballs. The SEM provides an estimate of the random error in the data observed during repeated impacts of a football and was used to calculate the MDD.

Good agreement was found between the theoretical and force platform calculated value of impulse that gave confidence in the measurements. Peak impact force and impulse were measured as these metrics characterise the shape of the force-time curve. Repeated impacts at both velocity conditions demonstrated high absolute ($CV \leq 10\%$) and relative ($ICC \geq 0.94$) repeatability. High repeatability in these metrics demonstrated that the force platform can consistently measure the dynamic response of a football when impacted above one of the corner sensors [39].

Slightly larger confidence intervals and lower repeatability statistics were observed at the higher velocity. This was attributed to the use of a motorised launch device, that introduced greater variation in the impact orientation and location on the force platform that could have resulted in a larger variation in impact variables [113].

Despite the variability, the MDDs of peak impact force and impulse at both velocity conditions accounted for less than 1% of the mean value of each variable. Providing the differences in impact variables exceed the MDD's, the force platform can be used to detect differences in loading behaviour between different models of footballs.

4.7 Conclusions

This chapter determined the repeatability of measuring the deformation and loading behaviour of a football using high-speed video and a Kistler 9281EA force platform for normal-inbound impacts at 6 and 20 $m \cdot s^{-1}$. These velocities were based on existing policy test protocols and a trajectory model estimating the upper limit of match-encountered impact velocities. The technical specifications of the force platform including the natural frequency and rigidity were carefully considered to avoid system vibrations corrupting the output signal. The results of the repeatability study showed high absolute and relative repeatability, which suggests the combination of equipment can consistently measure the dynamic response of a football with high sensitivity. Future research should measure the impact behaviour of the twelve difference footballs using the equipment and methodologies outlined in this chapter.

5 Dynamic Behaviour of a Football – Results

5.1 Introduction

In chapter 4, a laboratory-based experiment to measure impact variables that characterise the deformation and rebound characteristics of a football for a collision with a force platform was validated. In brief, a single high speed video camera was used to measure impact variables including the coefficient of restitution (COR), contact time, deformation and contact length. A force platform was used to measure the impact forces and to calculate the impulse of the collision.

The footballs will be impacted at two velocities; 6 and 20 $m \cdot s^{-1}$, which were consistent with the speeds studied by other researchers conducting similar experiments [36,58,59]. The velocity of 6 $m \cdot s^{-1}$ was stipulated to align with the FIFA certification test [1]. The higher velocity was chosen to represent the upper limit of normal in-bound velocities that a football could experience in match play. This velocity will involve larger deformations and impact forces which is thought to accentuate the influence of material composition on the results. However, no study has previously confirmed the statistical significance amongst results of multiple footballs to confirm this finding.

This chapter presents and discusses the results from impact tests performed on 12 different FIFA-Pro certified footballs. All procedures were approved by Sheffield Hallam University Research Ethics Board (ER45419121). The selection of these footballs was described in Chapter 3. This section works towards achieving objective 4 of the doctoral study and will serve as the data to develop relationships in Chapter 6.

5.2 Experimental Results

To compare the results between different footballs, a one-way ANOVA with a post-hoc Tukey test was performed on each of the impact variables using SPSS with a confidence level of 0.05. The Pearson’s product moment correlation coefficient was calculated using

SPSS to assess for linear correlations between impact variables. A significance level of 0.01 was used. Coefficients between $0 \leq r < |0.5|$ were interpreted as low correlations, coefficients between $|0.7| \leq r < |0.9|$ were interpreted as high and $|0.9| \leq r < |1|$ as very high [141].

5.2.1 Impact variables measured using High Speed Video.

The following section presents the results for the impact variables measured using the high-speed camera. These include the inbound velocity used to calculate the coefficient of restitution, the contact time, deformation and contact length, illustrated in Figure 40.

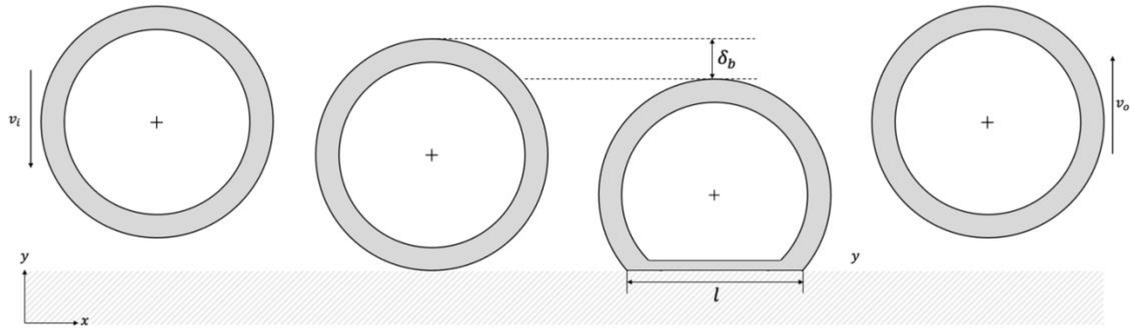

Figure 40 Sequence of ball impact depicting the measured impact variables: in and out-bound velocity, ball deformation and contact length.

Inbound Velocity

The average inbound velocities were 5.93 ± 0.1 m·s^{-1} and 19.2 ± 0.2 m·s^{-1}. Figure 41 presents the mean and standard deviation across 25 repeated impacts for each football. The variability among repeated impacts was larger at the higher velocity with a standard error of 0.1 m·s^{-1} compared to 0.01 m·s^{-1} at the 6 m·s^{-1}. The differences between the mean inbound velocity among the footballs were more pronounced at the higher velocity (Figure 41b) which led to a greater number of significant differences detected in the results of the ANOVA. Across the total number of pairings (66), 72% of velocities were statistically different ($p < 0.05$). At 6 m·s^{-1}, no statistically significant relationship ($p < 0.01$) was found between impact velocity and any other impact variable. A statistically significant but relatively weak relationship was found between the in- and out-bound velocity r < 0.5, $p < 0.05$. At the higher velocity, relatively weak significant relationships ($p < 0.01$) were observed with contact time (r = - 0.3), COR (r = - 0.2), impact force (r = 0.4) and impulse (r = 0.5).

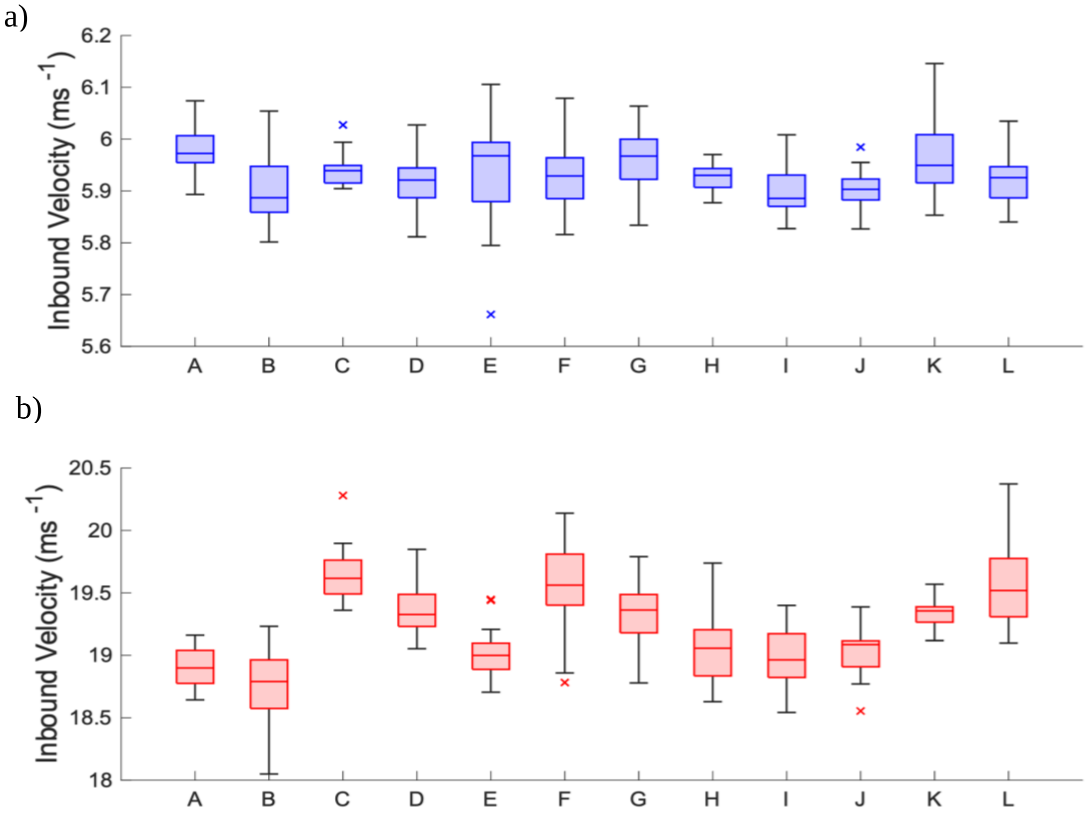

Figure 41 Box plots showing the distribution of inbound velocities for each football model at (a) 6 m·s^{-1} and (b) 20 m·s^{-1}. Outliers are indicated using a (x). The intervals on the y-axis have been adjusted to account for the increased range observed at 20 m·s^{-1} to ensure the variability among the repeats was depicted clearly.

Coefficient of restitution (COR)

To allow a direct comparison between the data at the two velocities, the results of the COR for each football are presented in Figure 42. The results for each football are grouped; the COR at 6 m·s^{-1} (labelled as CT: 'certification test') and 20 m·s^{-1} (labelled as HV: 'higher velocity') are shown by the blue and red lines, respectively, any outliers are indicated by crosshairs. The COR decreased from the 6 m·s^{-1} to 20 m·s^{-1}. Figure 42 shows that there was more variability between the upper and lower quartiles for the impacts at 20 m·s^{-1} compared to at 6 m·s^{-1}, where there were more significant differences observed among the footballs. The average difference: defined as the difference between the mean of two pairings of footballs, was larger at the higher velocity; 0.02 compared to 0.01.

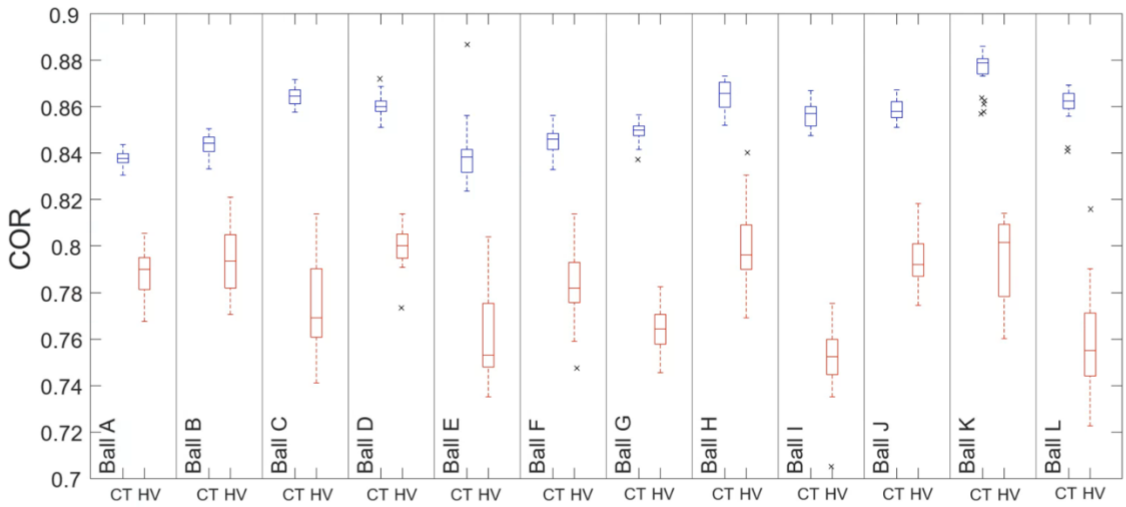

Figure 42 Box plots showing the COR for each football model: 6 m·s^{-1} ('CT'- blue) and 20 m·s^{-1} ('HV'- red). Outliers are indicated using a (x).

Contact Time

To allow a direct comparison between the data at the two velocities, the results of the contact time are shown in Figure 43. The average contact time among the footballs reduced from 9.0 ± 0.1 ms to 7.7 ± 0.2 ms for impacts at 6 m·s^{-1} and 20 m·s^{-1}, respectively. There were more significant differences detected between footballs at 6 m·s^{-1} (79% and 41% at 20 m·s^{-1}). Unlike the COR, the magnitude of difference between the footballs was larger at 6 m·s^{-1}; 0.3 ms compared to 0.2 ms.

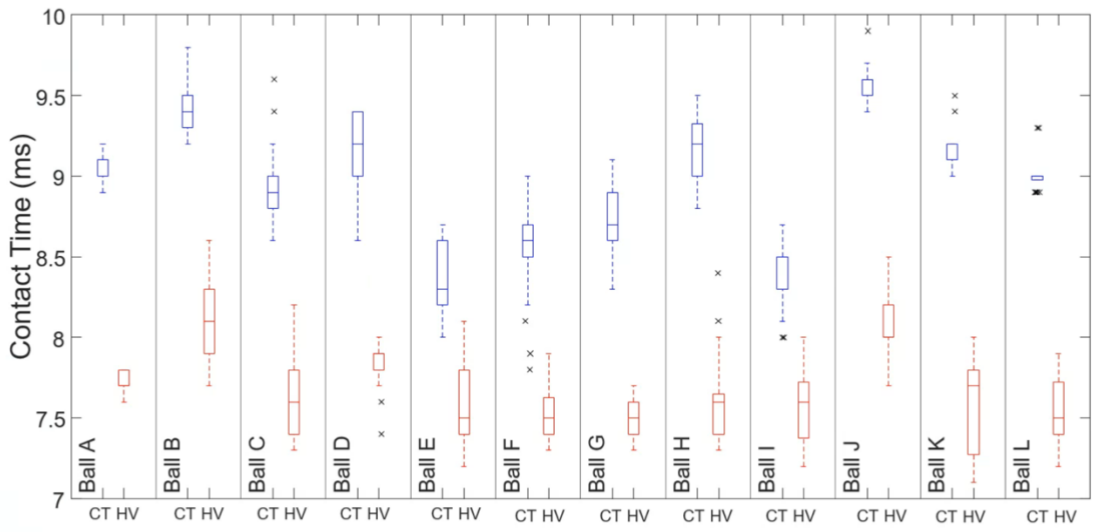

Figure 43 Box plots showing the contact time for each football model: 6 m·s^{-1} ('CT'- blue) and 20 m·s^{-1} ('HV'- red). Outliers are indicated using a (x).

Deformation

The average deformation among the footballs was 17.6 ± 0.6 mm and 49.0 ± 2.1 mm for the impacts at 6 m·s^{-1} and 20 m·s^{-1}, respectively. Figure 44 presents the mean and standard deviation across 25 repeated impacts for each football. Statistical differences were found between approximately 60% of pairings of footballs at both velocities. Larger differences between the mean results were observed for the higher velocity. The average magnitude of difference was 2.7 mm at the higher velocity compared to 1.0 mm at 6 m·s^{-1}.

The relationship between contact time with deformation is shown in Figure 45. A strong significant ($p < 0.01$) correlation was found between the contact time and deformation was observed for the impacts at 6 m·s^{-1} (Figure 45a, r = 0.96) and 20 m·s^{-1} (Figure 45b, r = 0.92).

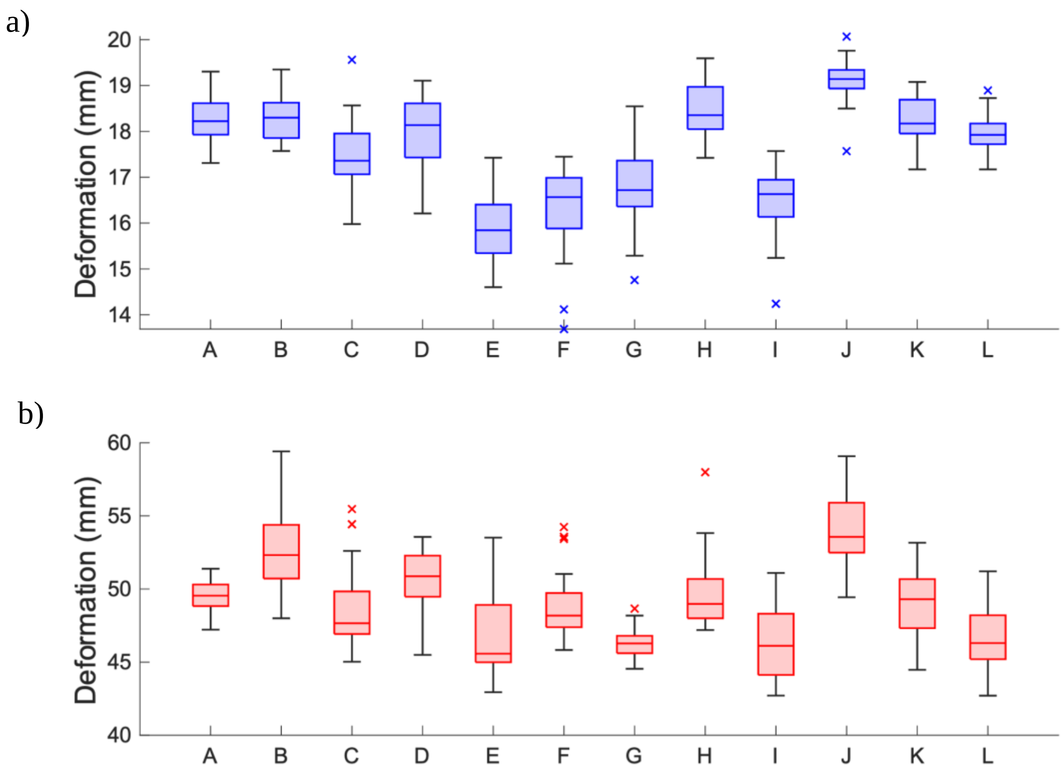

Figure 44 Box plots showing the distribution of the deformation for each football model at (a) 6 m·s^{-1} and (b) 20 m·s^{-1}. Outliers are indicated using a (x). The intervals on the y-axis have been adjusted to account for the increased range observed at 20 m·s^{-1} to ensure the variability among the repeats was depicted clearly.

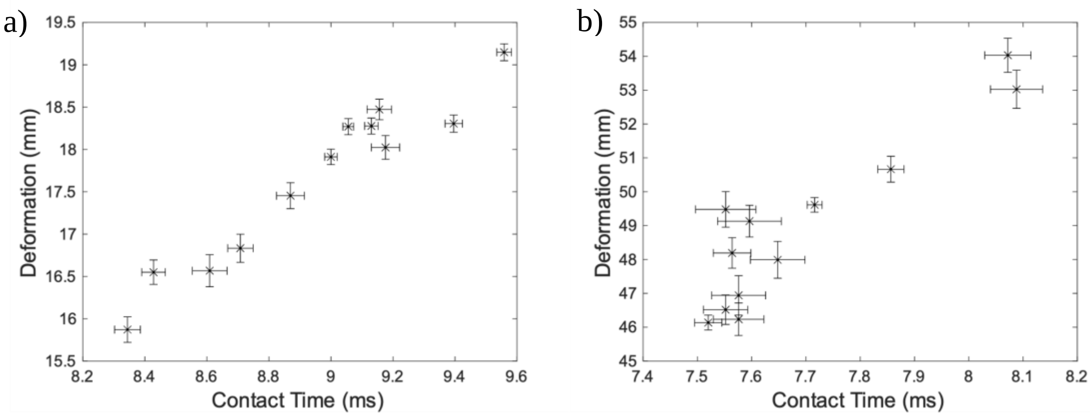

Figure 45 The deformation plotted against contact time for the impacts at (a) 6 m·s^{-1} and (b) 20 m·s^{-1}. The error bars outline the standard error of measurement for contact time (horizontal) and deformation (vertical). The intervals on the y-axis have been adjusted to account for the increased range observed at 20 m·s^{-1} to ensure the variability among the repeats was depicted clearly.

Contact Length

The results for contact length are shown in Figure 46, the amount of lateral deformation increased at the higher inbound velocity due to the increased vertical deformation. A lower number of significant differences were detected between footballs compared to the other variables; 54% and 32%. However, the average magnitude of difference between the footballs was the similar 3 mm compared to 2.4 mm for the impacts at 6 and 20 m·s^{-1} respectively.

a)

b)

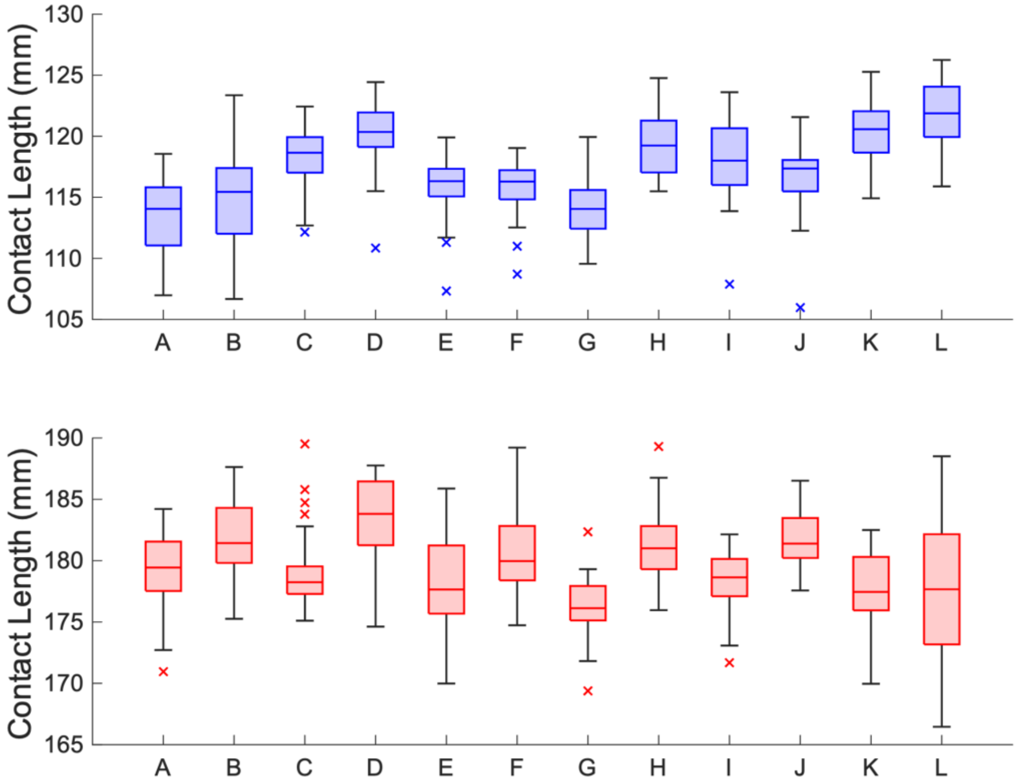

Figure 46 Box plots showing the distribution of the contact length for each football model. Certification velocity (a) and the higher velocity (b). Outliers are indicated using a (x). The limits of the y-axis have been adjusted to account for the variation among the repeats for the impacts at 20 m·s^{-1}.

5.2.2 Impact variables measured using a force platform.

Figure 47 presents the force-time curves for two randomly selected footballs at 6 m·s^{-1} (Figure 47a) and at 20 m·s^{-1} (Figure 47b). At the 6 m·s^{-1}, the force trace of all footballs was highly symmetrical around the peak force. At the higher velocity, the shape was asymmetric; the time taken during the initial deformation phase to peak impact force was 6% shorter than the restoration phase. Across the 25 repeated impacts there is visually more variation during the initial deformation phase of the curve at the higher velocity.

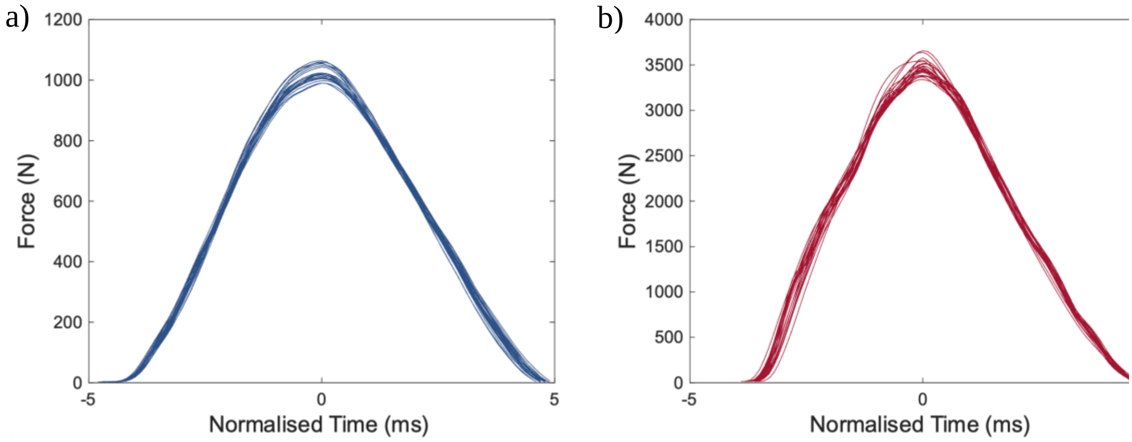

Figure 47 Force-time curves for a single football at (a) 6 and (b) 20 m·s^{-1} for 25 repeated impacts. The contact time has been aligned with the time position of the peak impact force. The limits of the y-axis have been adjusted to account for the increased magnitude at the higher velocity.

The force-time curve was highly sensitive to the impact orientation of the football, the curves for 6 consecutive impacts are shown in Figure 48. At the peak impact force, for the 6 m·s^{-1} the range was around 100 N whilst at 20 m·s^{-1} the range was 300 N.

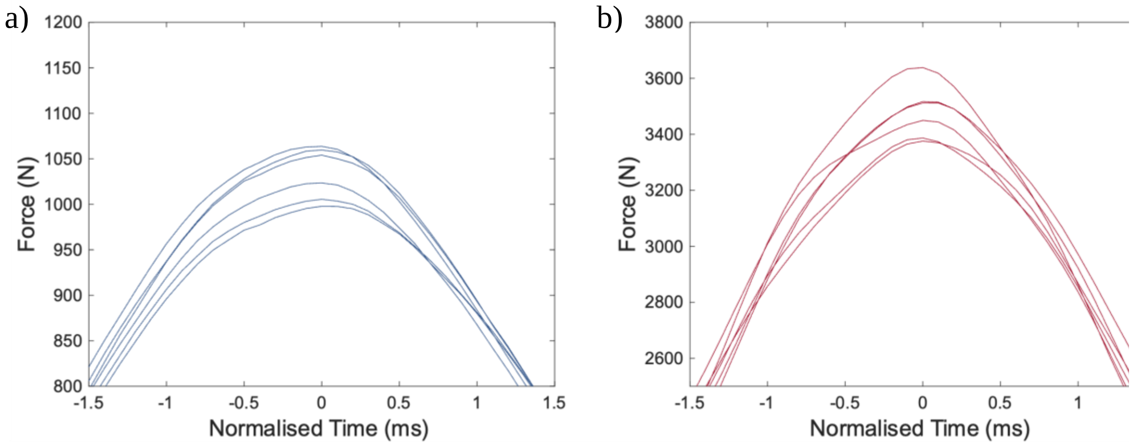

Figure 48 Enlarged portion of the force-time curves in Figure 47 showing -1.5 ms either side of the peak impact force for 6 impacts with visually different orientations at (a) 6 and (b) 20 m·s^{-1}.

Peak Impact Force

The results for peak impact force are shown in Figure 49. At 6 m·s^{-1}, 82% of pairings were significantly different compared to 52% at 20 m·s^{-1}. The magnitude of the difference was larger at the higher velocity 124.0 N compared to 42.5 N.

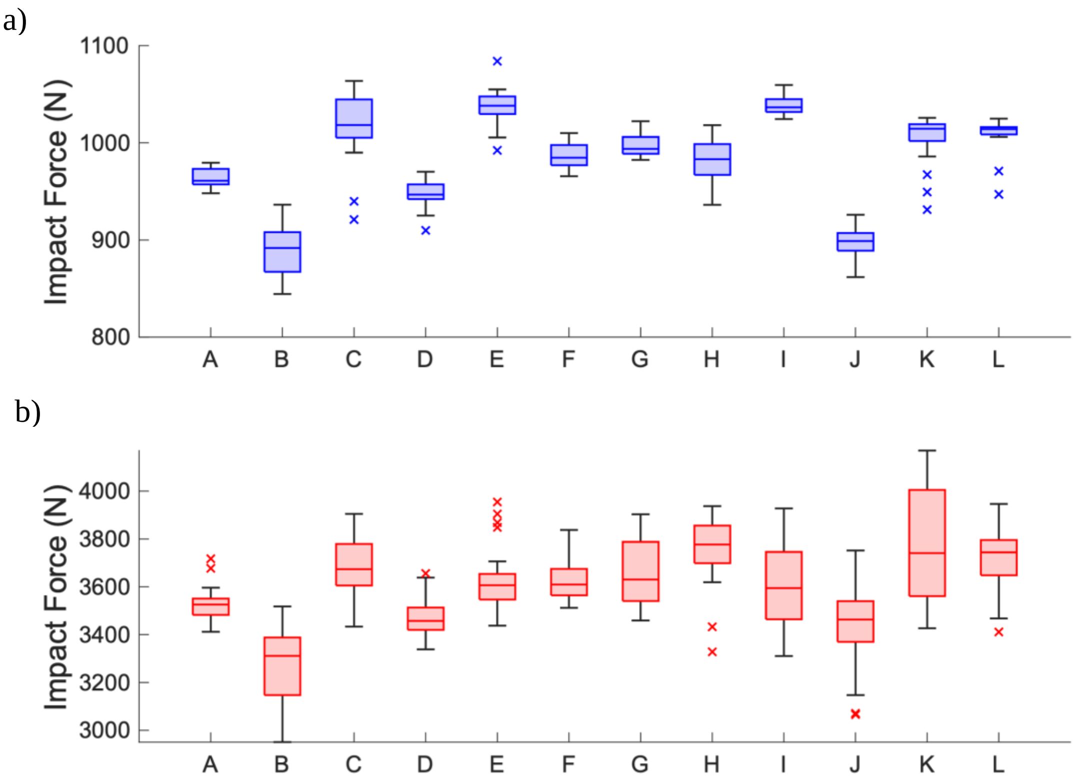

Figure 49 Box plots showing the distribution of the peak impact force for each football model at (a) 6 m·s^{-1} and (b) 20 m·s^{-1}. Outliers are indicated using a (x). The limits of the y-axis have been adjusted to account for the increased magnitude at 20 m·s^{-1}.

The relationship between impact force with contact time is shown in Figure 50. Multicollinearity was observed between impact force and contact time. There was a good significant ($p < 0.01$) negative correlation at both velocity conditions; at 6 m·s^{-1} $r = -0.82$ and $r = -0.85$ at 20 m·s^{-1}.

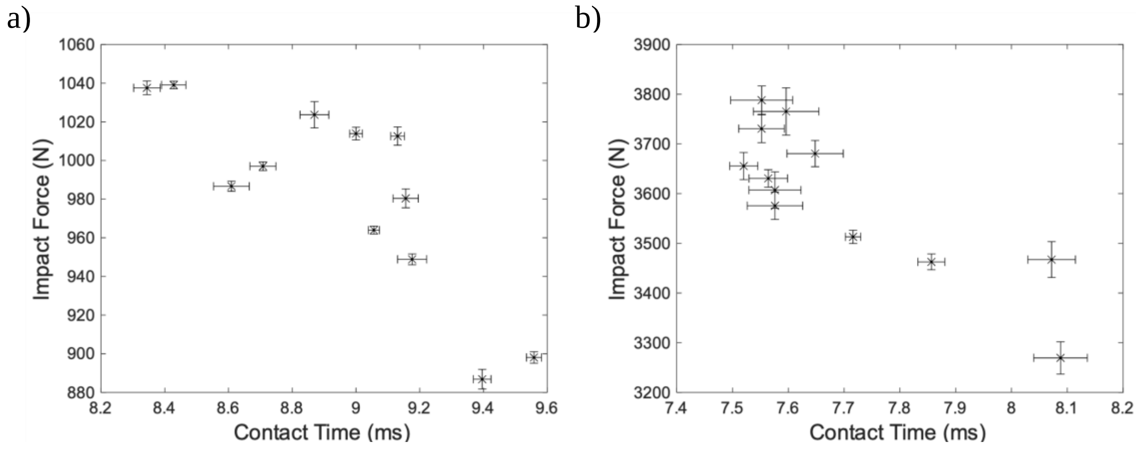

Figure 50 Graph showing the impact force plotted with contact time for the impacts at (a) 6 m·s^{-1} and (b) 20 m·s^{-1}. The error bars outline the standard error of measurement for contact time (horizontal) and impact force (vertical).

Contact Time Measured using the Force Platform

In the previous chapter it was shown that the contact time could be measured using both the high-speed video and force platform. The time stamp between the first visual contact on the high-speed camera and first increase of force measured using the force platform aligned within ± 1 frame, as outlined in Chapter 4 using an automated algorithm.

Figure 51 shows a single force trace marked with high-speed video frames to illustrate the difference in contact duration between the camera and the force platform. This figure shows that at the start of contact both time stamps between the two systems align. However, at the end of contact, the camera shows the football separated from the surface; a measured contact time of 8.7 ms. However, the force platform is still registering a force that that gives a contact time of 9.2 ms.

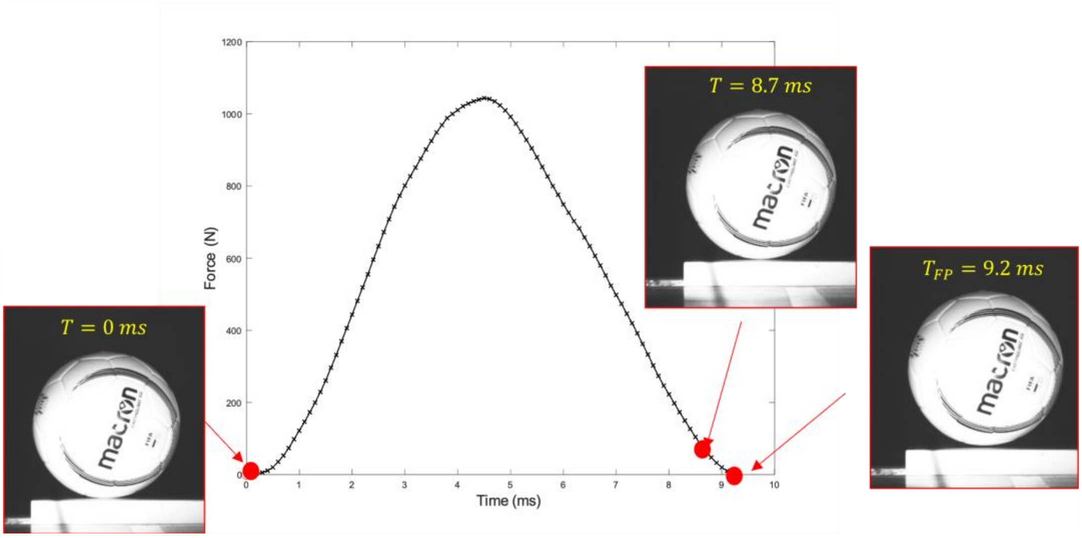

Figure 51 A force trace showed corresponding image shown on HSV. The initial contact at t=0, contact time measured by visually inspection the high-speed video frames and the contact time measured using the force platform showing the football has separated from the surface.

A Bland-Altman plot was used to assess the agreement between the duration of contact between the two systems [142]. The plots are shown in Figure 52, the negative y axes demonstrate that the contact duration measured using the force platform was longer for all impacts than when it was measured using the high-speed video. Since the resolution of contact time measured using the high-speed video was 0.1 ms, the limits of agreement in the Bland Altman plot were rounded to the nearest 0.1 ms. At 6 m·s^{-1}, the contact time may be 0.3 to 1.0 ms longer. At 20 m·s^{-1} the contact time may be 0.3 to 0.8 ms longer.

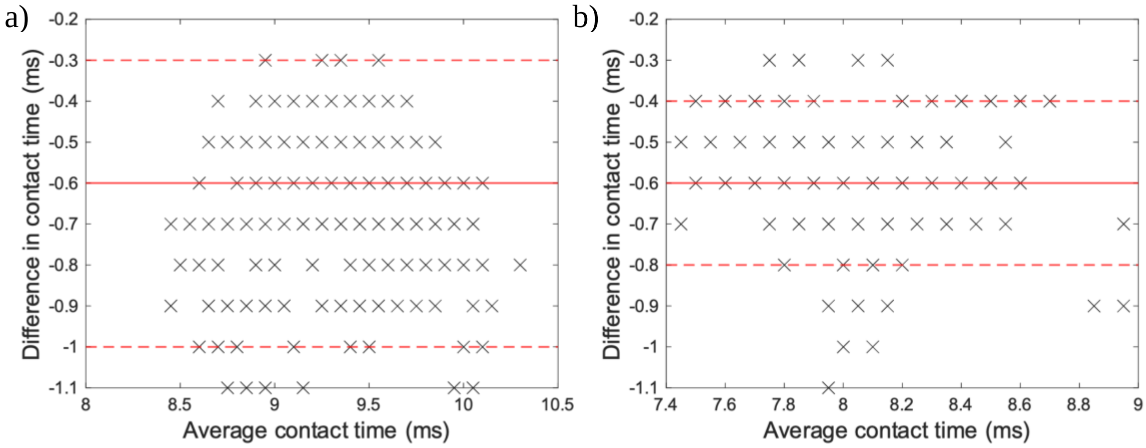

Figure 52 Bland Altman plots showing the difference between the contact time measured using the force platform to the high-speed camera at (a) 6 m·s^{-1} and (b) 20 m·s^{-1}.

The average random error for the contact duration between the two systems was 0.6 ms at both velocities. This error could influence the impulse measured using the force trace. In chapter 4 it was determined the precision of the force platform to measure the impulse was 0.01 Ns. Given that the discrepancy between the theoretical calculation of impulse and the measured value of impulse was 0.01 Ns, the impact of the error in the measurement of contact time on the calculated impulse was considered negligible.

5.2.3 Material anisotropy and deformation shapes

The effect of the anisotropy was alluded to during the static assessment of stiffness in Chapter 3. These effects were observed to influence the variability in the deformation behaviour and post-impact behaviour of the football during impact testing, which were particularly present at the higher velocity impacts where impact orientation was harder to control using the mechanical launch device. Figure 53 shows 4 frames captured at the maximum deformation for different impacts; the change in orientation of the football on impact can be appreciated by visually observing the change in position of the logo, highlighted in red, in the different frames. Across the 25 repeated impacts at the higher velocity, there was a range of 8.1 mm in deformation.

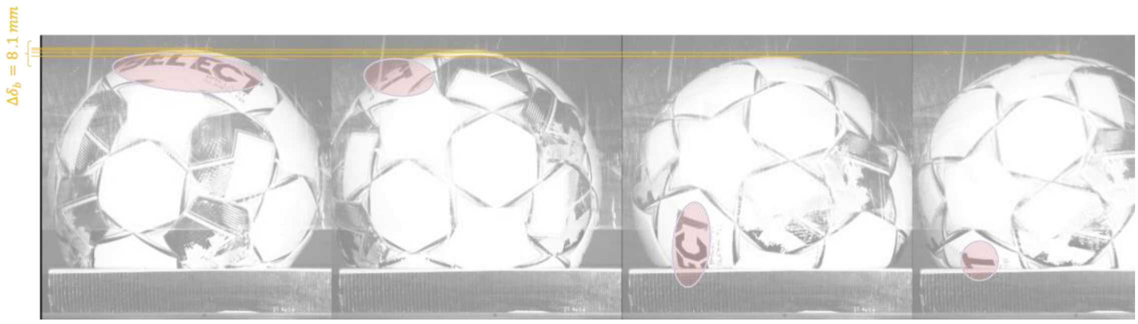

Figure 53 HSV images of the football at maximum deformation showing different orientations as indicated by the change in location of the single logo located on the football.

The location of the valve was observed to cause distortion of the football in the high-speed video frames. The sequence of events is shown in Figure 54b**,** arrows have been added to indicate the direction of travel. When the valve was located at either side of the centre of the geometry, the valve acted to displace the centre of the mass of the football. The added mass of the valve retains momentum towards the surface while the opposite of the football has entered the restitution phase (Figure 54b- sketch 3). The difference in localised motion causes lateral movement during rebound that generates a torque (Figure 54b-sketch 4) around the centre of mass that increases the rotational velocity of the football as it leaves the surface (Figure 54b- sketch 5).This phenomenon is further explained in Price's research [113].

a)

b)

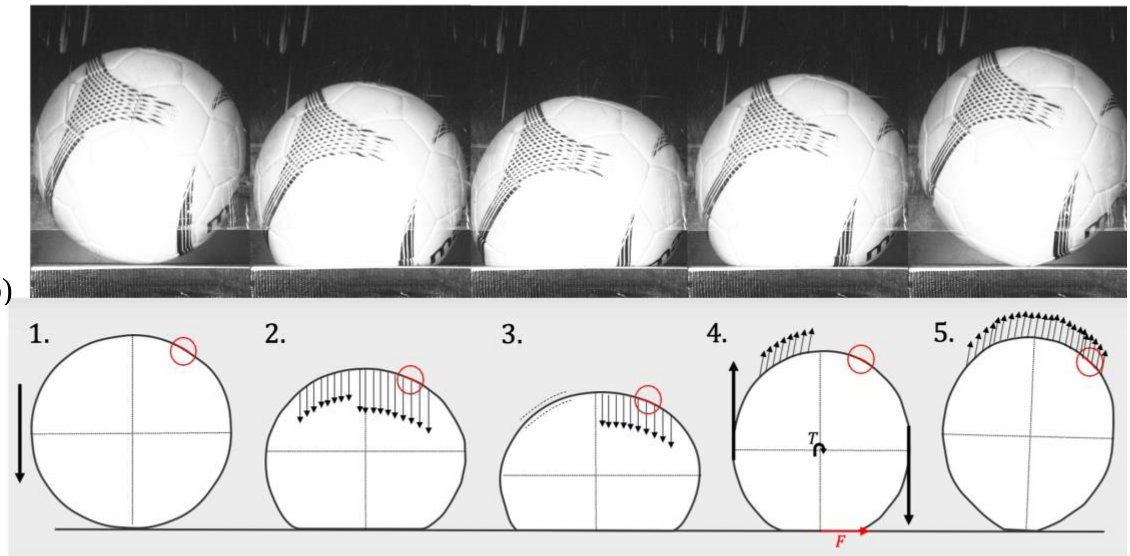

Figure 54 (a) Sequence of HSV images for an ball impact and (b) illustrations for an impact where the valve is located off centre. Arrows illustrate the direction of motion of the section of football. T (Toque), F (lateral force).

5.2.4 The correlation between static stiffness and dynamic impact variables

In Chapter 3 it was concluded that value of static stiffness of a football was influenced by way it was calculated. This factor could influence any perceived correlation between static and dynamic measurements. To ensure any potential correlation was not obscured by the method of calculation, the Pearson correlation was evaluated for each of the three stiffness values and the average measurement for each impact variable.

Figure 55 shows the stiffness of the football plotted against the average impact variable. Significant differences were only observed when the stiffness was evaluated using the 2nd order polynomial at a deflection of 3 mm. The significant differences were detected at varying strengths for contact time (6 m·s^{-1}; r = - 0.87, 20 m·s^{-1}; r = -0.58) and deformation (6 m·s^{-1}; r = - 0.87 and 20 m·s^{-1}; r = - 0.75) at both velocities.

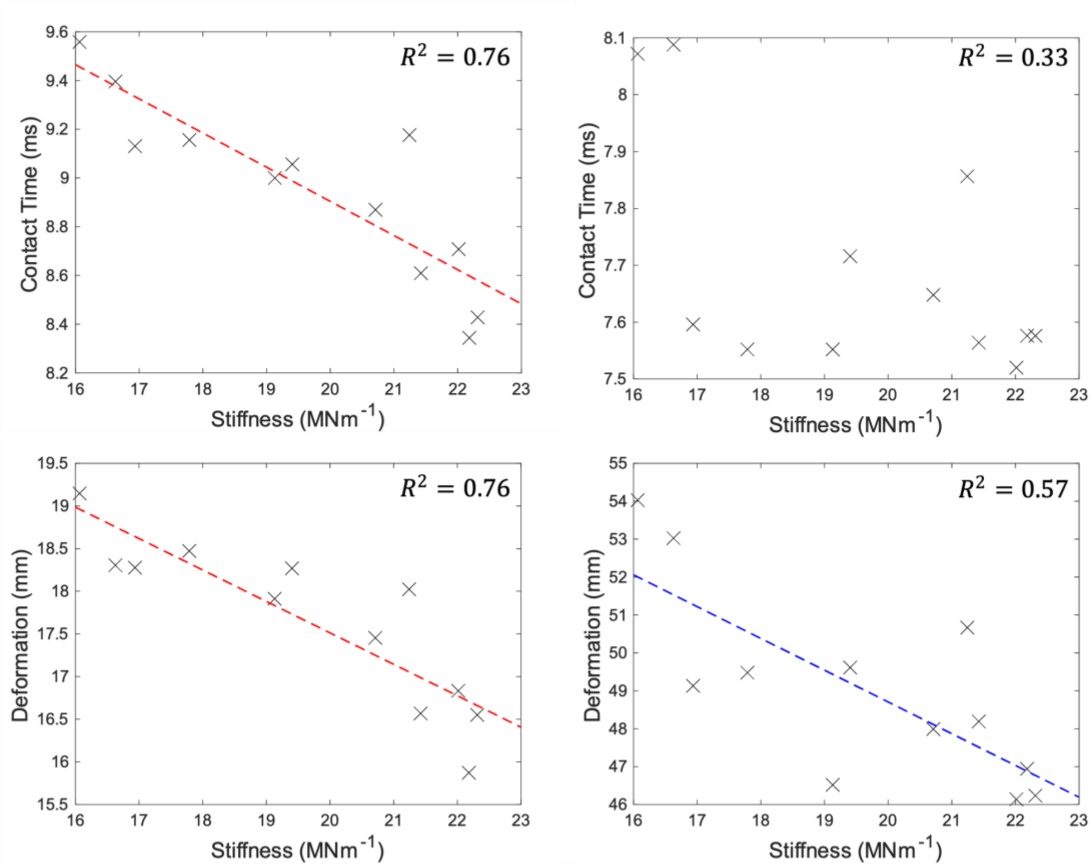

Figure 55 The quasi-static stiffness evaluated at 3 mm plotted against contact time and deformation at 6 m·s^{-1} and 20 m·s^{-1}. A dashed line was used to symbolised relationships that exceeded 0.7 for 6 m·s^{-1} (red) and 20 m·s^{-1} (blue).

No significant correlations were found between the stiffness and any of the impact variables that describe the damping properties of the football. Nor were any found when the stiffness was calculated using the other methods discussed in chapter 3.

5.3 Discussion

This chapter presented the experimental results for an impact between twelve different footballs and a force platform. The results showed that the sensitivity of the equipment was appropriate to detect statistical differences in the impact response for a relatively large number of footballs. Many more statistical differences were observed at 6 m·s^{-1} for the impact variables that are unrestricted by the existing certification policy such as contact time and deformation. The results of this investigation will be discussed in three parts, a) impact variables measured using high-speed video, b) impact variables measured using the force platform and c) the static and dynamic properties of footballs.

a) impact variables measured using high-speed video.

A larger number of statistical differences were found between the inbound velocities of the footballs at 20 $m \cdot s^{-1}$ than at 6 $m \cdot s^{-1}$. This was likely due to various factors including the feed direction, the properties of the football [29] and surface texture [67,143], that influenced the speed imparted onto the football using the mechanical device. These factors introduced more variability among the inbound velocities than simply releasing the ball from a height. Attempts to minimise the variations could not be achieved by altering the system parameters of the device, as the rotational speed of the mechanical wheels could only be increased by discrete intervals, that changed the imparted velocity far greater than the differences between the footballs. At both velocities, the outbound velocity had a weak significant relationship ($r = 0.4$) with inbound velocity, suggesting other mechanisms were responsible for the difference in outbound velocity such as material composition or the physical properties of the footballs. This suggests that despite variations in inbound velocity arising between the footballs at both impact velocities, it was not a confounding factor for the differences observed in the overall impact response between the footballs.

The dynamic impact response of the football was characterised by the COR, contact time, deformation and contact length.

As the FIFA Quality Programme (FQP) confines the interval for rebound height and the FIFA-Quality Pro certification has the narrowest acceptance interval, it was unsurprising that minimal differences were observed among the COR values for the different footballs at either velocity. The average difference between the football's outbound velocities was 0.1 at 6 $m \cdot s^{-1}$ and 0.3 at 20 $m \cdot s^{-1}$, the increase corresponding to the rise in inbound velocity. Whilst the differences were statistically significant, exceeding the standard error, it is unlikely they would be perceptible to players. Visual inspection of the high-speed video frames showed that the position of the valve affected the post-impact motion of the football. However, unlike previous work that had only considered the single inner-bladder layer [11], the results in this study showed lower variability among the repeated impacts for measurements of COR, contact time and deformation. The results demonstrated that footballs can be constructed using different materials yet exhibit similar damping behaviour, as supported by Hendee [32]. In a sport with frequent interactions between a player's body and the football, this finding holds potential for manipulating the mechanical properties of a football to achieve a desired impact response that minimises impact severity while maintaining consistent rebound behaviour in line with the current FQP standards.

The contact time is governed by the material properties and internal air pressure of the football, it is affected by how quickly the football can deform and then restore its spherical shape. When evaluated at a deflection of 3 mm, the quasi-static stiffness showed strong correlations with contact time and deformation, inferring that a football with a stiffer construction will exhibit lower deformation and shorter contact times but will exert higher restoring forces. A larger number of differences were observed between the contact times of the football at 6 $m \cdot s^{-1}$ but were not evident at 20 $m \cdot s^{-1}$. Previous research has demonstrated that when a football is impacted at velocities exceeding 30 $m \cdot s^{-1}$, the contact time tends to asymptotes towards a constant value beyond 20 $m \cdot s^{-1}$[36,43]. As the higher velocity in this study aligns with this behaviour, it explains why minimal differences in contact time were observed among the footballs at 20 $m \cdot s^{-1}$. This observation suggests that as the velocity increases, there is a threshold where the contact time may primarily be governed by the internal air pressure of the football, regardless of its material composition.

The shape of the football at maximum deformation was characterised by measurements of the deformation and contact length. For the impacts at 20 $m \cdot s^{-1}$ there was more variation in the shape of the football at the maximum deformation among the repeated impacts for a single football that arose due to more varied impact orientations as a result of using the mechanical device. These variations increased the spread of the results. The magnitude of deformation increased at 20 $m \cdot s^{-1}$ as the football possessed greater kinetic energy prior to the collision. Whilst, the deformation increased, the contact time decreased which indicated a faster rate of deformation and restoration.

b) impact variables measured using the force platform.

To the authors knowledge, this work serves as the first instance where a commercial force platform has been used to measure the loading behaviour of a relatively large sample size of footballs, considering the sensitivity of the platform as well as the standard error to make statistical comparisons.

The impacts at 20 $m \cdot s^{-1}$ highlighted the effects of material anisotropy and viscoelastic behaviour through the varying shape of the loading phase and position of the peak impact force on the loading curves with respect to time. In previous research, only a single force trace had been presented which could not allude to the variation in loading curves due to impact orientation as was seen in this study [36,39,59]. Greater variation in the loading phase between repeated impacts led to increased differences between the magnitude of peak force. The timing of the peak force occurred slightly before the mid-point of contact, suggesting the deformation happens much quicker than the restoration phase.

The force platform enables the automatic measure of contact time without the need for manual digitisation that would be beneficial in a large-scale testing environment. However, it was observed that different definitions of contact time can give different values depending on the measuring system that was used[28]. In this study, the contact time for the force platform was 0.6 ms longer than the contact time measured using the high-speed camera for both velocities. The discrepancy occurred after the initial frame of contact, as both systems were aligned at time = 0. This is a novel finding since previous studies tend to only define the contact time for a football impact using a single system.

c) static and dynamic properties of footballs

In chapter 3, the different calculation methods gave different values of quasi-static stiffness, and it was unclear which value should be used during modelling procedures to represent the stiffness properties of the football. While the three stiffness values showed some correlations with dynamic impact variables, relatively few met the significance level. When evaluated at a deflection of 3 mm, the quasi-static stiffness showed strong and statistically significant relationships with the contact time and deformation at both velocities. This finding demonstrates that conclusions surrounding the relationship between static and dynamic measurements can be skewed by the calculation method of stiffness. For the remainder of this work, the stiffness evaluated at 3mm will be used to represent the quasi-static stiffness of the football.

5.4 Conclusions

This study provides a more comprehensive analysis of impact behaviour compared to previous research, particularly by including a relatively large sample size of footballs and multiple measurements. It stands out as one of the first studies to suggest that despite passing standardised certification protocols, these footballs may exhibit different impact behaviours.

Among the repeated measurements for each football, lower variability was observed for the impact variables measured from the drop test than using the mechanical device, that led to more statistically significant comparisons. Greater differences were found between the footballs for the variables that aren’t directly measured during the FQP including the contact time, deformation, and peak impact force, compared to the COR that is restricted by the limits of the rebound test. Statistically significant correlations were found between the static stiffness, contact time and deformation but not with outbound velocity. This suggests that the impact behaviour of a football cannot be attributed to a single property but rather reflects a complex interaction between different properties. Future research should quantify the relationship between the mechanical properties of the football and its impact response. The weightings of the inputs can be used to establish whether the measurements in the FQP are accurately capturing the properties of the football that are responsible for determining the balls response to an impact.

6 Multivariable Modelling

6.1 Introduction

In the previous chapters, the mechanical properties of 12 different footballs have been measured using both static and dynamic tests. The correlation between the measurements of these different tests on the same ball has gained significant attention in previous research [27,28,32,77], leading to conflicting results. Many conclude that that a single measurement cannot be used in isolation to describe the impact behaviour of a ball [32].

The literature review revealed different modelling techniques that could be used to quantify the relationship between the mechanical properties of a football and its impact response. A statistical approach emerged as the preferred choice for this application due to its distinct advantages over other techniques. Analytical models, although insightful to fundamental mechanics, struggle to generalise across the wide range of football designs, limiting their applicability. Similarly, viscoelastic models may not be effective to investigate the interactive effects between footballs with different characteristics and impact variables. Computational models, although detailed, require extensive knowledge of the material properties and may not be practical for wider populations of footballs. In contrast, statistical models can effectively leverage the experimental data obtained in chapters 3 and 5 to generalise the findings amongst the population of footballs. Multivariable regression modelling emerged as a robust approach to comprehensively investigate the interaction between different properties that influence the dynamic impact response across a range of different footballs. This technique can consider multiple independent variables simultaneously such as the physical and mechanical properties of the football and the conditions of impact to assess their combined effect on impact behaviour.

This chapter presents the development of a multivariable model that will simultaneously consider the relationship between the mechanical properties of a football and its dynamic response. The mechanical properties were chosen to provide a holistic representation of the collective behaviour of the materials and internal air pressure of the football. This approach simplified the analysis, making it more generalisable across diverse football design that tends to practical implementation with established equipment regulations. The model will be used to understand if the mechanical properties of the 12 different footballs can explain the differences that were observed among their impact responses during the impact tests presented in Chapter 5. This works towards fulfilling objective 5 of the doctoral study.

6.2 General Modelling Procedure

The following section describes the procedure for developing multivariable regression models using the experimental results obtained previously.

6.2.1 Data-Fitting

In chapter 5, an impact test was carried out to measure the behaviour of 12 FIFA-certified footballs. A single high-speed camera and force platform were used to measure the deformation and loading behaviour of the footballs. Each football was impacted 25 times. Figure 56 shows the inbound velocities for each of the impacts and the corresponding outbound velocity.

A moderate trend ($r = 0.4$) was observed that as the inbound velocity increased so did the outbound velocity, however there was a large amount of scatter for both velocities. This suggests other factors beyond inbound velocity are influencing the outbound velocity of a football. The inbound velocity explained approximately 20 % of the variation observed in the outbound velocity. The unexplained variance is likely attributed to differences in the material composition and homogeneity of the footballs that introduce variations into the impact behaviour during repeated impacts. A mathematical model is necessary to quantify the contributions of various mechanical properties of the football on its impact response, to provide a more comprehensive understanding of the factors that influence the impact behaviour beyond just inbound velocity.

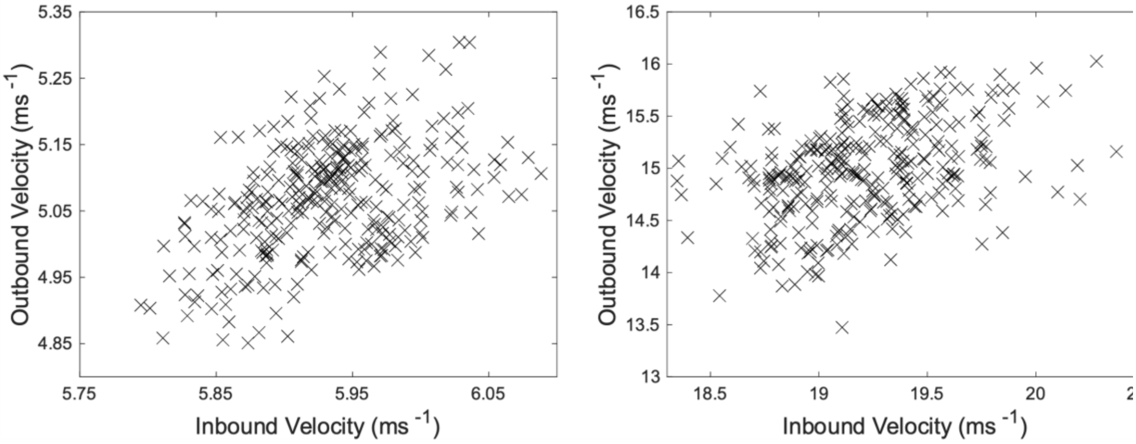

Figure 56 The inbound and corresponding outbound velocity for each impact in the study.

Multivariable Modelling

A simple linear regression model would establish a relationship between 2 variables. For Figure 56, it would reveal the relationship between the in- and out- bound velocity but would not account for any other experimental variable. This technique would not reveal the effect of the differences in the properties of the footballs used in the impact study on the outbound velocity. A multivariable regression model can be considered as an extension of a simple regression model. It predicts the dependent variable using a function of multiple independent variables, providing a more comprehensive understanding of how multiple parameters determine the overall outcome. The model applies a mathematical function such as a polynomial, an exponential, or an advanced technique such as gaussian process or neural network, to capture complex relationships between the dependant and independent variables.

The general form of a multivariable model for *n* independent variables is given by Equation 6-1.

$$Y = \beta_0 + \beta_1 x_1 + \beta_2 x_2 + \cdots + \beta_n x_n + E \tag{6-1}$$

Where $\beta_0, \beta_1, \beta_2 .. \beta_n$ are the regression coefficients, these are a set of weighted terms associated to the independent variables $x_1, x_2 \ldots x_n$ to predict the outcome Y. The error component (E) reflects the difference between the predicted response of Y and the true value. In the context of this experiment, the multivariable regression model predicts the impact variables of the football for given a set of input parameters. The input parameters are the experimental values obtained in chapters 3 and 5. These are the properties of the footballs; mass and stiffness and the impact variables determined experimentally. The magnitude of the weighted terms and the overall performance of the model can be used to improve the understanding of the relationship between the properties of a football and its impact behaviour at two different velocities.

Typically, the relationships governing the post-impact behaviour of other viscoelastic type balls follow linear or low-order polynomial relationships [23,55,57,86,94]. A polynomial multivariable model was employed to capture the complex impact behaviour of a football, using this base function, the model could account for potential non-linear interactions among the predictors. By incorporating first, second and third order terms, the model was able to flexibly represent the data to identify the best fit. To generate the multivariable model a MATLAB function, '*polyfitn*' was obtained from the online MATLAB community [144]. The function requires the user to specify the independent and dependant variables and order of the relationship. A series of weighted terms are generated that best fit a given set of experimental data. This approach uses the least square techniques to minimise the sum of the square errors between the observed response and those predicted by the model [145].

The function was incorporated into a custom-written MATLAB function to train and evaluate a 12-fold cross validation assessment of polynomial fits of order 1,2 and 3. A 12-fold cross-validation method was used to examine generality and over-fitting to compare the errors that arise from the models for each different football. As illustrated by Figure 57, the experimental data was split into each football to ensure that the model was evaluated against different ball characteristics rather than evaluating it against repeated impacts that may echo similarity and lead to inaccurate high performing models. Each fold consisted of the 25 impacts for each football. The model was trained on 11 folds and evaluated against the twelfth omitted fold. The process was repeated until each football had acted in the train and test data set. After 12 repeats, the model performance was assessed by averaging the evaluation metrics to give an indication of the suitability of the combination of input variables in the model. The results of the cross-validation procedure are shown in Appendix 10.6.

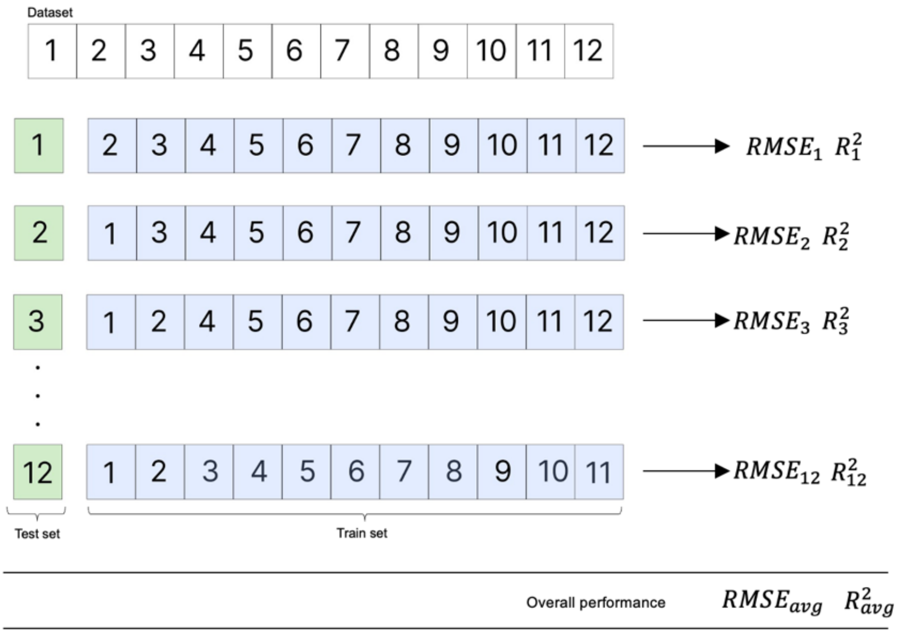

Figure 57 Cross-validation procedure

Prior to modelling, both the independent and dependant variables were normalised to have a mean of 0 and standard deviation of 1, using equation 6-2. This was done to aid interpretation of the coefficients in the model by accounting for the different scales and units of measurement between the variables to prevent one variable e.g., peak impact force, dominating the value coefficients simply due to the larger scale of measurement.

$$Z = \frac{x - \bar{x}}{\sigma} \quad \text{6-2}$$

Normalised data (Z), x value in data set, $\bar{x}$ mean of data set, σ standard deviation

The independent variables were inputted into the normalisation in the following units: inbound and outbound velocity in $m \cdot s^{-1}$, mass in kg, stiffness in $N \cdot m^{-1}$, energy loss in J, contact time in s, deformation in mm, and peak impact force in N.

6.2.2 Evaluating the performance of models

As the relationship between the independent and multiple dependant variables could not be graphically visualised, performance metrics and coefficient significance were used to indicate the model's ability to predict the experimental results. The performance metrics were the root-mean square error (RMSE) and the coefficient of determination (R^2). The RMSE quantifies the average value of the residuals between the experimental and predicted values, providing an insight into quality of the model predictions. The R^2 expresses the variance of the outbound velocity that is explained by the predictors as a percentage. The R^2 value was only calculated for the linear model as the non-linear models violate the assumptions of the calculation [146]. The RMSE and R^2 values were compared between the cross-validation and whole data training to examining over-fitting. A further assessment of the model was to evaluate the significance of the coefficients in the model. A significance level of 0.05 was used.

The outcome of multivariable modelling is a relationship with weighted terms associated to each of the input variables. Dominance analysis can be used to aid interpretation of the best-fitting model [147-149]. This technique assesses the relative importance of each input variable on the predictions, offering insight into the contribution to explain variability in the outcome variable. The definition of importance follows Budescu [147] and is based on the additional contribution of a single input variable in all subset models. The purpose of determining predictor importance is to identify the relative contribution of each input variable relative to the others in the final selected model. As such, dominance analysis will only be carried out on the final selected model, as it aids interpretation rather than model selection.

The confidence intervals (CI) were calculated to provide insight into the precision of the predictions made by the model. The interval was calculated using the design matrix, that considers the values of all predictors simultaneously. To aid interpretation, the confidence and prediction intervals were calculated using unstandardised data.,

For the general form of multivariable model given in equation 6-3, for any specific value of x_i, the predicted value $\hat{y}$ will be obtained.

$$\hat{y}_o = \beta_0 + \beta_1 x_1 + \beta_2 x_2 + \cdots + \beta_n x_n \quad \text{6-3}$$

If X_o represent a column array containing the values 1, x_1, x_2,… x_k, then equation 6-4 provides an unbiased estimate of the standard error of $\hat{y}_o$.

$$se = \sqrt{MS_{res}(X_0^T(X^TX)^{-1}X_o} \quad \text{6-4}$$

Where, MS_{res} mean square of the residuals, X_o column array of coefficient values, X design matrix.

The confidence interval is calculated by equation 6-5. A t_{crit} value of 1.65 was found from standard probability tables for a degree of freedom equal to 295 with a significance level of 0.05.

$$y \pm t_{crit}(se) \quad \text{6-5}$$

The prediction interval (PI) was calculated by equation 6-7, by considering the variance as the variance of the residual.

$$y \pm t_{crit} \cdot \sqrt{MS_{res}(1 + X_0^T(X^TX)^{-1}X_o} \quad \text{6-6}$$

6.3 Multivariable Model – Static Mechanical Properties

In this section, a multivariable model will be developed to establish the relationship between the mechanical properties of the footballs and their impact response. This model will be used to determine whether the mechanical properties of a football, obtained in using static assessments in chapter 3, can be used to explain variances in the dynamic impact behaviour of the footballs. In this model, the independent variables are the properties of the football: mass, static stiffness, and the inbound velocity. The dependant variables will be the outbound velocity, contact time, deformation, and peak impact force. A single model will be created for each velocity.

The multivariable model will take the form of equation 6-7.

$$Y = Av_i + Bm_b + Ck_s + constant \quad (6\text{-}7)$$

Where v_i is the inbound velocity, m_b is the mass of the football and k_s is the static stiffness of the football. Two models will be considered in this section. The results presented in section 6.3.1, will encompass all the data captured during the experimental investigation (n = 300). The results presented in section 6.3.2, will use the average of 25 impacts for each football model (n = 12).

6.3.1 Results using all impact data.

The results for each dependant variable will be presented.

Outbound velocity

The results of the multivariable regression model with outbound velocity as the dependant variable are presented in Table 15. The margins of error were 0.01 and 0.04 m·s^{-1} at the certification test velocity and high velocity condition, respectively.

Table 15 Performance statistics for the multivariable models for outbound velocity using static measurements.

Condition	RMSE	R^2	CI (m·s^{-1})	PI (m·s^{-1})
Certification test	0.82	0.33	[5.06, 5.08]	[4.95, 5.19]
Higher velocity	0.78	0.39	[14.9,15.0]	[14.4,15.6]

The value of the coefficients associated to each independent variable are shown in Table 16, along with the significance level. The significance level was met for all independent variables.

Table 16 The value and significance of the coefficients in the multivariable models for outbound velocity using static measurements.

Condition	Coefficients and significance			
	Inbound Velocity	Mass	Static Stiffness	Constant
Certification test	0.49 $p < 0.05$	0.23 $p < 0.05$	-0.38 $p < 0.05$	0.00 $p > 0.05$
Higher velocity	0.50 $p < 0.05$	-0.29 $p < 0.05$	-0.26 $p < 0.05$	0.00 $p > 0.01$

The results of the dominance analysis, presented in Table 17, showed that outbound velocity was largely dominated by the inbound velocity.

Table 17 The weighting associated to each coefficient calculated using the dominance analysis in the model of outbound velocity.

Condition	Inbound Velocity	Mass	Static Stiffness
Certification test	0.16	0.02	0.06
Higher velocity	0.15	0.06	0.04

Contact Time

The results of the multivariable regression model with contact time as the dependant variable are presented in Table 18. The R^2 at the certification velocity was much higher at 0.6 compared to 0.2 at the higher velocity. The margin of error was 0.03 ms at both velocities.

Table 18 Performance statistics for the multivariable models for contact time using static measurements.

Condition	RMSE	R^2	CI (ms)	PI (ms)
Certification test	0.62	0.61	[8.9, 9.0]	[8.6, 9.3]
Higher velocity	0.82	0.22	[7.7, 7.8]	[7.3, 8.1]

The value of the coefficients associated to each independent variable are shown in Table 19, along with the significance level. In each model, the static stiffness was the only independent variable to meet the significance level.

Table 19 The value and significance of the coefficients in the multivariable models for contact time using static measurements.

Condition	Coefficients and significance			
	Inbound Velocity	Mass	Static Stiffness	Constant
Certification test	0.003 $p > 0.05$	0.005 $p > 0.05$	-0.81 $p < 0.05$	0.00 $p > 0.05$
Higher velocity	-0.21 $p < 0.05$	0.03 $p > 0.05$	-0.38 $p < 0.05$	0 $p > 0.05$

The results of the dominance analysis, presented in Table 20, showed that the stiffness of the football dominated the model at both velocities.

Table 20 The weighting associated to each coefficient calculated using the dominance analysis in the model of outbound velocity.

Condition	Inbound Velocity	Mass	Static Stiffness
Certification test	0.01	0.01	0.34
Higher velocity	0.04	0.01	0.08

Deformation

The results of the multivariable regression model with deformation as the dependant variable are presented in Table 21. The margins of error were 0.1 and 0.3 mm at the certification test and higher velocity, respectively.

Table 21 Performance statistics for the multivariable models for deformation using static measurements.

Condition	RMSE	R^2	CI (mm)	PI (mm)
Certification test	0.69	0.53	[17.5,17.7]	[16.4,18.8]
Higher velocity	0.83	0.31	[49.4,48.8]	[44.7,53.6]

The value of the coefficients associated to each independent variable is shown in Table 22, along with the significance level. In both models' stiffness was the only coefficient that met the required level of significance.

Table 22 The value and significance of the coefficients in the multivariable models for deformation using static measurements.

Condition	Coefficients and significance			
	Inbound Velocity	Mass	Static Stiffness	Constant
Certification test	0.04	0.11	-0.78	0.00
	$p > 0.05$	$p < 0.05$	$p < 0.05$	$p > 0.05$
Higher velocity	-0.09	-0.09	-0.47	0.00
	$p > 0.05$	$p > 0.05$	$p < 0.05$	$p > 0.05$

As with contact time, the stiffness dominated the relationship, as shown by the outputs of the dominance analysis, presented in Table 23.

Table 23 The weighting associated to each coefficient calculated using the dominance analysis in the model of deformation.

Condition	Inbound Velocity	Mass	Static Stiffness
Certification test	0.01	0.02	0.30
Higher velocity	0.01	0.02	0.12

Peak impact force

The results of the multivariable regression model with peak impact force as the dependant variable are presented in Table 24. The margins of error were 5.9 and 20.5 N at the certification test and higher velocity, respectively.

Table 24 Performance statistics for the multivariable models for peak impact force using static measurements.

Condition	RMSE	R^2	CI (N)	PI (N)
Certification test	0.75	0.44	[975,987]	[918, 1044]
Higher velocity	0.93	0.14	[3575,3617]	[3297, 3893]

The value of the coefficients associated to each independent variable are shown in Table 25, along with the significance level. At the lower velocity, all independent variables met the significance level. However, at the higher velocity only the inbound velocity met the significance level.

Table 25 The value and significance of the coefficients in the multivariable models for peak impact force using static measurements.

Condition	Coefficients and significance			
	Inbound Velocity	Mass	Static Stiffness	Constant
Certification test	0.01	0.24	0.49	0.00
	$p < 0.05$	$p < 0.05$	$p < 0.05$	$p > 0.05$
Higher velocity	0.34	0.08	0.05	0.00
	$p < 0.05$	$p > 0.05$	$p > 0.05$	$p > 0.05$

Table 26 shows the weightings associated to each of the independent variables. The weightings shifted between the two velocities.

Table 26 The weighting associated to each coefficient calculated using the dominance analysis in the model of peak impact force.

Condition	Inbound Velocity	Mass	Static Stiffness
Certification test	0.01	0.06	0.15
Higher velocity	0.07	0.01	0.01

6.3.2 Results using average measurements.

The results for each dependent variable will be presented.

Outbound Velocity

The results of the multivariable regression model using average measurements with outbound velocity as the dependant variable are presented in Table 27. The model that used all the measurements (n = 300) displayed a better ability to explain the variance in the outbound velocity; lower RMSE and higher R^2 values compared to the average measurements (n = 12) at the certification test velocity. However, a larger margin of error was observed for the smaller dataset; 0.03 and 0.15 $m \cdot s^{-1}$ at the certification test and higher velocity.

Table 27 Performance statistics for the multivariable models for outbound using average independent variables.

Condition	RMSE	R^2	CI ($m \cdot s^{-1}$)	PI ($m \cdot s^{-1}$)
Certification test	0.87	0.17	[5.04, 5.10]	[4.96, 5.28]
Higher velocity	0.63	0.57	[14.8, 15.1]	[14.7, 15.3]

The value of the coefficients associated to each independent variable is shown in Table 28, along with the significance level. Most independent variables did not meet the significance level.

Table 28 The value and significance of the coefficients in the multivariable models for outbound velocity using the average independent variables.

Condition	Coefficients and significance			
	Inbound Velocity	Mass	Static Stiffness	Constant
Certification test	0.16 $p > 0.05$	0.29 $p > 0.05$	-0.47 $p > 0.05$	0.00 $p > 0.05$
Higher velocity	0.58 $p < 0.05$	-0.35 $p > 0.05$	-0.37 $p > 0.05$	0.00 $p > 0.05$

Contact Time

The results of the multivariable regression model using average measurements with contact time as the dependant variable are presented in Table 29. The model that using the average measurements showed better ability to explain the variance in the contact time. However, the model had a larger margin of error of 0.1 ms at both velocities compared to the model using the larger sample size.

Table 29 Performance statistics for the multivariable models for contact time using average independent variables.

Condition	RMSE	R^2	CI (ms)	PI (ms)
Certification test	0.46	0.77	[8.9, 9.0]	[8.7, 9.3]
Higher velocity	0.72	0.44	[7.6, 7.8]	[7.4, 8.0]

The value of the coefficients associated to each independent variable are shown in Table 30, along with the significance level. Between the two model approaches, at the certification test velocity, there was no change in the significance of the independent variables across the two models. No variables met the significance level for the average measures model at the higher velocity.

Table 30 The value and significance of the coefficients in the multivariable models for contact time using the average independent variables.

Condition	Coefficients and significance			
	Inbound Velocity	Mass	Static Stiffness	Constant
Certification test	-0.09	0.01	-0.86	0.00
	$p > 0.05$	$p > 0.05$	$p < 0.05$	$p > 0.05$
Higher velocity	-0.32	0.06	-0.52	0.00
	$p > 0.05$	$p > 0.05$	$p > 0.05$	$p > 0.05$

Deformation

The results of the multivariable regression model using average measurements with deformation as the dependant variable are presented in Table 31. As above, the model using average measurement showed better ability to explain the variance in deformation between the footballs. The margin of error was 0.25 and 1.33 mm at the certification and higher velocity.

Table 31 Performance statistics for the multivariable models for deformation using average independent variables.

Condition	RMSE	R^2	CI (ms)	PI (ms)
Certification test	0.47	0.76	[17.4, 17.9]	[16.8, 18.3]
Higher velocity	0.59	0.62	[47.7, 50.3]	[46.2, 51.8]

The value of the coefficients associated to each independent variable is shown in Table 32, along with the significance level.

Table 32 The value and significance of the coefficients in the multivariable models for deformation using the average independent variables.

Condition	Coefficients and significance			
	Inbound Velocity	Mass	Static Stiffness	Constant
Certification test	-0.01	0.09	-0.916	0.00
	$p > 0.05$	$p > 0.05$	$p < 0.05$	$p > 0.05$
Higher velocity	-0.22	-0.08	-0.64	0.00
	$p > 0.05$	$p > 0.05$	$p < 0.05$	$p > 0.05$

Peak Impact Force

The results of the multivariable regression model using average measurements with peak impact force as the dependant variable are presented in Table 33. The model showed better ability to explain the variance in the peak impact force than the model using all impact data. The margin of error is 18.4 and 82.6 N.

Table 33 Performance statistics for the multivariable models for peak impact force using average independent variables.

Condition	RMSE	R^2	CI (ms)	PI (ms)
Certification test	0.66	0.53	[963, 1000]	[925, 1040]
Higher velocity	0.77	0.35	[3513, 3678]	[3420, 3771]

The value of the coefficients associated to each independent variable is shown in Table 34, along with the significance level. None of the independent variables in the average measures model met the significance level.

Table 34 The value and significance of the coefficients in the multivariable models for peak impact force using the average independent variables.

Condition	Coefficients and significance			
	Inbound Velocity	Mass	Static Stiffness	Constant
Certification test	0.25 $p > 0.05$	0.26 $p > 0.05$	0.45 $p > 0.05$	0.00 $p > 0.05$
Higher velocity	0.59 $p > 0.05$	0.13 $p > 0.05$	-0.07 $p > 0.05$	0.00 $p > 0.05$

6.3.3 Discussion

Multivariable regression has previously been used to investigate the factors affecting the impact response of a ball [35,150]. The models developed in this section examined the relationship between the mechanical properties determined using static tests and the dynamic impact response for twelve different footballs. The model was created to examine whether the stiffness, football mass and the inbound velocity, could explain the variations observed between the impact behaviours amongst the balls. A first-order multivariable model was found to be the most appropriate fit to represent the data. The cross-validation procedure performed prior to model training, displayed evidence of over-fitting beyond this order of fit. In addition, there was a lack of significance amongst the terms in models above this order, that indicated higher-order effects were negligible or difficult to discern within the given interval of inbound velocity. Given that the purpose of k_s is to evaluate the linear stiffness between footballs, with inbound velocity relatively controlled within the experiment tests, the non-linear effects on the relative stiffness were negligible [77].

Two approaches were considered in this chapter; a model created using all data points (n = 300) and using average measurements (n = 12). The model with the larger sample size provided a more detailed view of the patterns arising in the dataset, i.e. the weighting associated to each independent variable, that was observed through higher significance of the individual terms. The model containing average measurements (n = 12), reduced the variability in the data which appeared to be masking the strength of the relationships between the independent and dependant variables, and higher R-squared values were observed. However, due to a significant reduction in the sample size, wider confidence intervals reduced the precision of statistical tests and resulted in fewer statistically significant relationships. The results of both approaches revealed that to some extent measurements evaluating the properties of the footballs using static tests could allude to some of the variation that arose in the impact variables. These tended to be greater at the lower velocity than at the higher velocity, a common observation amongst mathematical models examining the impact response of a football [90].

The stiffness of the football was found to dominant many of the relationships for contact time, deformation, and peak impact force. These variables are typically associated to the stiffness properties of balls. As FIFA-certified footballs were used, the amount of variation that can exist within the independent variables of mass and inbound velocity was limited by the passing requirements of the FIFA Quality Programme (FQP), leaving the stiffness as the sole property of the football not strictly constrained. Consequently, the coefficients associated with mass and velocity did not consistently attain statistical significance, leading to fluctuations in their effect sizes or even changes in polarity between the models at the two velocities. This reinforced findings in chapter 5 that saw more variation among the impact variables of deformation and contact time shown here to be a response of the stiffness of the football.

The model showed that the stiffness of the football explains some the variance in the impact behaviour of the FIFA-certified footballs. However, the R-squared values obtained in this chapter showed slight differences to the R-squared obtained when solely fitting a first-order linear relationship between a single independent variable and the static stiffness in Chapter 5. For deformation, the value of R-squared decreased between the linear model in chapter 5 (6 $m \cdot s^{-1}$: R^2=0.93 and 20 $m \cdot s^{-1}$: R^2 =0.73) and the multivariable model (6 $m \cdot s^{-1}$: R^2=0.76 and 20 $m \cdot s^{-1}$: R^2 =0.62). This highlights the importance of considering simultaneously multiple properties of the football as it suggests that the interactions among mass and inbound velocity might partially explain a portion of the variance previously explained the two highly correlated variables.

The results of both models showed that the differences in the mechanical properties of the footballs, obtained using static tests, accounted for some of the variance among the dynamic impact response. The value of the coefficients between both approaches were comparable, which implied robust trends observed amongst the independent and dependant variables. By averaging the measurements this appeared to minimise the impact of the experimental variability and led to more stable reflection of the strength of the underlying relationships. Higher R-squared and lower RMSE values, that suggested better overall performance was found at certification test velocity than at the higher velocity. This is associated to factors including increased energy loss and greater emphasis on the football's viscoelastic properties at the higher velocity, that were not accounted for in the model. While the mechanical properties obtained during static compression tests provided valuable information to suggest differences among the footballs, they do not represent the properties of the football during a dynamic impact. In these impacts, the football is subject to greater forces, higher deformation rates and larger energy loss. In the next section, the mechanical properties of the football will be calculated directly from impact tests to achieve more accurate representation of the football under dynamic conditions.

6.4 Multivariable Model – Dynamic Mechanical Properties Measurements

The model presented in section 6.3 revealed that the mechanical properties measured during a quasi-static compression test could not fully explain the variations within the dependant variables ($R^2 \leq 0.77$), particularly at the higher impact speed. It was suggested that the weakness of the model arose due to the neglection of any energy loss mechanisms and oversimplification of the rate-dependency of the materials.

The next section looks to address the limitations of the first model by evaluating the mechanical properties of the footballs using dynamic measurements.

6.4.1 Model Derivation

Chapter 4 described an experimental investigation that measured the force-time behaviour for a football impact using a force platform. In this section, the mechanical properties were calculated using the loading curve obtained during a dynamic impact.

The dynamic stiffness of the football $k_{dyn}$was calculated by applying Newton's second law of motion to obtain the displacement of the centre-of-mass (COM) x_b of the football. The force-time curve was divided by the mass $m_b$of the football, to obtain the acceleration $\ddot{x_b}$, and then integrated twice over time to obtain x_b. The boundary conditions applied to estimate the constant were: (1) at time t = 0 the inbound velocity was v_i, obtained using the high-speed video in chapter 5, and (2) at time t = 0 x_b= 0.

The dynamic stiffness was calculated using equation 6-8.

$$F = k_{dyn}(x_b) \qquad \text{6-8}$$

The hysteresis loss (η), which will be referred to in this chapter as energy loss, was calculated as the integral of the force-displacement curve over a complete loading-unloading cycle. The area enclosed by this curve represents the energy dissipated during the impact due to friction, damping and other dissipative mechanisms within the material.

In this section, the independent variables will be inbound velocity, mass, dynamic stiffness, and energy loss. As before, a single model will be created for each inbound velocity.

The multivariable model will take the form of equation 6-9.

$$Y = Av_i + Bm_b + Ck_{dyn} + De_{loss} + constant \qquad \text{6-9}$$

Where v_i is the inbound velocity, m_b is the mass of the football and k_{dyn} is the dynamic stiffness of the football and e_{loss} is the energy loss.

6.4.2 Results using all data points

Figure 58 shows a sequence of graphs required to derive the data to calculate the dynamic properties of a football. The graphs represent a single impact and were repeated to give 25 measurements per ball. Figure 58c showing the displacement against time indicates that the football does not fully reform to its original shape when loosing contact with the force platform.

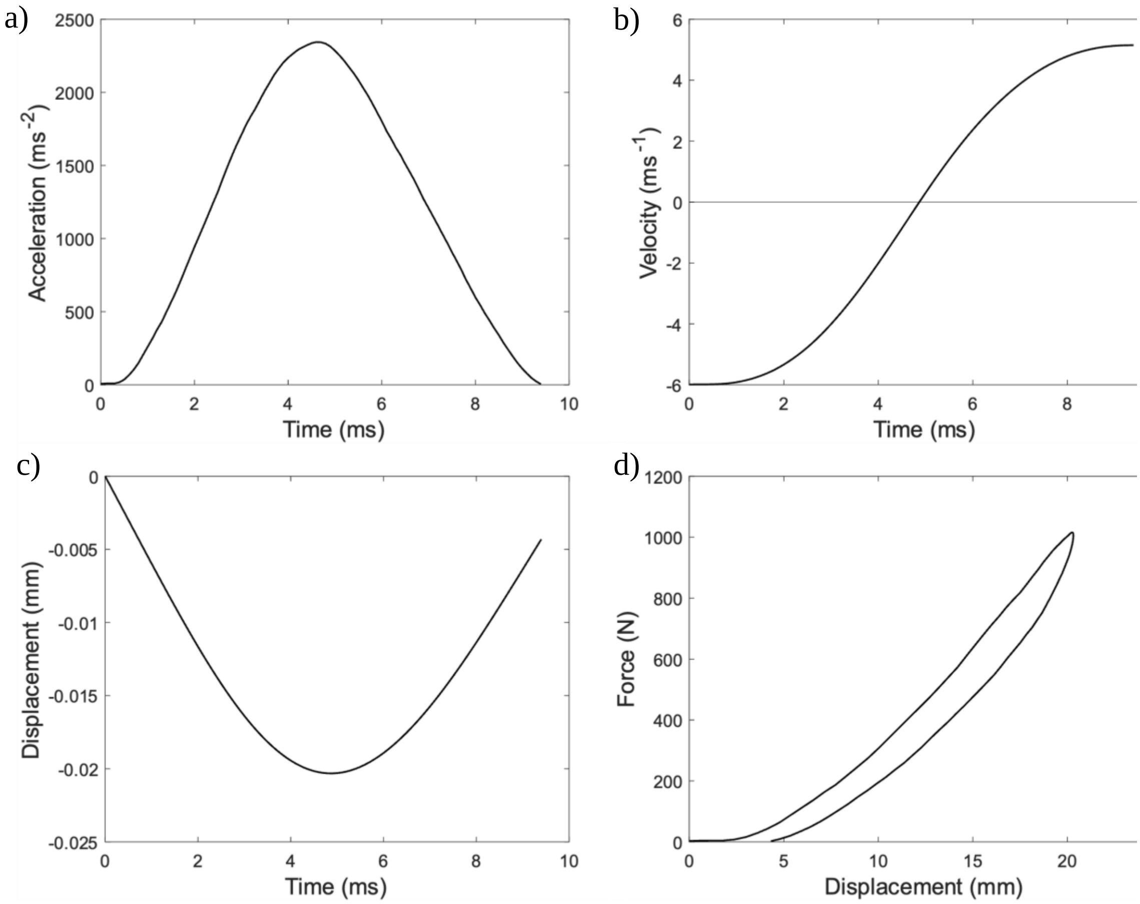

Figure 58 The sequence of graphs to calculate the displacement of the football as measured by the force platform; (a) acceleration (b) velocity, (c) displacement verses time and (d) the dynamic hysteresis curve.

Outbound Velocity

The results of the multivariable regression model using average measurements with outbound velocity as the dependant variable are presented in Table 35. The margin of error was 0.02 and 0.03 m·s^{-1} at the certification test and higher velocity.

Table 35 Performance statistics for the multivariable models for outbound velocity using dynamic measurements.

Condition	RMSE	R^2	CI	PI
Certification test	0.76	0.41	[5.05, 5.08]	[4.97, 5.17]
Higher velocity	0.64	0.59	[14.9, 15.0]	[14.5, 15.5]

The value of the coefficients associated to each independent variable are shown in Table 36, along with the significance level. In the model of certification test velocity inbound velocity and energy loss were the only terms to reach statistical significance, whereas at the higher velocity, all terms met this level.

Table 36 The value and significance of the coefficients in the multivariable models for outbound velocity using dynamic measurements.

Condition	Coefficients and significance				
	Inbound Velocity	Mass	Dynamic Stiffness	Energy Loss	Constant
Certification test	0.88 $p < 0.05$	0.05 $p > 0.05$	-0.04 $p > 0.05$	-0.60 $p < 0.05$	0.00 $p > 0.05$
Higher velocity	1.31 $p < 0.05$	-0.10 $p < 0.05$	-0.20 $p < 0.05$	-1.03 $p < 0.05$	0.00 $p > 0.05$

Table 37 shows the weightings associated to each of the independent variables. The inbound velocity and energy loss had the highest weightings.

Table 37 The weighting associated to each coefficient calculated using the dominance analysis in the model of outbound velocity.

Condition	Inbound Velocity	Mass	Dynamic Stiffness	Energy Loss
Certification test	0.34	0.01	0.01	0.13
Higher velocity	0.35	0.09	0.05	0.18

Contact Time

The results of the multivariable regression model using average measurements with contact time as the dependant variable are presented in Table 38. The margin of error was 0.05 and 0.02 ms at the certification test and higher velocity.

Table 38 Performance statistics for the multivariable models for contact time using dynamic measurements.

Condition	RMSE	R^2	CI (ms)	PI
Certification test	0.60	0.64	[8.9, 9.0]	[8.6,9.3]
Higher velocity	0.73	0.46	[7.7, 7.8]	[7.4, 8.0]

The value of the coefficients associated to each independent variable are shown in Table 39, along with the significance level. All independent variables met the required level of significance in the models for the two velocities.

Table 39 The value and significance of the coefficients in the multivariable models for contact time using dynamic measurements.

	Coefficients and significance				
Condition	Inbound Velocity	Mass	Dynamic Stiffness	Energy Loss	Constant
Certification test	0.12 $p < 0.05$	-0.09 $p < 0.05$	-0.71 $p < 0.05$	-0.29 $p < 0.05$	0.00 $p > 0.05$
Higher velocity	0.10 $p < 0.05$	0.03 $p < 0.05$	-0.55 $p < 0.05$	-0.45 $p < 0.05$	0 .00 $p > 0.05$

Table 40 shows the weightings associated to each of the independent variables. The inbound velocity and energy loss had the highest weightings. The dynamic stiffness dominated the model at both velocities, with the energy loss term slightly more pronounced at the higher impact velocity.

Table 40 The weighting associated to each coefficient calculated using the dominance analysis in the model of contact time.

Condition	Inbound Velocity	Mass	Dynamic Stiffness	Energy Loss
Certification test	0.01	0.05	0.47	0.05
Higher velocity	0.03	0.01	0.31	0.07

Deformation

The results of the multivariable regression model using average measurements with outbound velocity as the dependant variable are presented in Table 41. The margin of error was 0.19 and 0.26 mm at the certification and higher velocity.

Table 41 Performance statistics for the multivariable models for deformation using dynamic measurements.

Condition	RMSE	R^2	CI (mm)	PI (mm)
Certification test	0.73	0.47	[17.4, 17.8]	[16.4, 18.8]
Higher velocity	0.72	0.49	[48.9, 49.4]	[45.2, 53.0]

The value of the coefficients associated to each independent variable are shown in Table 42, along with the significance level. The inbound velocity, dynamic stiffness and energy loss met the required level of significance in both models.

Table 42 The value and significance of the coefficients in the multivariable models for deformation using dynamic measurements.

Condition	Coefficients and significance				
	Inbound Velocity	Mass	Dynamic Stiffness	Energy Loss	Constant
Certification test	0.18 $p < 0.05$	-0.06 $p > 0.05$	-0.59 $p < 0.05$	-0.31 $p < 0.05$	0.00 $p > 0.05$
Higher velocity	0.48 $p < 0.05$	-0.06 $p > 0.05$	-0.45 $p < 0.05$	-0.79 $p < 0.05$	0.00 $p > 0.05$

Table 43 shows the weightings associated to each of the independent variables. The inbound velocity and energy loss had the highest weightings. The dynamic stiffness dominated the models at both velocities.

Table 43 The weighting associated to each coefficient calculated using the dominance analysis in the model of deformation.

Condition	Inbound Velocity	Mass	Dynamic Stiffness	Energy Loss
Certification test	0.02	0.03	0.33	0.05
Higher velocity	0.05	0.04	0.21	0.14

Peak Impact Force

The results of the multivariable regression model using average measurements with outbound velocity as the dependant variable are presented in Table 44. The margin of error was 6.4 and 16.1 N at the certification and higher velocity.

Table 44 Performance statistics for the multivariable models for peak impact force using dynamic measurements.

Condition	RMSE	R^2	CI (N)	PI (N)
Certification test	0.49	0.76	[974, 987]	[940, 1021]
Higher velocity	0.72	0.49	[3590, 3611]	[3356, 3834]

The value of the coefficients associated to each independent variable are shown in Table 45, along with the significance level. While at variables met the significance level at the certification velocity, this reduced to only the inbound velocity and dynamic stiffness at the higher velocity.

Table 45 The value and significance of the coefficients in the multivariable models for peak impact force using dynamic measurements.

Condition	Coefficients and significance				
	Inbound Velocity	Mass	Dynamic Stiffness	Energy Loss	Constant
Certification test	0.23 $p < 0.05$	0.18 $p < 0.05$	0.77 $p < 0.05$	-0.10 $p < 0.05$	0.00 $p > 0.05$
Higher velocity	0.42 $p < 0.05$	0.07 $p > 0.05$	0.59 $p < 0.05$	-0.10 $p > 0.05$	0.00 $p > 0.05$

Table 46 shows the weightings associated to each of the independent variables. The dynamic stiffness dominated the response at both velocities.

Table 46 The weighting associated to each coefficient calculated using the dominance analysis in the model of peak impact force.

Condition	Inbound Velocity	Mass	Dynamic Stiffness	Energy Loss
Certification test	0.02	0.10	0.55	0.01
Higher velocity	0.06	0.01	0.35	0.03

6.4.3 Results using average measurements

The results for each dependent variable will be presented.

Outbound velocity

The results of the multivariable regression model using average measurements with outbound velocity as the dependant variable are presented in Table 47. The margin of error was 0.01 and 0.27 $m \cdot s^{-1}$ at the certification test and higher velocity.

Table 47 Performance statistics for the multivariable models for outbound velocity using average independent variables.

Condition	RMSE	R^2	CI ($m \cdot s^{-1}$)	PI ($m \cdot s^{-1}$)
Certification test	0.36	0.86	[5.06, 5.07]	[5.4, 5.1]
Higher velocity	0.57	0.65	[14.7, 15.3]	[14.6,15.4]

The value of the coefficients associated to each independent variable is shown in Table 48, along with the significance level. The majority of the independent variables did not meet the significance level.

Table 48 The value and significance of the coefficients in the multivariable models for outbound velocity using the average independent variables.

Condition	Coefficients and significance				
	Inbound Velocity	Mass	Dynamic Stiffness	Energy loss	Constant
Certification test	0.79	-0.09	0.24	-1.22	0.00
	$p < 0.05$	$p > 0.05$	$p > 0.05$	$p < 0.05$	$p > 0.05$
Higher velocity	1.24	-0.06	-0.26	-0.93	0.00
	$p < 0.05$	$p > 0.05$	$p > 0.05$	$p > 0.05$	$p > 0.05$

Contact Time

The results of the multivariable regression model using average measurements with contact time as the dependant variable are presented in Table 49. The margin of error was 0.02 ms and 0.07 ms.

Table 49 Performance statistics for the multivariable models for contact time using average independent variables.

Velocity	RMSE	R^2	CI ($m \cdot s^{-1}$)	PI ($m \cdot s^{-1}$)
Certification	0.20	0.96	[8.9, 9.0]	[8.9,9.0]
Higher	0.37	0.85	[7.6, 7.8]	[7.6,7.8]

The value of the coefficients associated to each independent variable is shown in Table 50, along with the significance level. The majority of the independent variables did not meet the significance level.

Table 50 The value and significance of the coefficients in the multivariable models for contact time using the average independent variables.

Condition	Coefficients and significance				
	Inbound Velocity	Mass	Dynamic Stiffness	Energy Loss	Constant
Certification test	0.17	-0.03	-0.92	-0.23	0.00
	$p > 0.05$	$p > 0.05$	$p < 0.05$	$p > 0.05$	$p > 0.05$
Higher velocity	-0.26	0.05	-0.81	-0.07	0.00
	$p > 0.05$	$p > 0.05$	$p < 0.05$	$p > 0.05$	$p > 0.05$

Deformation

The results of the multivariable regression model using average measurements with deformation as the dependant variable are presented in Table 51. The margin of error was 0.19 and 1.04 mm.

Table 51 Performance statistics for the multivariable models for deformation using average independent variables.

Condition	RMSE	R^2	CI ($m \cdot s^{-1}$)	PI ($m \cdot s^{-1}$)
Certification test	0.34	0.87	[17.4, 17.8]	[17.1, 18.2]
Higher velocity	0.49	0.74	[16.6,18.7]	[16.0,19.3]

The value of the coefficients associated to each independent variable is shown in Table 52, along with the significance level. The majority of the independent variables did not meet the significance level.

Table 52 The value and significance of the coefficients in the multivariable models for deformation using the average independent variables.

Condition	Coefficients and significance				
	Inbound Velocity	Mass	Dynamic Stiffness	Energy Loss	Constant
Certification test	0.32 $p > 0.05$	-0.03 $p > 0.05$	-0.81 $p < 0.05$	-0.40 $p > 0.05$	0.00 $p > 0.05$
Higher velocity	0.21 $p > 0.05$	0.05 $p > 0.05$	-0.64 $p < 0.05$	-0.65 $p > 0.05$	0.00 $p > 0.05$

Peak Impact Force

The results of the multivariable regression model using average measurements with peak impact force as the dependant variable are presented in Table 53. The margin of error was 3.36 and 18.8 N at the certification and higher velocity.

Table 53 Performance statistics for the multivariable models for peak impact force using average independent variables.

Condition	RMSE	R^2	CI ($m \cdot s^{-1}$)	PI ($m \cdot s^{-1}$)
Certification test	0.17	0.97	[979, 986]	[972,993]
Higher velocity	0.31	0.70	[964, 1001]	[952,1013]

The value of the coefficients associated to each independent variable is shown in Table 54, along with the significance level. The majority of the independent variables did not meet the significance level.

Table 54 The value and significance of the coefficients in the multivariable models for peak impact force using the average independent variables.

Condition	Coefficients and significance				
	Inbound Velocity	Mass	Dynamic Stiffness	Energy Loss	Constant
Certification test	0.31 $p < 0.05$	0.05 $p > 0.05$	0.96 $p < 0.05$	-0.39 $p < 0.05$	0.00 $p > 0.05$

Higher velocity	0.70 $p < 0.05$	0.02 $p > 0.05$	0.75 $p < 0.05$	-0.33 $p > 0.05$	0.00 $p > 0.05$

6.4.4 Summary of models using the mechanical properties of footballs

This section will compare the performance of the models using static and dynamic mechanical properties. The model presented in section 6.3, where the relationship was a function of the static stiffness is denoted by $f(k_s)$. The model presented in section 6.4, where the relationship was a function of the dynamic stiffness and energy loss is denoted by $f\left(k_{dyn} + e_{loss}\right)$.

a) Certification test velocity

Table 55 shows the R-squared values for the four models presented in this chapter for every dependant variable at the certification test velocity.

Table 55 The R-squared value for the models using static and dynamic mechanical properties at the certification test velocity for each dependent variable.

	Raw measurements		Average measurements	
Impact Variable	$f(k_s)$	$f(k_{dyn} + e_{loss})$	$f(k_s)$	$f(k_{dyn} + e_{loss})$
Outbound Velocity	0.33	0.42	0.16	0.86
Contact time	0.61	0.64	0.77	0.96
Deformation	0.53	0.47	0.76	0.85
Peak impact force	0.44	0.76	0.53	0.97

b) Higher velocity

Table 56 shows the R-squared values for the four models presented in this chapter for every dependant variable at the higher velocity.

Table 56 The R-squared value for the models using static and dynamic mechanical properties at the higher velocity for each dependent variable.

	Raw measurements		Average measurements	
Impact Variable	$f(k_s)$	$f(k_{dyn} + e_{loss})$	$f(k_s)$	$f(k_{dyn} + e_{loss})$
Outbound Velocity	0.39	0.59	0.57	0.65
Contact time	0.22	0.46	0.44	0.85
Deformation	0.31	0.49	0.62	0.74
Peak impact force	0.14	0.49	0.35	0.70

c) Percentage of variance explained for each independent variable

Table 57 expresses the weightings of the variables as a percentage of the total model performance. The results show that the properties governing the response of the independent variable remains relatively consistent across the two velocity conditions.

Table 57 The weighting of each independent variable expressed as a percentage. The top diagonal shows the percentage at 6 m·s^{-1} and lower diagonal shows the percentage at 20 m·s^{-1}.

Impact variable	Percentage Explained (%)			
	Outbound Velocity	Contact Time	Deformation	Peak Impact Force
Inbound velocity	69 / 52	2 / 7	5 / 11	3 / 13
Mass	2 / 13	9 / 2	7 / 9	15 / 2
Dynamic Stiffness	2 / 7	81 / 74	77 / 48	81 / 78
Energy loss	27 / 27	9 / 17	12 / 32	1 / 7

6 m·s^{-1} / 20 m·s^{-1}

6.4.5 Discussion

This model investigated whether the mechanical properties of footballs calculated directly from the impact tests could explain the variations observed between their impact behaviour. The mechanical properties were calculated from the output of the force platform [30,77,151]. To overcome the limitations of the first modelling attempt, the static stiffness was substituted for the dynamic stiffness, and an additional term of energy loss was incorporated to represent the material damping. The results showed that the dynamic mechanical properties exhibited better ability to explain the variances in impact behaviour among the footballs.

The influence of experimental variability on the performance of the model was minimised by averaging the repeated impacts. Across the two approaches, the values of the coefficients of the independent variables showed minimal change, that implies robust relationships. While the smaller sample size led to larger confidence intervals that reduced the statistical significance of the coefficients, it revealed the true strength of the relationships. The regression model showed that the combination of inbound velocity, mass, dynamic stiffness, and energy loss accounted for 86 % of the variation in outbound velocity, 96 % of the variation in contact time, 85 % of the variation in deformation and 97 % of the variation in peak impact force at the certification test velocity. At the higher velocity, the combination of properties accounted for 65 % of the variation in outbound velocity, 85 % of the variation in contact time, 74 % of the variation in deformation and 70 % of the variation in peak impact force. These results suggest the most important properties that govern the impact response of a football were identified.

The portion of the variation not accounted by properties can be attributed to the assumptions of the models. The impact response of an inflated ball has previously been associated to the stiffness, material damping and elastic properties [30,84]. While the first two properties were included, the elasticity of the football was assumed negligible. This characteristic is likely to have the greatest influence the outbound velocity, by influencing the storage and release of potential energy during rebound. Moreover, the texture of the football and interaction between the panels may affect the deformation behaviour and interaction with the force platform surface and could subsequently introduce spin on the separation of the surface which introduces additional dynamics to the collision, which the model currently considers negligible [13,101]. Between the two velocities, the model performance for peak impact force showed the largest change. This may be caused by the assumption that any contribution by the phenomenon of momentum flux was negligible. This phenomenon accounts for the reaction force that results from the transfer of mass from the outer circumference of the football to the stationary portion that is in contact with the surface. This phenomenon has been encountered by many researchers mathematically modelling the impact response of a pressurised sphere as an additional mechanism of energy loss [28,55,152]. The results would suggest that this phenomenon has more influence on the impact response of footballs at higher velocities.

The results demonstrated that the impact response arose from a complex interaction between all properties of the football, as well as the conditions of the impact. While existing research has been largely speculative as to the reasons differences may occur for the impact behaviour between footballs often associating the difference broadly to material composition, this study identifies the properties responsible for explaining the differences in impact behaviour between various footballs. It has shown that the impact response of a football is primarily governed by its dynamic stiffness, that significantly influences the contact time, the deformation and the peak impact force. The inbound velocity is a key determinant of rebound speed but also affects deformation and impact force, especially at higher speeds. Energy loss consistently influences rebound speed. The mass properties explained relatively little of the variation across all the impact variables, with some influence on peak impact force at the lower speed. This research provides strong evidence to suggest solely measuring the rebound height of a football during certification does not capture the stiffness characteristics of a football. A ball meeting the rebound height standard might be assumed to perform well in all aspects, which could be misleading, as this measure provides an incomplete assessment of the properties governing the impact response of a football. Two footballs with similar rebound heights might behave differently in other important aspects such as impact force, contact time and deformation. This could lead to inconsistencies in how a ball feels and performs in different situations, potentially affecting gameplay quality and player performance. The next section of this chapter will investigate whether the properties obtained during the certification test are able to explain variations in impact behaviour encountered at higher velocities. This is critical in the regulation of footballs.

6.5 Relationships between the Two Impact Velocities

The impact response of a football has been shown to vary with impact velocity. Typically, this has been shown by observing the decrease of the COR for a football at an increasing inbound velocity, rather than considering the change in mechanical properties of the footballs. Replicating the magnitude and rate of deformation of dynamic impacts in a controlled laboratory environment to measure the properties of a football is challenging. Standardised quasi-static test machines cannot replicate the conditions of impact tests, whereas relatively low speed drop tests are easy to perform in controlled environments. The mathematical models derived in this chapter have shown that by estimating the mechanical properties from dynamic impact tests, these properties could explain the variations in impact response at each respective velocity.

To establish comprehensive policies to effectively regulate the standard of footballs, it is essential to quantitatively understand the properties under different conditions. While the FQP rebound test aims to verify whether a football meets the standards and specifications outlined by FIFA, understanding how well the procedure accurately reflects the behaviour of a football in various conditions it will encounter in real world applications is essential for assessing the footballs performance in practical scenarios. It is necessary to investigate whether the differences in the dynamic mechanical properties between the footballs obtained from the FQP rebound test, can explain the variation in impact response at a higher impact velocity.

6.5.1 Model overview

In the work up to this point, the two velocities have been considered separate, with individual models established at both velocities for the impact variables. In this section, the dynamic mechanical properties obtained at the certification test velocity will be the independent variables and the dynamic impact variables measured at the high velocity will be the dependant variables.

The model will take the form:

$$Y = Av_{i(HV)} + Bm_b + Ck_{dyn(CT)} + De_{loss(CT)} + constant$$

Where $v_{i(HV)}$ is the inbound velocity at the higher velocity, m_b is the mass of the football and $k_{dyn(CT)}$ is the dynamic stiffness of the football and $e_{loss(CT)}$ is the energy loss measured at the certification test velocity.

For this model, the independent and dependant variables were non-concurrent, i.e. the independent variables were captured separately from the dependent variables. To minimise the potential impact of variability introduced by the different experiment conditions, the average of the 25 repeat measurements from each football (n = 12) were used. This approach is common practice in scientific research when dealing with non-concurrent datasets as it gives a more representative depiction of the relationship between the independent and dependant variables, improving the generalisation of the results.

6.5.2 Results

In this section, the results of the model using the mechanical properties calculated from the impacts at the certification velocity with dependant variables from the higher velocity are presented.

Table 58 presents the performance metrics along with the coefficients and their significance for each dependant variable.

Table 58 The performance and coefficients for each dependent variable at the higher velocity using the mechanical properties evaluated at the certification test velocity.

Condition	RMSE	R^2	Coefficient and significance				
			Inbound Velocity	Mass	Dynamic Stiffness	Energy Loss	Constant
Outbound velocity	0.50	0.73	0.59 $p < 0.05$	-0.27 $p > 0.05$	-0.55 $p > 0.05$	-0.08 $p > 0.05$	0.00 $p > 0.05$
Contact Time	0.38	0.85	-0.25 $p > 0.05$	0.23 $p > 0.05$	-0.91 $p > 0.05$	0.01 $p > 0.05$	0.00 $p > 0.05$
Deformation	0.27	0.92	-0.21 $p > 0.05$	-0.01 $p > 0.05$	-0.85 $p < 0.05$	-0.07 $p > 0.05$	0.00 $p > 0.05$
Peak Impact Force	0.60	0.60	0.36 $p > 0.05$	-0.21 $p > 0.05$	0.68 $p > 0.05$	-0.32 $p > 0.05$	0.00 $p > 0.05$

In Table 58, mass was consistently observed to not meet the required level of significance. A second iteration was devised without mass to ensure this variable was not inhibiting the significance of other independent variables. The results of the second iteration are presented in Table 59. While slight reductions in the overall performance of the model, the dynamic stiffness was observed to meet the required level of significance in more of the models.

Table 59 The performance and coefficients for each dependent variable at the higher velocity using the mechanical properties evaluated at the certification test velocity with mass removed from the independent variables.

Condition	RMSE	R^2	Coefficient and significance			
			Inbound Velocity	Dynamic Stiffness	Energy loss	Constant
Outbound velocity	0.55	0.67	0.62 $p < 0.05$	-0.71 $p < 0.05$	-0.03 $p > 0.05$	0.00 $p > 0.05$
Contact Time	0.42	0.81	-0.27 $p > 0.05$	-0.78 $p < 0.05$	-0.03 $p > 0.05$	0.00 $p > 0.05$
Deformation	0.27	0.92	-0.21 $p > 0.05$	-0.86 $p < 0.05$	-0.07 $p > 0.05$	0.00 $p > 0.05$
Peak Impact Force	0.63	0.57	0.38 $p > 0.05$	0.56 $p > 0.05$	-0.28 $p > 0.05$	0.00 $p > 0.05$

6.5.3 Discussion

This model investigated whether the mechanical properties captured during the rebound test could explain the variation observed between the footballs at the higher velocity. The regression model showed that the combination of mechanical properties captured during the rebound test accounted for 67 % of the variation in outbound velocity, 81 % of the variation in contact time, 92 % of the variation in deformation and 57 % of the variation in peak impact force. To achieve statistical significance among the terms, the mass of the football had to be removed. This was attributed to the limited range of this variable in the model, that was partly restricted by the passing requirements of the FQP. The elements of impact behaviour such as contact time and deformation that are associated to the stiffness properties of the football were well accounted for by the properties captured at the lower velocity. Whereas the outbound velocity and peak impact force suffered from the assumption of negligible contributions from other mechanisms such as elasticity and momentum flux, that have greater emphasis at the higher velocity. These initial findings suggest that the mechanical properties obtained from the rebound test performed as part of the FQP could be used to predict the response of the football at higher velocities even though the trend cannot be clearly quantified due to the relatively small sample size. However, despite this limitation, these findings suggest that the rebound test in the FQP, designed to assess the impact behaviour of a football, may also offer insights into the performance of a football at higher impact velocities. Expanding the sample size in future research could provide a more robust relationship that would enable the ability to predict football behaviour across a broader range of velocities.

6.6 Conclusions

The results of the multivariable regression models showed that when in combination with the inbound velocity and mass, the dynamic mechanical properties of stiffness and energy loss explained a considerable portion of the variation observed in the impact response of footballs. At the two velocities, 6 and 20 $m \cdot s^{-1}$, these properties accounted for 86 % and 65 % of the variation in outbound velocity, 96 % and 85 % of the variation in contact time, 85 % and 75 % of the variation in deformation and 97 % and 70 % of the variation in peak impact force, suggesting these are the two most important properties in governing a football's response to an impact. The unexplained variance was attributed to the assumption of negligible influence by the panel interactions, elasticity of the football and momentum flux. These assumptions affected the performance of the models at 20 $m{\cdot}s^{-1}$ for the outbound velocity and peak impact force more than the contact time and deformation, that demonstrated strong correlations with stiffness.

The results of the four multivariable regression models showed that the dynamic mechanical properties captured during the rebound test accounted for 67 % of the variation in outbound velocity, 81 % of the variation in contact time, 92 % of the variation in deformation and 57 % of the variation in peak impact force at the higher velocity. This is a novel finding to suggest the properties captured during rebound test can explain variations in impact response at higher velocities. The significance of these relationships suffered due to the relatively low sample size that resulted from averaging the repeated impacts to minimise the effect of random variability masking the true strength of the relationship when comparing between the two non-concurrent datasets, but could be overcome by increasing the sample size, and considering a wider range of football designs.

The mechanical properties of footballs encapsulate the collective behaviour of the material composition and internal air pressure of the football, encompassing crucial aspects such as stiffness, material damping, elasticity, and momentum flux, which play a pivotal role in determine the football's response to an impact. The mechanical properties measured from quasi-static tests struggled to explain variations in impact response, suggesting while they can be used to provide a baseline comparison between structural properties of footballs, they not represent the properties of footballs during dynamic impacts. The dynamic stiffness properties showed significant influence on the way a football responds at both velocity conditions yet is not directly examined by the governing body. The findings demonstrate that solely measuring the rebound height of a football during certification may provide an incomplete assessment of the properties governing the impact response of a football. By overlooking the stiffness properties of a football that primarily govern the contact time, deformation and impact force it could lead to inconsistencies in how a ball feels and performs in different match situations, potentially affecting game play and player performance.

The knowledge developed in this chapter enables a data-driven approach to regulation, facilitating evidence-based decision-making that allows certification standards to evolve with scientific advancements. By understanding the mechanisms that govern the impact behaviour of a football, FIFA can proactively enhance their performance standards to ensure a comprehensive assessment of a football. As technology advances, football design and manufacturing technologies will evolve, making it essential to consider the mechanical properties to keep regulations relevant. This ensures that FIFA stay abreast of technological advancements, enhancing the overall safety, fairness and playability of footballs under various conditions. The next chapter will consider the integration of these findings into the existing test protocols of the FQP.

7 Practical Applications to Regulate Football Performance

7.1 Introduction

In chapter 6, a multivariable regression model was developed that showed the mechanisms governing the impact behaviour of a football. Implementing a programme of tests to examine the overall performance of a football takes a more macroscopic approach than mathematical modelling. While the doctoral study has delved into the properties and behaviours of footballs to detect subtle differences and improve knowledge, policy implementation aims to categorise footballs into distinct performance categories rather than pinpointing to minor disparities. To effectively regulate the standard of footballs used at the top level of the game, standardised test protocols must be established that can simulate real-world impact scenarios but fundamentally are designed to offer an objective evaluation of a football's performance with minimal measurement error. For that reason, additional considerations are required to ensure that the test procedures are repeatable and applicable to various football brands and types. Moreover, any change to the current policy should add substantial value to the test programme while aligning with the overarching goal of enhancing the integrity of the sport and consistency of football performance standards.

This chapter will discuss how the results of the doctoral study can be implemented into the FIFA Quality Programme (FQP). This will work towards successfully achieving objective 6 of the doctoral study.

7.2 Modification opportunities in the Rebound test

It is imperative that any proposed developments or modifications to the rebound test preserve the integrity and objectivity of the assessment. There three areas that could be modified are (1) the apparatus (and the subsequent impact velocity), (2) the impact surface and (3) the measurements taken. Each aspect will be discussed below.

a) The apparatus

Chapter 4 presented two methods to project the football towards the surface; these included the drop test currently employed in the FQP and a mechanical device to project the football to a higher velocity of 20 $m{\cdot}s^{-1}$. However, the model developed in Chapter 6 demonstrated that increasing the inbound speed to 20 $m{\cdot}s^{-1}$ does not improve the assessment of football behaviour or better distinguish performance differences compared to the current test. This conclusion is based on the observation that the properties governing the outbound velocity, a parameter closely correlated with rebound height, remained consistent across both velocity conditions. Therefore, the additional financial and logistical challenges of incorporating an additional device to increase the impact speed is not justified.

b) The impact surface

In the current test protocol, the impact surface is metal. Replacing this with alternative materials, such as turf, would compromise the integrity of the rebound measurement. However, an alternative approach could involve directly impacting a force platform, which would enhance the measurement capabilities and provide additional data without compromising the accuracy and reliability of the test.

c) The measurements

The model in chapter 6 alluded that the current test protocol may not provide a comprehensive assessment of the properties of a football that govern the impact response. Specifically, the sole measurement of rebound height captures the energy loss characteristics and may not fully address the stiffness properties that influence the contact duration, deformation and impact force. The results indicated that the stiffness properties captured during the drop test could account for variations in the impact response of the footballs at the higher velocity. While some discrepancies in the strength of the relationships were attributed to the assumptions made in the mathematical models, relying solely on the rebound height may not effectively protect the integrity of the game. Capturing the stiffness properties during the drop test could provide a more robust assessment of football performance under various conditions.

This section has highlighted the potential areas for innovation within the rebound test of the FQP. The next section will establish the feasibility and potential methods to integrate these learnings into the current test protocol FQP.

7.3 Application of Findings

FIFA's motivation around this work was to ensure that the measurements taken in the FQP are appropriate to ensure the impact behaviour of a football remains consistent to protect the integrity of the game. The findings of the models suggest that additional parameters associated with the stiffness properties of the football should be introduced into the test protocols of the FQP to offer a robust assessment of the performance of the football across various conditions.

For a change to occur, it will involve going through the following process:

1. Modification to test protocol identified
2. Background data capture to establish validity and define passing thresholds
3. Results and presentation to TAG*
4. Vote for integration
5. Integration into the test protocol

*The FIFA Technical Advisory Group (TAG) for footballs is a group consisting of several representatives from FIFA licencees, test institutes and academia, formed to exchange on technical discussions about improving the standards for football.

The background data capture is an important stage for assessing the applicability of additional measures across a diverse sample of footballs. This process, performed alongside the existing rebound height measurement during certification, helps to determine if a new measurement is suitable for regulating impact behaviour and setting pass-fail criteria. To enable background data capture to occur, it should involve minimal changes to the existing rebound test that allow it to be conducted simultaneously with the rebound height measurement. This would involve maintaining the current metal impact surface. Directly measuring the stiffness would require a force platform, which is inappropriate due to conflicts with the current manual and European standards.

The current rebound test employs either a video-based or acoustic measurement, with neither technique predominantly used across various test institutes. Therefore, a proxy for dynamic stiffness that could be measured using either an audio or visual method would be required. It is important to acknowledge that each of the variables used to describe the football's impact response have a degree of correlation. The contact time and deformation, which are heavily determined by the stiffness, directly affect the footballs' ability to absorb and dissipate energy, consequently affecting the rebound behaviour and potentially leading to variations in outbound velocity. A single variable that can be measured visually and acoustically is contact time, that conveniently emerged as the variable with the highest correlation with dynamic stiffness ($r = 0.96$, $p<0.01$). While the FIFA manual specifies accuracy for acoustic measurements at 1 ms (per EN 12235: 2013), it does not specify a minimum sampling frequency. Conversations with test institutes have shown through UKAS (UK accreditation service) assessments the accuracy of their equipment falls far below the specified requirement at approximately 0.1 ms. A visual method must be accurate to ± 1 cm, but likewise no minimum sample frequency is specified. Across the data collection of the 12 footballs used in this study, the difference in contact time for the rebound test was 2.1 ms, but it is unknown what minimum accuracy would be required to identify distinct performance categories of footballs. Therefore, the exploratory data collection should use the highest accuracy equipment available. Since many test institutes only have high-speed visual systems capable of operating at 2000 Hz, giving a resolution of 0.5 ms, it would be suitable for test institutes to use acoustic equipment accurate to 0.1 ms for the initial collection. This can then be refined and reviewed based on the data collected.

7.4 Conclusions

Three areas for potential modification in the existing rebound test were the apparatus, impact surface and the measurements. There was no evidence from previous chapters to warrant changes to the inbound velocity. However, the stiffness captured during the rebound test could account for variations in behaviour for impacts at higher speeds, indicating its potential as a robust measure for evaluating the performance of a football across diverse conditions. Thus, while assessing the rebound height alone may not be effective to safeguard the integrity of the game, incorporating an additional measurement that directly or indirectly reflects the stiffness of a football could provide a more comprehensive evaluation of a footballs impact behaviour.

The practical application of these findings was considered and recommends that contact time is the best proxy for dynamic stiffness and should be assessed during the regulation of footballs. To apply this finding within the FIFA Quality Programme would require suitable criteria for the approval bounds to be identified. Defining this criterion fell beyond the scope of this research. However, a route to establish if measuring contact time in the FQP is an appropriate additional measurement to regulate the impact behaviour of footballs has been identified and the next steps outlined.

8 Conclusions

8.1 Introduction

This chapter will consolidate the findings from this doctoral study. The chapter will present a summary of the findings for each objective that was outlined in Chapter 1. It will then highlight the conclusions from the research and present possible future directions to progress this area of research.

8.2 Summary of Study

The aim of this research was to develop a greater understanding of the influence that the mechanical properties of a football have on its impact response at a low and at a match-representative velocity. To achieve this aim, six objectives were formed. This section presents a short summary of the findings from each objective.

Objective 1 - To analyse and evaluate existing research relevant to this study.

All footballs used in a competitive environment must adhere to the standards outlined in the FIFA Quality Programme (FQP). The rebound test has been used to regulate the impact behaviour of a football since 1996 with minimal alterations to the methodology and approval bounds. However, there remains uncertainty to whether this test is appropriate to safeguard against future developments in football design detrimentally affecting the sport. Previous research efforts have explored the impact behaviour of a football using experimental investigations, mathematical modelling, and computational simulations. The main weaknesses of the published material were the inconsistencies in experimental protocols between impact studies and that often only a single football had been considered during the development of previous models. Efforts to characterise the properties of a football have been limited in scope and often performed separate to impact studies. This posed challenges in synthesising results across different studies to conclude the influence of a ball's properties on its impact behaviour, fuelling the doctoral study.

Objective 2 - Measure the quasi-static stiffness properties of a football.

The structural stiffness of 12 different footballs, that represented a typical range of footballs adhering to the FQP standards, was obtained using a quasi-static compression test. It was found that the relative stiffness of the footballs was dependant on the magnitude of the deformation. The results confirmed differences among the physical properties of the footballs.

Objective 3 - Validate an experimental set-up to measure the force and deformation during a football-surface impact.

An experiment was carried out to replicate the rebound test from the FQP at 6 $m{\cdot}s^{-1}$ and using a mechanical device to project a football at a force platform at 20 $m{\cdot}s^{-1}$. Repeated impacts at both velocity conditions demonstrated high absolute and relative repeatability indicating that the combination of high-speed video and a force platform could consistently measure the dynamic response of a football to an appropriate sensitivity that would allow statistically significant comparisons between different footballs.

Objective 4 - Measure the impact response of a football during a collision with a surface at appropriate velocities.

Impact tests were carried out on the 12 footballs and several impact variables were determined empirically for each football. The differences in the physical properties of the footballs were reflected in variations in their dynamic impact response. Typically footballs that exhibited higher stiffness exhibited lower contact times and deformation compared to footballs of lower stiffness'. It was found that the footballs exhibited similar material damping properties during the rebound test. Higher variability was found between the footballs in the impact variables attributed to the stiffness properties at both inbound velocities. The rebound test demonstrated lower variability in a single impact variable among the repeated impacts for each football compared to the mechanical device, particularly in the measurements of inbound velocity and permitted more control over the impact orientation.

Objective 5 - Develop a mathematical model between the mechanical properties of a football and appropriate variables that characterise the impact response of a football.

A first-order multivariable regression model was developed to examine the relationship between the mechanical properties and dynamic impact response of a football. This model assessed the contribution of mass, stiffness and energy loss on the impact response, demonstrating that variations between different footballs impact response were best explained by incorporating properties derived from dynamic impact tests. The findings revealed that the impact response is a result of the complex interaction between all the footballs properties and impact conditions. This study is the first to observe that the mechanical properties a football measured during relatively low-impact scenarios may allude to variations in impact behaviour at higher velocities. Further improvement to the accuracy of the models could be achieved by considering additional properties such as elasticity, characteristics of the impact such as panel interactions and additional impact phenomenon's such as momentum flux. This approach represents a significant advancement on prior approaches as it considers a broader range of footballs, offering a more comprehensive understanding of how their physical properties affect the impact behaviour.

Objective 6 - *Consider the practical applications of the research findings in the context of the FIFA Quality Programme for Footballs.*

The rebound test in the FQP is fundamentally designed to provide an objective evaluation of a football's performance. However, findings have demonstrated that solely measuring the rebound height during certification offers an incomplete assessment of the properties governing a football's impact response. Incorporating an additional measurement of contact time can be incorporated into the existing test protocol to provide a comprehensive assessment of the mechanisms governing a footballs impact response.

8.3 Conclusions

The main conclusions of this study are listed below:

- FIFA-certified footballs exhibited different structural stiffness' that resulted in variations in the impact behaviour of the footballs, particularly in measurements of contact time, deformation, and peak impact force.

- A first-order multivariable model effectively quantified the relationship between different mechanical properties, the impact conditions, and the impact response of a football.

- Properties measured from static tests could not predict dynamic behaviour, due to lower compression rates and differing deformation shapes that fail to accurately represent a football's response across representative impact speeds. This highlights the need for a dynamic approval test within the FQP to maintain high standards of performance.

- The governing role of different mechanical properties of a football during impact stages highlights that a single measurement cannot comprehensively evaluate the impact performance of a football.

- Solely measuring the rebound height during the certification of footballs provides an incomplete assessment of the properties governing the impact response of a football. Overlooking the stiffness properties may lead to inconsistencies in football performance.

8.4 Contribution to knowledge

Chapter 7 discussed the practical applications of the research findings, specifically addressing their relevance to the policies governing football performance in global competitions. However, this research also contributes significantly to the broader understanding of football impact mechanics.

The research demonstrated the effectiveness of a commercially available force platform as a measuring system for quantifying and comparing the impact force for different footballs. It quantified the minimal detectable difference in measuring the peak impact force and impulse for footballs inflated to 0.8 bar for impacts at 6 and 20 $m \cdot s^{-1}$. The repeatability statistics identified the threshold at which any detected change in impact variable can be attributed solely to the differences in football construction, rather than variability in the measurement system. Although the statistics obtained at 20 $m \cdot s^{-1}$ may have limited applicability due to the use of a bespoke launching device, the impacts at 6 $m \cdot s^{-1}$ used a standard drop protocol with commercially available equipment, so can offer valuable insights to the broader research community by identifying minimum thresholds necessary for detecting genuine changes.

This research measured the stiffness properties of a football using both static and dynamic tests. It highlighted that the calculation method used with quasi-static force-deflection measurements affects the magnitude of stiffness and subsequent correlation with dynamic impact variables, such as contact time. The use of a 2nd order polynomial evaluated at a deflection of 3 mm showed higher correlations with dynamic impact variables than linear models. This research identified the mechanical properties that govern the impact response of a football at two velocities, 6 and 20 $m \cdot s^{-1}$. It identified the mechanical properties that explained the variance in impact behaviour for several variables; outbound velocity, contact time, deformation, and peak impact force. Furthermore, it revealed that the dominant properties governing the impact response of a football change with different velocities. This emphasises that differences in the properties of a football, that could directly influence the impact behaviour during high-speed impacts, are unidentifiable through solely measuring the COR at 6 $m \cdot s^{-1}$.

This research has established a dataset of football properties and their corresponding impact response for multiple FIFA certified footballs. This dataset provides researchers a valuable resource for understanding the relationship between various ball characteristics and their impact behaviour. Manufacturers can leverage this dataset to refine product development, gaining an understanding of how prototype footballs compare to a variety of currently certified models. Researchers can build on this dataset to explore more complex relationships between football properties and impact response, leading to ongoing advancements in the field.

8.5 Limitations

In each chapter, several limitations have been identified. There are three that require the most consideration. Firstly, the use of a bespoke mechanical device introduced variability into the impact variables of the football at the higher velocity. This variability reduced the number of statistical differences by widening the confidence intervals. Secondly, across the programme of research, a single inflation pressure was considered. As a result, the contribution of internal air pressure over material composition on the properties of a football cannot be distinguished using the current dataset. Finally, the assumption of negligible elasticity within the mathematical model of outbound velocity may not accurately capture real-word behaviour.

8.6 Future Research

This investigation has highlighted the potential for further research, which are discussed below:

a) *Investigating the role of football construction modifications in mitigating head injury risk*

Researchers have often explored the mitigation of sports injuries through equipment modification. The current FQP standards do not explicitly examine characteristics of the ball related to player safety. This is largely because the relationship between impact variables and the mechanisms of injury are not fully understood. Given the increasing public and scientific concern around short and long-term neurodegenerative diseases, a critical area of research should involve how modifications to a football's construction might reduce the impact magnitude of headers. This research should extend the understanding between ball properties including size, weight, internal air pressure and material composition on the force and energy transfer during collisions. This knowledge will be crucial for advancing policy on football construction with a focus on player welfare and developing effective injury mitigation strategies across all levels of the sport.

b) Oblique impacts

This study considered a normal-inbound impact to ensure the impact response solely reflected the properties of the footballs. A natural progression would be to consider more advanced impact scenarios such as oblique impacts. Unlike normal-inbound impacts that focus on the properties of the football, oblique impacts introduce additional factors such as the coefficient of friction between the football and surface, impact angle, variable contact area and distribution of forces. The rebound behaviour will also require additional factors to quantify the angle and spin. To effectively analyse the impact behaviour of a football during an oblique impact many additional impact variables would have to be incorporated into the model. However, advancing knowledge in this area would not only enhance our understanding of football behaviour, but it could also lead to more realistic testing protocols by providing insights into how the existing rebound test relates to oblique impacts encountered during match play.

c) Using instrumented footballs in impact studies to measure impact severity.

An avenue that poses many exciting opportunities is the growing emergence of instrumented footballs. These footballs integrate an inertial measuring unit (IMU) that measures precise changes in acceleration and deceleration during impacts. Incorporating such technology into the experimental methodologies of impact studies offers a novel approach to quantify the impact magnitude and duration of an impact, as well as determining the forces exerted on a football. This may enable a direct quantification of impact severity experienced by players, such as during heading, without the need for simplified experimental setups aimed at replicating human-like behaviour. However, the predominant use of instrumented footballs is in touch detection for officiating purposes. Therefore, it is imperative to determine the full-scale range of acceleration to identify whether the current capabilities of these footballs would be a viable tool for use in impact studies. The real-time data provided by IMU's holds immense potential and would allow immediate feedback on the impact severity during training sessions and matches. This information could be used by coaches and medical staff to make informed decisions regarding player safety, making a significant step forward in research centred around player welfare.

9 References

[1] Fédération Internationale de Football Association, " Testing Manual FIFA Quality Programme for Footballs ," 2018.

[2] The International Football Association Board, *The Laws of the Game.* 2021.

[3] Fédération Internationale de Volleyball, *Homologation Procedures for Manufacturers Volleyball & Beach Volleyball.* . 2014.

[4] Fédération Internationale de Basketball, *Basketball Rules and Basketball Equipment* . 2022.

[5] R&A and United States Golf Association, *The Equipment Rules.* 2020.

[6] World Baseball and Softball Confederation, *The Official Rules of Baseball* . 2023.

[7] The Fédération Internationale de Hockey, *Performance Requirements and Test Procedures for Hockey Balls* . 1999.

[8] International Tennis Federation, *ITF Approved Tennis Balls, Classified Surfaces & Recognised Courts: A Guide to Products and Test Methods* 2023.

[9] FIFA, "Youth Football Specification Recommendations," 2021.

[10] R. Zouari, S. B. Amar and A. Dogui, "Experimental and numerical analyses of fabric off-axes tensile test," *Journal of the Textile Institute,* vol. 101, *(1),* pp. 58-68, 2010. DOI: 10.1080/00405000802231341.

[11] D. S. Price, "Advanced Modelling of Soccer Balls ." , Loughborough University, 2005.

[12] D. T. Kirkendall, S. E. Jordan and W. E. Garrett, "Heading and Head Injuries in Soccer," *Sports Medicine,* vol. 5, *(31),* pp. 369-386, DOI: 0112-1642/01/0005-0369/$22.00/0.

[13] D. S. Price *et al*, "Viscoelasticity of multi-layer textile reinforced polymer composites used in soccer balls," *J. Mater. Sci.,* vol. 43, *(8),* pp. 2833-2843, 2008. DOI: 10.1007/s10853-008-2526-0.

[14] S. Tuplin *et al*, "The application of simulation to the understanding of football flight," *Proceedings of the Institution of Mechanical Engineers, Part P: Journal of Sports Engineering and Technology,* vol. 226, *(2),* pp. 134-142, 2012. DOI: 10.1177/1754337112444402.

[15] M. A. Passmore *et al*, "Experimental studies of the aerodynamics of spinning and stationary footballs," *Proc. Inst. Mech. Eng. Part C,* vol. 222, *(2),* pp. 195-205, 2008. DOI: 10.1243/09544062JMES655.

[16] M. Passmore *et al*, "The aerodynamic performance of a range of FIFA-approved footballs," *Proceedings of the Institution of Mechanical Engineers, Part P: Journal of Sports Engineering and Technology,* vol. 226, *(1),* pp. 61-70, 2012.

[17] M. J. Carré, S. R. Goodwill and S. J. Haake, "Understanding the effect of seams on the aerodynamics of an association football," *Proc. Inst. Mech. Eng. Part C,* vol. 219, *(7),* pp. 657-666, 2005. DOI: 10.1243/095440605X31463.

[18] S. Hong and T. Asai, "Effect of panel shape of soccer ball on its flight characteristics," *Scientific Reports,* vol. 4, 2014. DOI: 10.1038/srep05068.

[19] B. Thompsett, A. Harland and J. Roberts, "Investigating the relationship between physical properties of a football and player perceptions," in *11th Conference of the International Sports Engineering Association;* 2016, pp. 519-525.

[20] J. T. Bauman, *Fatigue, Stress, and Strain of Rubber Components : A Guide for Design Engineers.* 2008.

[21] D. C. Leigh and W. Lu, "Dynamics of the Interactions Between Ball, Strings, and Racket in Tennis," *International Journal of Sport Biomechanics,* vol. 8, pp. 181-206, 1992.

[22] R. Cross, "The bounce of a ball," *Am. J. Phys,* vol. 67, *(3),* 1999.

[23] M. J. Carré, D. M. James and S. J. Haake, "Impact of a non-homogeneous sphere on a rigid surface," *J. Mechanical Engineering Science,* vol. 218, 2004.

[24] F. Collins, D. Brabazon and K. Moran, "Viscoelastic impact characterisation of solid sports balls used in the Irish sport of Hurling," *Sports Engineering,* vol. 14, *(1),* pp. 15-25, 2011. DOI: 10.1007/s12283-011-0067-2.

[25] A. Bryson and L. Smith, "Impact response of sports materials," in 2010, DOI: 10.1016/j.proeng.2010.04.095.

[26] H. Brody, "The physics of tennis. III. The ball–racket interaction," *American Journal of Physics,* vol. 65, *(10),* pp. 981-987, 1997. DOI: 10.1119/1.18701.

[27] R. J. Dignall, "Modelling the Impact of Tennis Balls on Court Surfaces." , The University of Sheffield, 2004.

[28] S. R. Goodwill, "The Dynamics of Tennis Ball Impacts on Tennis Rackets." , The University of Sheffield, 2002.

[29] M. J. Carré, "The Dynamics of Cricket Ball Impacts and the Effect of Pitch Construction." , The University of Sheffield, 2000.

[30] F. Schneider *et al*, "Analysis of mechanical properties of different volleyballs," *Proceedings of the Institution of Mechanical Engineers, Part P: Journal of Sports Engineering and Technology,* vol. 233, *(2),* pp. 292-300, 2019. DOI: 10.1177/1754337118823996.

[31] A. Karimi *et al*, "Measurement of the mechanical properties of soccer balls using digital image correlation method," *Sport Sciences for Health,* vol. 12, *(1),* pp. 69-76, 2016. DOI: 10.1007/s11332-015-0255-8.

[32] S. P. Hendee, R. M. Greenwald and J. J. Crisco, " Static and Dynamic Properties of Various Baseballs," *Journal of Applied Biomechanics,* vol. 14, pp. 390-400, 1998.

[33] G. Holmes and M. J. Bell, "effect of football type and inflation pressure on rebound resilience," pp. 132-135, 1985.

[34] T. A. Levendusky *et al*, "Impact characteristics of two types of soccer balls," in *First World Congress of Science and Football,* 1987, pp. 385-393.

[35] N. Wiart *et al*, "Effect of temperature on the dynamic properties of soccer balls," *Proceedings of the Institution of Mechanical Engineers, Part P: Journal of Sports Engineering and Technology,* vol. 225, *(4),* pp. 189-198, 2011. DOI: 10.1177/1754337111411644.

[36] T. Iga *et al*, "Basic mechanical analysis of soccer ball impact," in *Proceedings of the 31st International Conference on Biomechanics in Sports * 2013, .

[37] Z. Taha and M. H. A. Hassan, "A reaction-force-validated soccer ball finite element model," *Proceedings of the Institution of Mechanical Engineers, Part P: Journal of Sports Engineering and Technology,* vol. 231, *(1),* pp. 43-49, 2017. DOI: 10.1177/1754337115626636.

[38] A. Koizumi *et al*, "A study of impact force on modern soccer balls," in *2014 Conference of the International Sports Engineering Association* 2014, pp. 423-428.

[39] J. Auger *et al*, "Factors affecting peak impact force during soccer headers and implications for the mitigation of head injuries," *PLoS ONE,* vol. 15, *(10),* 2020. DOI: 10.1371/journal.pone.0240162.

[40] T. Asai *et al*, "The curve kick of a football I: impact with the foot," *Sports Engineering,* vol. 5, pp. 183-192, 2002.

[41] H. Shinkai *et al*, "Ball impact dynamics of instep soccer kicking," *Med. Sci. Sports Exerc.,* vol. 41, *(4),* pp. 889-897, 2009. DOI: 10.1249/MSS.0b013e31818e8044.

[42] D. S. Price, R. Jones and A. R. Harland, "Computational modelling of manually stitched soccer balls," *Proceedings of the Institution of Mechanical Engineers, Part L: Journal of Materials: Design and Applications,* vol. 220, *(4),* pp. 259-268, 2006. DOI: 10.1243/14644207JMDA83.

[43] D. S. Price, R. Jones and A. R. Harland, "Advanced finite-element modelling of a 32-panel soccer ball," *Proc. Inst. Mech. Eng. Part C,* vol. 221, *(11),* pp. 1309-1319, 2007. DOI: 10.1243/09544062JMES711.

[44] R. E. Jacobson, *The Manual of Photography.* (9. ed. ed.) 2000.

[45] R. Hartley and A. Zisserman, *Multiple View Geometry in Computer Vision.* 2003.

[46] M. Dunn *et al*, "Reconstructing 2d planar coordinates using linear and non-linear techniques," in *30th Annual Conference of Biomechanics in Sports * 2012, .

[47] Z. Zhang, "Flexible camera calibration by viewing a plane from unknown orientations," in 1999, DOI: 10.1109/iccv.1999.791289.

[48] *Check 2D - Camera calibration tool for 2D kinematic analysis*. Sheffield Hallam University. Sports Engineering Research Group. http://www.check2d.co.uk

[49] *Check 3D - Camera calibration tool for 3D kinematic analysis*. Sheffield Hallam University. Sports Engineering Research Group. http://www.check3d.co.uk

[50] C. B. Daish, *The Physics of Ball Games.* 1972.

[51] R. Cross, "The coefficient of restitution for collisions of happy balls, unhappy balls, and tennis balls," *Am. J. Phys,* vol. 68, *(11),* pp. 1025-1031, 2000.

[52] H. Nunome, K. Ball and H. Shinkai, "Myth and fact of ball impact dynamics in football codes," *Footwear Science, (2),* pp. 105-118, 2014. DOI: 10.1080/19424280.2014.886303.

[53] G. Homes. and M. Bell., "Effect of football type and inflation pressure on rebound resilience," *Journal of the Sports Turf Research Institute,* vol. 61, 1985.

[54] B. W. Johnson, S. R. Reid and R. Trembaczowski-Ryderr, "The impact, rebound and flight off a well inflated pelliclee as exemplified in associationn footballl," in *Manchester Association of Engineers,* 1973, .

[55] M. Hubbard and W. J. Stronge, "Bounce of hollow balls on flat surfaces," *Sports Engineering,* vol. 4, pp. 49-61, 2001.

[56] L. P. Rica, "Contact and compression of elastic spherical shells: the physics of a 'ping-pong' ball," *Philos. Mag. B,* vol. 78, *(2),* pp. 225-233, 1998. DOI: 10.1080/014186398258285.

[57] R. Cross, "Dynamic properties of tennis balls," *Sports Engineering,* vol. 2, pp. 23-33, 1999.

[58] A. Rezaei *et al,* "Finite element modelling and experimental study of oblique soccer ball bounce," *J. Sports Sci.,* vol. 29*, (11),* pp. 1201-1213, 2011. DOI: 10.1080/02640414.2011.587443.

[59] T. Iga *et al*, "Novel mathematical model to estimate ball impact force in soccer," *Sports Biomechanics,* vol. 17*, (4),* pp. 477-493, 2018.

[60] S. AminiAghdam, R. Müller and R. Blickhan, "Locomotor stability in able-bodied trunk-flexed gait across uneven ground," *Human Movement Science,* vol. 62, pp. 176-183, 2018. DOI: 10.1016/j.humov.2018.10.011.

[61] S. AminiAghdam and R. Blickhan, "The effects of an expected twofold perturbation on able-bodied gait: Trunk flexion and uneven ground surface," *Gait and Posture,* vol. 61, pp. 431-438, 2018. DOI: 10.1016/j.gaitpost.2018.02.013.

[62] M. Günther *et al*, "Transverse pelvic rotation during quiet human stance," *Gait and Posture,* vol. 27*, (3),* pp. 361-367, 2008. DOI: 10.1016/j.gaitpost.2007.05.014.

[63] B. De La Fuente, F. Garcia and R. Arellano, "Are the forces applied during vertical countermovement jump related to the forces applied during the swimming start? ," in *Biomechanics and Medicine in Swimming*. University of Saint-Etienne, 2003, pp. 207-212.

[64] S. W. Lipfert, M. Günther and A. Seyfarth, "Diverging times in movement analysis," *J. Biomech.,* vol. 42*, (6),* pp. 786-788, 2009. DOI: 10.1016/j.jbiomech.2008.12.020.

[65] T. R. Derrick, "Signal processing," in *Research Methods in Biomechanics,* 2nd ed., D. G. E. Robertson *et al*, Ed. 2014, .

[66] R. Bartlett, *Introduction to Sports Biomechanics: Analysing Human Movement Patterns.* (2nd ed.) 2007.

[67] R. Sasaki *et al*, "The Friction Force Between the Soccer Ball and the Goalkeeper Glove Material," *Procedia Engineering,* vol. 72, pp. 654-659, 2014. DOI: 10.1016/j.proeng.2014.06.111.

[68] Kistler Group, "Multicomponent Force Plate," *(9281E_000-711e-02.14),* 2014.

[69] M. F. Bobbert and H. C. Schamhardt, "Accuracy of determining the point of force application with piezoelectric force plates," 1990. DOI: 10.1016/0021-9290(90)90169-4.

[70] H. Schmiedmayer and J. Kastner, "Parameters influencing the accuracy of the point of force application determined with piezoelectric force plates," *J. Biomech.,* vol. 32, pp. 1237-1242, 1999.

[71] S. G. Psycharakis and S. Miller, "Estimation of errors in force platform data," *Res. Q. Exerc. Sport,* vol. 77, *(4),* pp. 514-518, 2006. DOI: 10.1080/02701367.2006.10599386.

[72] N. Chockalingam, G. Giakas and A. Iossifidou, "Do strain gauge force platforms need in situ correction?" *Gait and Posture,* vol. 16, pp. 233-237, 2002.

[73] R. Cross, "Standing, walking, running, and jumping on a force plate," *American Journal of Physics,* vol. 67, *(4),* pp. 304-309, 1999. DOI: 10.1119/1.19253.

[74] C. Payton and R. Bartlett, *Biomechanical Evaluation of Movement in Sport and Exercise: The British Association of Sport and Exercise Sciences Guidelines.* 2007DOI: 10.4324/9780203935750.

[75] N. Hori *et al*, "Reliability of performance measurements derived from ground reaction force data during countermovement jump and the influence of sampling frequency," *J. of Strength and Conditioning Research,* vol. 23, *(3),* pp. 874-882, 2009.

[76] M. R. Gudavalli *et al*, "Effect of sampling rates on the quantification of forces, durations, and rates of loading of simulated side posture high-velocity, low-amplitude lumbar spine manipulation," *J. Manipulative Physiol. Ther.,* vol. 36, *(5),* pp. 261-266, 2013. DOI: 10.1016/j.jmpt.2013.05.010.

[77] L. V. Smith, A. M. Nathan and J. G. Duris, "A determination of the dynamic response of softballs," *Sports Engineering,* vol. 12, *(4),* pp. 163-169, 2010. DOI: 10.1007/s12283-010-0041-4.

[78] D. Knudson and R. Bahamonde, "Effect of endpoint conditions on position and velocity near impact in tennis," *J. Sports Sci.,* vol. 19, *(11),* pp. 839-844, 2001. DOI: 10.1080/026404101753113787.

[79] P. Bardella *et al*, "Optimal sampling frequency in recording of resistance training exercises," *Sports Biomechanics,* vol. 16, *(1),* pp. 102-114, 2017. DOI: 10.1080/14763141.2016.1205652.

[80] G. Smith, "Padding point extrapolation techniques for the butterworth digital filter," *Journal of Biomechanics,* vol. 22, *(8),* pp. 967-971, 1989. DOI: 10.1016/0021-9290(89)90082-1.

[81] H. Nunome *et al*, "Impact phase kinematics of instep kicking in soccer," *J. Sports Sci.,* vol. 24, *(1),* pp. 11-22, 2006. DOI: 10.1080/02640410400021450.

[82] A. Haron and K. A. Ismail, "Coefficient of restitution of sports balls: A normal drop test," in *IOP Conference Series: Materials Science and Engineering,* 2012, .

[83] N. J. Bridge, "The way balls bounce," *Physics Education,* vol. 33, *(3),* pp. 174-181, 1998. DOI: 10.1088/0031-9120/33/3/018.

[84] N. J. Bridge, "The way balls really bounce," *Physics Education,* vol. 33, *(4),* pp. 236-241, 1998. DOI: 10.1088/0031-9120/33/4/012.

[85] B. F. Bayman, "Model of the behavior of solid objects during collision," *American Journal of Physics,* vol. 44, *(7),* pp. 671-676, 1976. DOI: 10.1119/1.10353.

[86] E. Falcon *et al*, "Behavior of one inelastic ball bouncing repeatedly off the ground," *European Physical Journal B,* vol. 3, *(1),* pp. 45-57, 1998. DOI: 10.1007/s100510050283.

[87] D. M. James, "Understanding the Playing Performance of Cricket Pitches." , The Universtity of Sheffield, 2004.

[88] D. M. James, M. J. Carré and S. J. Haake, "The playing performance of county cricket pitches," *Sports Engineering,* vol. 7, *(1),* pp. 1-14, 2004. DOI: 10.1007/bf02843969.

[89] D. M. James *et al*, "Predicting the playing character of cricket pitches," *Sports Engineering,* vol. 8, pp. 193-207, 2005.

[90] T. Maruyama *et al*, "Influence of foot angle and impact point on ball behavior in side-foot soccer kicking," *Crossref,* vol. 42, *(16),* pp. 403-408, 2007. DOI: 10.1016/j.jbiomech.2009.08.025.

[91] H. Ishii *et al*, "Numerical study of ball behavior in side-foot soccer kick based on impact dynamic theory," *J. Biomech.,* vol. 42, *(16),* pp. 2712-2720, 2009. DOI: 10.1016/j.jbiomech.2009.08.025.

[92] A. Christenson, P. Cao and J. Tang, "Optimal Football Pressure as a Function of a Footballer’s Physical Abilities," *Proceedings,* vol. 2, *(6),* pp. 236, 2018. DOI: 10.3390/proceedings2060236.

[93] C. F. Babbs, "Biomechanics of heading a soccer ball: implications for player safety," *TheScientificWorldJournal,* vol. 1, pp. 281-322, 2001. DOI: 10.1100/tsw.2001.56.

[94] M. Nagurka and S. Huang, "A mass-spring-damper model of a bouncing ball," in 2004, DOI: 10.23919/acc.2004.1383652.

[95] M. J. TURNER *et al*, "Stiffness and Deflection Analysis of Complex Structures," *Journal of the Aeronautical Sciences,* vol. 23, *(9),* pp. 805-823, 1956. DOI: 10.2514/8.3664.

[96] W. J. Stronge and A. D. C. Ashcroft, "Oblique impact of inflated balls at large deflections," *Int. J. Impact Eng.,* vol. 34, *(6),* pp. 1003-1019, 2007. DOI: 10.1016/j.ijimpeng.2006.04.006.

[97] T. Allen, J. Ibbitson and S. Haake, "Spin generation during an oblique impact of a compliant ball on a non-compliant surface," *Proceedings of the Institution of Mechanical Engineers, Part P: Journal of Sports Engineering and Technology,* vol. 226, *(2),* pp. 86-95, 2012. DOI: 10.1177/1754337111430444.

[98] K. Arakawa *et al*, "Dynamic contact behaviour of a Golf Ball during oblique impact: Effect of friction between the ball and target," *Exp. Mech.,* vol. 47, *(2),* pp. 277-282, 2007. DOI: 10.1007/s11340-006-9018-4.

[99] S. Haake, M. Carre and S. R. Goodwill, "Modelling of oblique tennis ball impacts on tennis surfaces," in *Tennis Science and Technology 2*Anonymous 2003, .

[100] S. J. Haake *et al*, "Oblique impact of thick walled pressurized spheres as used in tennis," *Proc. Inst. Mech. Eng. Part C,* vol. 219, *(11),* pp. 1179-1189, 2005. DOI: 10.1243/095440605X32084.

[101] R. Cross, "Grip-slip behavior of a bouncing ball," *American Journal of Physics,* vol. 70, *(11),* pp. 1093-1102, 2002. DOI: 10.1119/1.1507792.

[102] D. G. Kleinbaum *et al*, *Applied Regression Analysis and Other Multivariable Methods.* (4. ed. ed.) 2008.

[103] T. Allen *et al*, "Effect of temperature on golf ball dynamics," in 2012, DOI: 10.1016/j.proeng.2012.04.108.

[104] P. Drane and J. Sherwood, "Characterization of the effect of temperature on baseball COR performance," *The Engineering of Sport,* vol. 2, 2004.

[105] G. J. Lewis, J. C. Arnold and I. W. Griffiths, "The dynamic behavior of squash balls," *American Journal of Physics,* vol. 79, *(3),* pp. 291-296, 2011. DOI: 10.1119/1.3531971.

[106] S. Choppin, "Modelling of Tennis Racket Impacts in 3d using Elite Players." , ProQuest Dissertations Publishing, 2008.

[107] C. Smith *et al*, "The Application of an Exploratory Factor Analysis to Investigate the Inter-Relationships amongst Joint Movement During Performance of a Football Skill," *Journal of Sports Science and Medicine,* vol. 5, *(4),* pp. 417-524, 2006.

[108] K. BRAY and D. KERWIN, "Modelling the flight of a soccer ball in a direct free kick," *Journal of Sports Sciences,* vol. 21, *(2),* pp. 75-85, 2003. DOI: 10.1080/0264041031000070994.

[109] K. Bray and D. Kerwin, "Modelling the long throw in soccer using aerodynamic drag and lift," *Sports Engineering,* vol. 7, *(4),* 2004.

[110] J. E. Goff, T. Asai and S. Hong, "A comparison of Jabulani and Brazuca non-spin aerodynamics," *Proceedings of the Institution of Mechanical Engineers, Part P: Journal of Sports Engineering and Technology,* vol. 228, *(3),* pp. 188-194, 2014. DOI: 10.1177/1754337114526173.

[111] J. E. Goff *et al*, "Wind-tunnel experiments and trajectory analyses for five non-spinning soccer balls," in *11th Conference of the International Sports Engineering Association;* 2016, pp. 32-37.

[112] D. S. Price *et al*, "Viscoelasticity of multi-layer textile reinforced polymer composites used in soccer balls," *J. Mater. Sci.,* vol. 43, *(8),* pp. 2833-2843, 2008. DOI: 10.1007/s10853-008-2526-0.

[113] D. S. Price, R. Jones and A. R. Harland, "Soccer ball anisotropy modelling," *Materials Science and Engineering A,* vol. 420, *(1-2),* pp. 100-108, 2006. DOI: 10.1016/j.msea.2006.01.079.

[114] A. G. Kistler Holding, "Installation and Maintenance of All Types of Forces Plates
for Biomechanics," pp. 29, .

[115] L. H. P. Vieira *et al*, "Kicking Performance in Young U9 to U20 Soccer Players: Assessment of Velocity and Accuracy Simultaneously," *Res. Q. Exerc. Sport,* vol. 89, *(2),* pp. 210-220, 2018. DOI: 10.1080/02701367.2018.1439569.

[116] J. Velasco, G. Cuadrado and A. Trigueros, "Estudio de factores antropométricos y fisco: Técnicos en el fútcol juvenil de élite en función de la posición habitual de juego," unpublished.

[117] G. Markovic, D.Dizdar and S.Jaric, "Evaluation of tests of maximum kicking performance," *The Journal of Sports Medicine and Physical Fitness,* vol. 46, *(2),* pp. 215-220, 2006.

[118] W. R. Barfield, D. T. Kirkendall and B. Yu. W. R. Barfield, D. T. Kirkendall and B. Yu. Kinematic instep kicking differences between elite female and male soccer players. 2002 Available: http://www.jssm.org.

[119] R. van den Tillaar and P. å Fuglstad, "Effect of Instructions Prioritizing Speed or Accuracy on Kinematics and Kicking Performance in Football Players," *J. Mot. Behav.,* vol. 49, *(4),* pp. 414-421, 2017. DOI: 10.1080/00222895.2016.1219311.

[120] L. Kershaw, F. A. Moura and A. Lees, "The three-dimensional nature of the maximal instep kick in soccer ," in *Science and Football* Anonymous 2005, .

[121] T. B. Andersen and H. C. Dörge, "The influence of speed of approach and accuracy constraint on the maximal speed of the ball in soccer kicking," *Scandinavian Journal of Medicine and Science in Sports,* vol. 21*, (1),* pp. 79-84, 2011. DOI: 10.1111/j.1600-0838.2009.01024.x.

[122] J. Scurr and B. Hall, "The effects of approach angle on penalty kicking accuracy and kick kinematics with recreational soccer players," *Journal of Sports Science and Medicine,* vol. 8*, (2),* pp. 230-234, 2009.

[123] C. D. Egan, M. H. G. Verheul and G. J. P. Savelsbergh, "Effects of experience on the coordination of internally and externally timed soccer kicks," *J. Mot. Behav.,* vol. 39*, (5),* pp. 423-432, 2007. DOI: 10.3200/JMBR.39.5.423-432.

[124] A. Katis and E. Kellis, "Is soccer kick performance better after a "faking" (cutting) maneuver task?" *Sports Biomech.,* vol. 10*, (1),* pp. 35-45, 2011. DOI: 10.1080/14763141.2010.547594.

[125] M. A. Khorasani, N. A. A. Osman and A. Yusof, "Biomechanical responds of instep kick between different positions in professional soccer players," in 2009, DOI: 10.2478/v10078-009-0019-0.

[126] N. P. Linthorne and D. S. Patel, "Optimum projection angle for attaining maximum distance in a soccer punt kick," *Journal of Sports Science and Medicine,* vol. 10, pp. 203-214, 2011.

[127] K. Bray and D. G. Kerwin, "Modelling the long throw in soccer using aerodynamic drag and lift," in *Engineering of Sport,* M. Hubbard, R. Mehta and J. Pallis, Eds. International sports engineering association, 2004, pp. 56-62.

[128] C. J. Payton and R. M. Bartlett. C. J. Payton and R. M. Bartlett. Biomechanical evaluation of movement in sport and exercise: The British association of sport and exercise sciences guidelines.

[129] B. PUEO, "High speed cameras for motion analysis in sports science," *Journal of Human Sport and Exercise,* vol. 11*, (1),* pp. 53-73, 2016.

[130] C. Robbe *et al*, "Quantification of the uncertainties of high-speed camera measurements," *International Journal of Metrology and Quality Engineering,* vol. 5*, (2),* 2014. DOI: 10.1051/ijmqe/2014007.

[131] Z. Wang *et al*, "Recognition and location of the internal corners of planar checkerboard calibration pattern image," *Applied Mathematics and Computation,* vol. 185*, (2),* pp. 894-906, 2007. DOI: 10.1016/j.amc.2006.05.210.

[132] F. Zheng and B. Kong. F. Zheng and B. Kong. Calibration of linear structured light system by planar checkerboard. Calibration of linear structured light system by planar checkerboard. 2004.

[133] G. Atkinson and A. M. Nevill, "Statistical methods for assessing measurement error (reliability) in variables relevant to sports medicine," *Sports Medicine*, vol. 26, *(4)*, pp. 217-238, 1998. DOI: 10.2165/00007256-199826040-00002.

[134] J. P. Weir. J. P. Weir. Quantifying test-retest reliability using the intraclass correlation coefficient and the sem. 2005.

[135] W. Newman, R. O. Duda and P. E. Hart. W. Newman, R. O. Duda and P. E. Hart. Graphics and use of the hough transformation to detect lines and curves in pictures.

[136] P. Royston and W. Sauerbrei, "Improving the robustness of fractional polynomial models by preliminary covariate transformation: A pragmatic approach," *Computational Statistics and Data Analysis*, vol. 51, *(9)*, pp. 4240-4253, 2007. DOI: 10.1016/j.csda.2006.05.006.

[137] A. G. Kistler Holdings, "Electronics & Software 64ch DAQ system with BioWare Data acquisition and analysis system for Biomechanics," .

[138] G. Atkinson and A. M. Nevill, "Statistical methods for assessing measurement error (reliability) in variables relevant to sports medicine," *Sports Medicine*, vol. 26, *(4)*, pp. 217-238, 1998. DOI: 10.2165/00007256-199826040-00002.

[139] T. C. M. Brock *et al*, "The minimum detectable difference (MDD) and the interpretation of treatment-related effects of pesticides in experimental ecosystems," *Environmental Science and Pollution Research*, vol. 22, *(2)*, pp. 1160-1174, 2015. DOI: 10.1007/s11356-014-3398-2.

[140] G. D. Israel. G. D. Israel. Determining sample size 1 the level of precision. Determining sample size 1 the level of precision. 1992.

[141] D. E. Hinkle, W. Wiersma and S. G. Jurs, "Applied statistics for the behavioural sciences," 2003.

[142] J. M. Bland and D. G. Altman, "Statistical methods for assessing agreement between two methods of clinical measurement," *International Journal of Nursing Studies*, vol. 47, *(8)*, pp. 931-936, 2010. DOI: 10.1016/j.ijnurstu.2009.10.001.

[143] Adin Ming Tan *et al*, "The Coefficient of Friction of Soccer Balls," *Proceedings*, vol. 49, *(92)*, pp. 92, 2020. DOI: 10.3390/proceedings2020049092.

[144] John D'Errico. *polyfitn*. Available: https://www.mathworks.com/matlabcentral/fileexchange/34765-polyfitn.

[145] N. R. Draper and H. Smith, *Applied Regression Analysis.* (3rd ed. ed.) 1998DOI: 10.1002/9781118625590.

[146] A. Spiess and N. Neumeyer, "An evaluation of R-Squared as an inadequate measure for nonlinear models in pharmacological and biochemical research: a Monte

Carlo approach," *BMC Pharmacology*, vol. 10, pp. 6, 2010. DOI: 10.1186/1471-2210-10-6.

[147] R. Azen and D. V. Budescu, "The Dominance Analysis Approach for Comparing Predictors in Multiple Regression," *Psychological Methods,* vol. 8, *(2),* pp. 129-148, 2003. DOI: 10.1037/1082-989X.8.2.129.

[148] R. Azen and D. V. Budescu. Comparing predictors in multivariate regression models: An extension of dominance analysis.

[149] M. T. Braun, P. D. Converse and F. L. Oswald, "The accuracy of dominance analysis as a metric to assess relative importance: The joint impact of sampling error variance and measurement unreliability," *J. Appl. Psychol.*, vol. 104, *(4),* pp. 593-602, 2019. DOI: 10.1037/apl0000361.

[150] S. B. Choppin. S. B. Choppin. Modelling of tennis racket impacts in 3d using elite players. Modelling of tennis racket impacts in 3d using elite players.

[151] L. V. Smith. Measuring the hardness of softballs. Measuring the hardness of softballs.

[152] A. L. Percival, "The impact and rebound of a football," in *Manchester Association of Engineers,* 1976-1977, pp. 17-28.

[153] Daniel Zwillinger, *CRC Standard Mathematical Tables and Formulae.* Baton Rouge: CRC Press LLC, 2011.

10 Appendix

10.1 The Hysteresis Curve

The atoms making up the polymeric material involved in football construction are joined by distant-dependent interactions called Van Der Waals bonds. They act as weak chemical bonds, therefore are susceptible to disturbance. The making and breaking of Van Der Waal bonds are the primary cause of the internal friction during compression and extension cycles illustrated in the hysteresis loop.

The deformation of a sports ball occurring upon impact with a surface, will cause the bonds to be broken by differential displacement of adjacent elastomer chains. The motion, existing due to differing stiffness properties and lengths of adjacent chains causing bonds to break and then re-establish in more favourable locations.

The temporary forming of Van Der Waal bonds increases the stiffness of the elastomer. This can be illustrated in Figure 59, using a spring model outlined from Bauman [20].

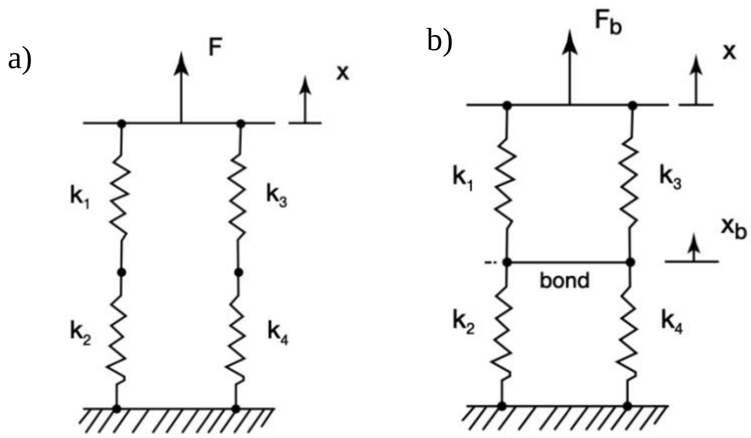

Figure 59 Spring model representing the stiffness of an elastomer (a) without and (b) with the temporary forming of Van Der Waal bonds. Reproduced from [20]

If the stiffness of each spring is assumed to be different, the equivalent stiffness of the system when no bond is present can be expressed by:

$$k_{eq} = \frac{(k_1)(k_2)}{k_1 + k_2} + \frac{(k_3)(k_4)}{k_3 + k_4}$$

The sum of the force to extend the polymer chains, is given by:

$$F = \left[\frac{(k_1)(k_2)(k_3 + k_4) + (k_3)(k_4)(k_1 + k_2)}{(k_1 + k_2)(k_3 + k_4)}\right] x$$

When the Van Der Waals bond are introduced, they act to join the springs in parallel. The system now consists of two parallel systems joined in series. The equivalent stiffness is expressed as:

$$\frac{1}{k_{eq}} = \frac{1}{(k_1 + k_3)} + \frac{1}{(k_2 + k_4)}$$

$$k_{eq} = \frac{(k_2 + k_4)(k_1 + k_3)}{(k_1 + k_2 + k_3 + k_4)}$$

The force required to extend the polymer chains is given by:

$$F = \left[\frac{(k_2 + k_4)(k_1 + k_3)}{(k_1 + k_2 + k_3 + k_4)}\right] x$$

Through a simple substitution of arbitrary values, it can be seen a greater force is required to cause the extension of the specimen when Van Der Waal bonds are present. This increases the stress observed during the loading curve of the hysteresis. During unloading of the material, these bonds act against the retraction force of the polymer chains, reducing the stress measured. The presence of these bonds acts as an explanation of the shape of hysteresis observed during tensile testing of polymeric materials.

10.2 Quasi-static Force-Deflection Curves for all Footballs

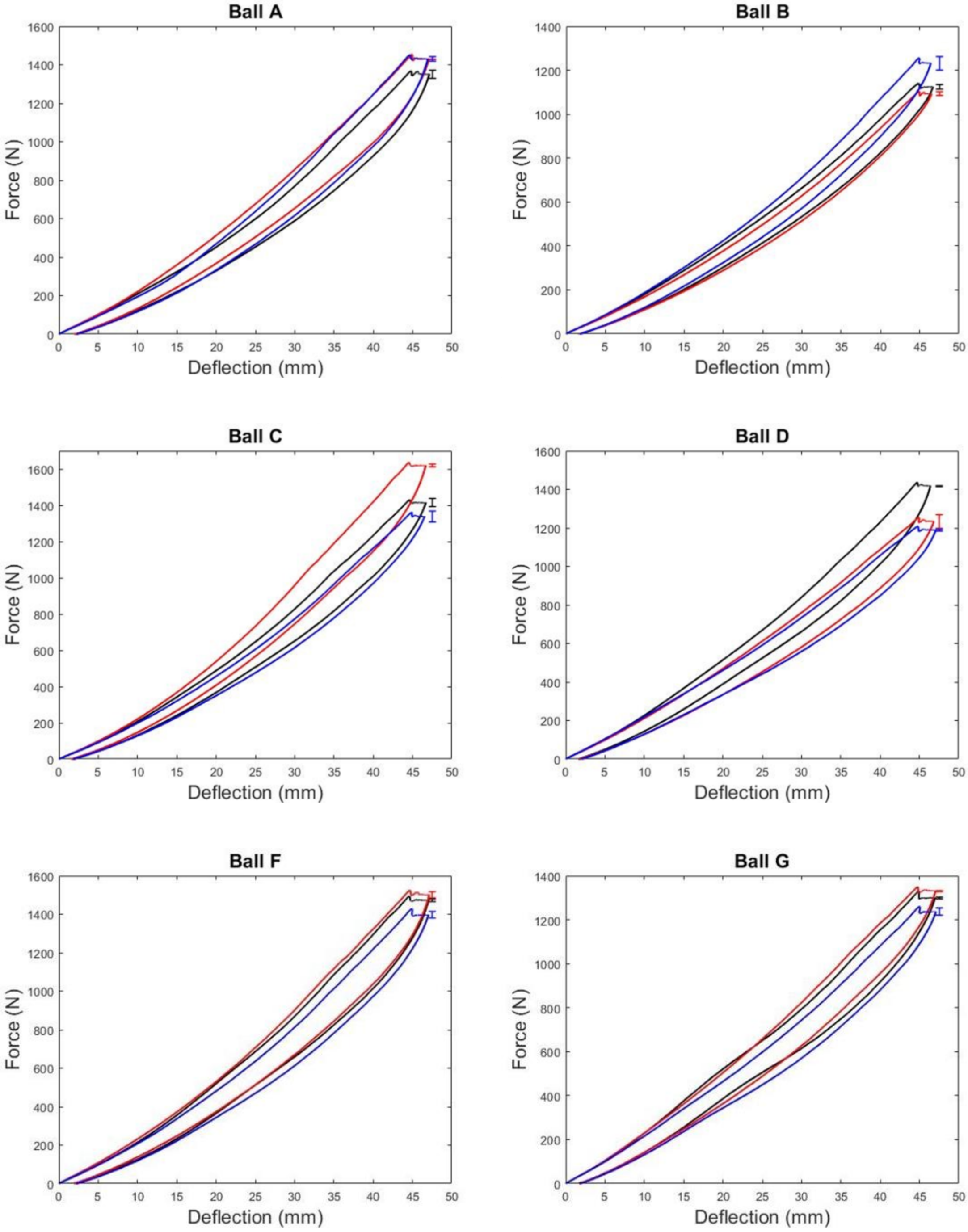

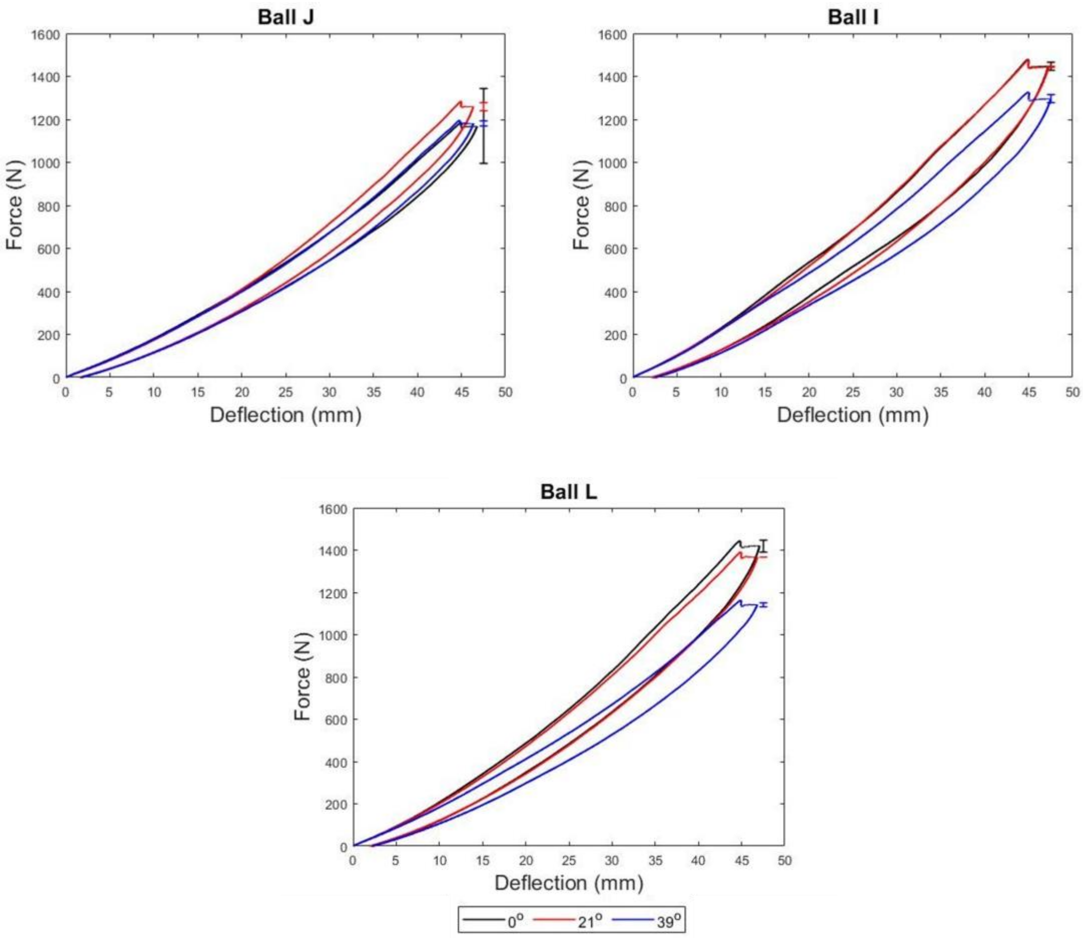

Figure 60 The force-deflection curve for the three loading directions for the remaining footballs.

10.3 Quantification of Spatial and Off-plane Errors

Preliminary assessments were carried out to establish the correct position of the high-speed camera with respect to the force platform edge. The camera was placed perpendicular to the impact plane to minimise parallax errors noted by Carré [88]. Many previous studies do not specify the distance between the impact area and the high-speed camera, it is also not specified in the FQP test manual [1]. The laboratory space at Sheffield Hallam University allows a maximum distance of 30 m, therefore it was necessary to investigate the errors associated with camera distance to minimise errors due to incorrect framing or caused by impacts out of the extrinsic calibration plane.

a) spatial errors

Spatial errors may arise if the camera is not placed at a sufficient distance away from the force platform. Incorrectly framing the football will cause the diameter to appear smaller when the camera is placed too close, as illustrated in Figure 61a. A to-scale drawing was created in Microsoft Visio to measure the change in radius with respect to increasing camera distance. As shown in Figure 61b, the error reduced as the camera-to-football distance increased. Beyond 2 m, the error in radius fell below 1 mm.

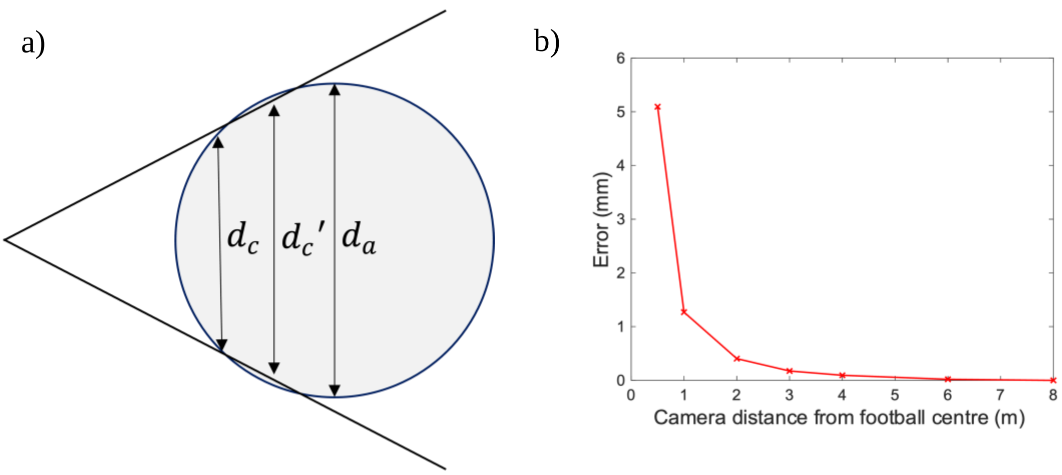

Figure 61 (a) Illustration of how incorrect framing of the football can cause the diameter of the football to appear smaller (d_c, d_c') than the actual diameter (d_a,). (b) The error is radius against camera distance from the football centre.

b) off-plane impacts

Uncontrollable variation in the impact location of the football can arise when using the mechanical device. An investigation was carried out to quantify the difference in velocity observed at different camera positions for impacts ± 20 mm from the extrinsic plane. A single checkerboard was placed 20 mm in front and behind the impact plane, as shown in Figure 62. The positions of the outer four corners were digitised to calculate the x and y distances. The pixel coordinates were transformed into world coordinates using DLT. To estimate the change in velocity across the three planes, the time taken to travel 100 pixels in the impact plane was calculated, assuming a constant velocity of 6 $m \cdot s^{-1}$. The time taken was applied across the distances in the other two planes. The error was calculated as the change in velocity between the forward and backward planes. The calculations were repeated for 20 $m \cdot s^{-1.}$

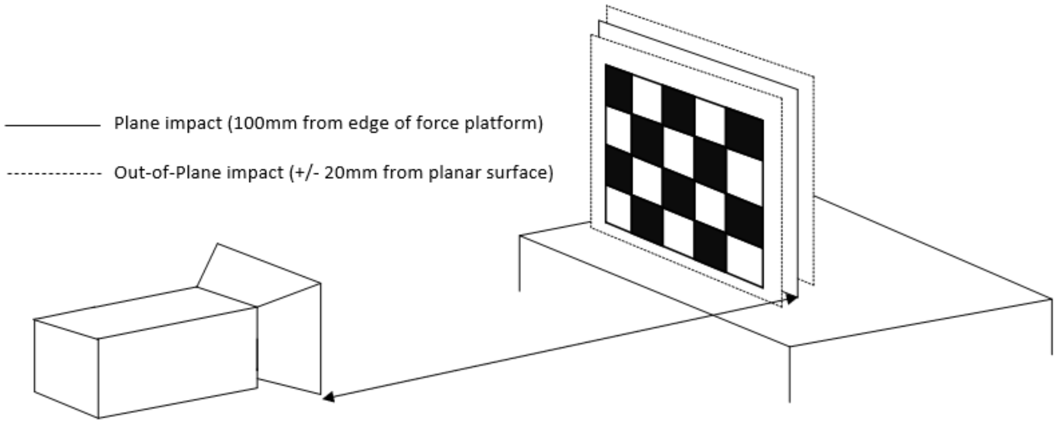

Figure 62 The assessment of off-plane errors uses a single checkerboard placed 20 mm in front and then behind of the plane used for the extrinsic camera parameter.

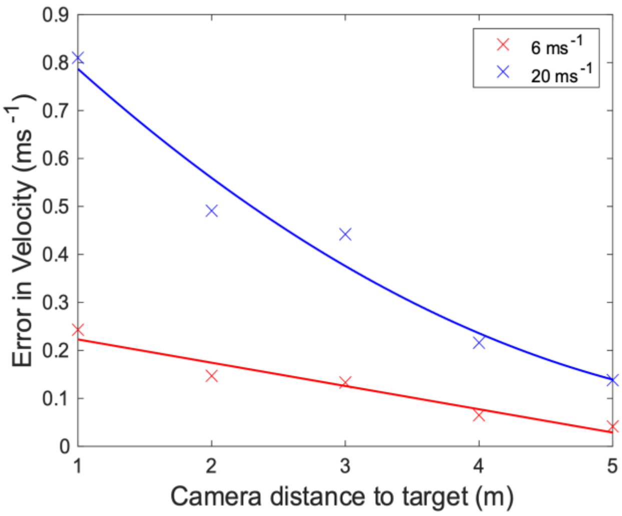

Figure 63 The error in velocity estimates for the corresponding camera distance

Figure 63 shows the difference in velocity between the forward and backward plane reduced as the camera distance was increased. While, to minimise occlusion errors a minimum distance between the camera and impact area was 2 m, the investigation to out-of-plane errors showed the error was almost halved by doubling the distance to 4 m. The clarity of image was influenced by the increase in distance therefore there is a trade-off between minimise the errors discussed above and the sharpness of the ball. For both data collections the camera should be placed at a minimum distance of 4 m from the force platform edge.

10.4 Derivation of Air Resistance Trajectory Model

Air resistance is a widely considered drag force in many trajectory modelling applications. Often for simplicity, the velocity of a falling object is approximated using the acceleration of gravity and the drop height, however, this does not consider the air resistance. When air resistance is not considered it leads to overestimations. In practice, a football will continue to accelerate towards the surface as it falls until it collides with it. Resolving the forces acting on the football can give much better approximations and provide insight into the velocity that will be encountered during laboratory testing. This can assess the decision to use the appropriate fitting techniques to estimate the impact velocity.

The forces due to drag and weight were resolved to make velocity the subject. The derivation is detailed below. Standard mathematical integral tables were used to express the velocity as a function of time. The velocity-time curve was integrated using the trapezium rule to obtain displacement. To calculate the impact velocity, the time required for a 2 m fall was inputted into equation 10-1.

$$F_D = \left(\frac{1}{2}\rho A C_d\right) v^2$$

$$F_N = ma$$

$$F_w = mg$$

$$F_w - F_D = F_N$$

$if\ k = \frac{1}{2}\rho A C_D$

$$mg - kv^2 = ma$$

$$m\frac{dv}{dt} = mg - kv^2$$

$$\frac{dv}{dt} = g - \frac{kv^2}{m}$$

$$= \frac{-k}{m}(v^2 - \frac{mg}{k})$$

$$\int_0^v \frac{1}{(v^2 - \frac{mg}{k})}\,dv = \int_0^t \frac{-k}{m}dt$$

$let\ b^2 = \frac{mg}{k}$

$$\int_0^v \frac{1}{(v^2 - b^2)}\,dv = \int_0^t \frac{-k}{m}dt$$

Using standard integral tables [153]

$$y = tanh^{-1}(v) = \frac{1}{2}\ln\left(\frac{1+v}{1-v}\right)$$

$$-\frac{1}{b}tanh^{-1}\left(\frac{v}{b}\right) = \frac{-kt}{m}$$

$$\sqrt{\frac{k}{mg}}tanh^{-1}\left(\frac{v}{\sqrt{\frac{mg}{k}}}\right) = \frac{kt}{m}$$

$$\frac{v}{\sqrt{\frac{mg}{k}}} = \tanh\left(\sqrt{\frac{gk}{m}}\right)$$

$let\ V_T = \sqrt{\frac{mg}{k}}$

$$v(t) = V_T \tanh\left(\sqrt{\frac{gk}{m}}t\right)$$

$$v(t) = V_T \tanh\left(\frac{gt}{V_T}\right) \quad (10\text{-}1)$$

Equation 10-1 above was used to plot Figure 64b that was differentiated with respect to time to obtain the displacement. The falling height from a 2 m with respect to time is shown in Figure 64a. The time taken for a football to fall from a 2 m and impact the surface was 0.63 s. This was inputted into equation 10-1 to give an impact velocity of 5.98 m·s^{-1}.

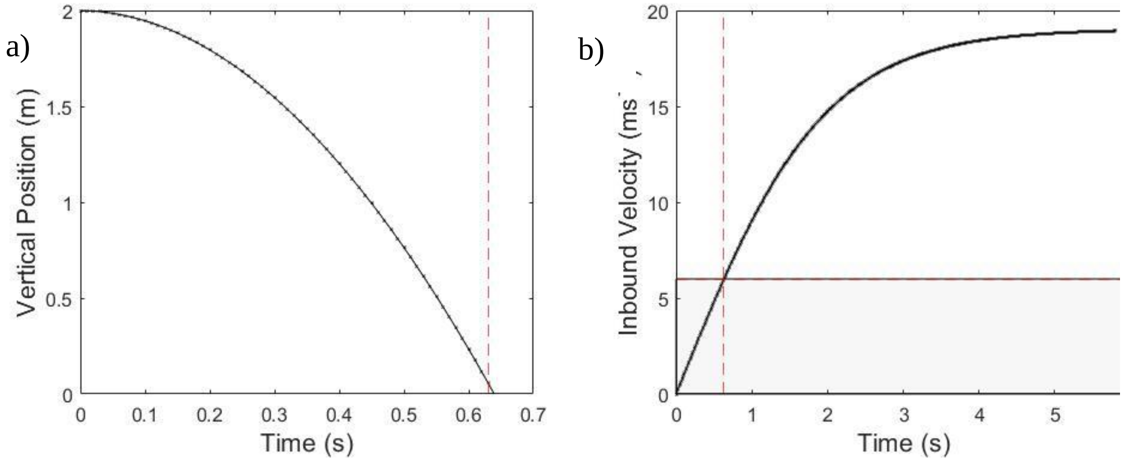

Figure 64 (a) The vertical position calculated for a football falling from 2 m. (b) The calculation of inbound velocity with respect to time. C_d=0.5, ρ =1.23 kg·m^{-3}, A=0.04 m^2 g=9.81 m·s^{-2} m=430g.

The calculated velocity was lower than the simplified calculation gives; 5.98 compared to 6.25 m·s^{-1}. The velocity obtained using this approach was used a guideline for the impact velocity that could be encountered during laboratory testing.

10.5 Sampling Frequency of the Force Platform

Previous studies had used a sampling frequency of 10 kHz to record the loading behaviour of a football, but its appropriateness was uncertain. The force platform was operated using Bioware which allowed a sampling frequency up 125 kHz. To investigate the influence of sampling frequency on the value of peak impact force, a football was released from 2 m and the force was sampled at 50 kHz and then downsampled by an integer factor using MATLAB.

Table 60 Forces measured during the down sampling of a 50 kHz signal.

Sampling Frequency (kHz)	Peak force (N)
1	1230.3
2	1266.8
5	1267.4
10	1267.8
25	1267.8
50	1268.9

The results in Table 60 showed that the 10 kHz was sufficient to capture the peak impact force. Above 5 kHz, the difference to the peak force at 50 kHz was 0.1 %. The force platform and high-speed camera were synchronised using a single trigger, which meant the sampling frequency must be the same for both systems. A sampling frequency of 10,000 fps was chosen to optimise the quality of the image captured by the high-speed camera whilst minimising measurement error. This frame rate accompanied by additional light sources allowed short exposure times to be achieved to minimise motion blur.

10.6 Multivariable modelling - Cross-validation modelling procedure

The performance statistics for the cross-validation procedure considering different order relationships using static measurements are presented in Table 61 for the certification test velocity and Table 62 for the higher velocity. The R-squared value is only presented for the linear model since higher order relationships violate the underlying assumptions of the calculation. In the calculation of R-squared the ratio of sum of square regression and total variance must produce a value between 0 and 1, whereas in nonlinear models, the variance explained by the regression model and the error variance do not equal the total variance, and therefore the R-squared value may no longer fall between 0 and 1.

Table 61 Performance statistics for cross-validation procedure at the certification test velocity for the multivariable regression model using static mechanical properties.

		Cross-Validation		Training		
Impact variable	Polynomial	RMSE	R^2	RMSE	R^2	Majority significant terms?
Outbound Velocity	1	0.81	0.34	0.82	0.33	Yes
	2	0.73	-	0.75	-	No
	3	0.55	-	0.67	-	No
Contact Time	1	0.62	0.61	0.62	0.61	Yes
	2	0.56	-	0.57	-	No
	3	0.44	-	0.44	-	No
Deformation	1	0.69	0.53	0.69	0.53	Yes
	2	0.62	-	0.62	-	No
	3	0.55	-	0.55	-	No
Peak Impact Force	1	0.74	0.44	0.75	0.44	Yes
	2	0.68	-	0.70	-	No
	3	0.41	-	0.47	-	No

Table 62 Performance statistics for cross-validation procedure at the higher velocity for the multivariable regression model using static mechanical properties.

		Cross-Validation		Training		
Impact variable	Polynomial	RMSE	R^2	RMSE	R^2	Majority significant terms?
Outbound Velocity	1	0.77	0.39	0.78	0.39	Yes
	2	0.71	-	0.72	-	No
	3	0.59	-	0.59	-	No
Contact Time	1	0.88	0.22	0.88	0.22	Yes
	2	0.81	-	0.81	-	No
	3	0.73	-	0.73	-	No
Deformation	1	0.83	0.31	0.83	0.31	Yes
	2	0.77	-	0.77	-	No
	3	0.67	-	0.67	-	No
Peak Impact Force	1	0.92	0.15	0.93	0.14	Yes
	2	0.84	-	0.85	-	No
	3	0.71	-	0.73	-	No

As the order of the polynomial increased, the number of terms also increases; for the first order, there are only four terms, for the second order this increases to 10 and then to 20 at the third order. Despite this increase in complexity, the improvement in the RMSE between the first and second order relationship was not substantial for each impact variable. In some cases, the third order exhibited signs of over-fitting through discrepancies between the RMSE of the cross-validation to training models. Given these findings, the added complexity and reduction in statistically significant terms associated with the higher-order polynomials did not justify the selection of a second-order relationship for this application, given that the impact behaviours are confined to a small inbound velocity interval, where a first-order model sufficed.

End of document.